University of North Dakota
UND Scholarly Commons

Theses and Dissertations | Theses, Dissertations, and Senior Projects

January 2015

Regulation Of Vectorial Active Transport In Human Proximal Tubule Cells By MT-3: The Role Of The C-Terminal Domain On E-And N-Cadherin Expression And The Confirmation Of Protein-Protein Interactions

Andrea Marie Nore

Follow this and additional works at: https://commons.und.edu/theses

Recommended Citation
Nore, Andrea Marie, "Regulation Of Vectorial Active Transport In Human Proximal Tubule Cells By MT-3: The Role Of The C-Terminal Domain On E-And N-Cadherin Expression And The Confirmation Of Protein-Protein Interactions" (2015). *Theses and Dissertations*. 1938.
https://commons.und.edu/theses/1938

This Dissertation is brought to you for free and open access by the Theses, Dissertations, and Senior Projects at UND Scholarly Commons. It has been accepted for inclusion in Theses and Dissertations by an authorized administrator of UND Scholarly Commons. For more information, please contact zeineb.yousif@library.und.edu.

REGULATION OF VECTORIAL ACTIVE TRANSPORT IN HUMAN PROXIMAL TUBULE CELLS BY MT-3: THE ROLE OF THE C-TERMINAL DOMAIN ON E-AND N-CADHERIN EXPRESSION AND THE CONFIRMATION OF PROTEIN-PROTEIN INTERACTIONS

by

Andrea Marie Nore
Bachelor of Science, Minnesota State University Moorhead, 2010

A Dissertation
Submitted to the Graduate Faculty

of the

University of North Dakota School of Medicine and Health Sciences

in partial fulfillment of the requirements

for the degree of

Doctor of Philosophy

Grand Forks, North Dakota
December
2015

Copyright 2015 Andrea Nore

This dissertation, submitted by Andrea Nore in partial fulfillment of the requirements for the Degree of Doctor of Philosophy from the University of North Dakota, has been read by the Faculty Advisory Committee under whom the work has been done and is hereby approved.

Scott H. Garrett

Seema Somji

Donald A. Sens

John B. Shabb

Jane R. Dunlevy

This dissertation is being submitted by the appointed advisory committee as having met all of the requirement of the School of Graduate Studies at the University of North Dakota and is hereby approved.

Wayne Swisher
Dean of the School of Graduate Studies

Date

PERMISSION

Title REGULATION OF VECTORIAL ACTIVE TRANSPORT IN HUMAN PROXIMAL TUBULE CELLS BY MT-3: THE ROLE OF THE C-TERMINAL DOMAIN ON E-AND N-CADHERIN EXPRESSION AND THE CONFIRMATION OF PROTEIN-PROTEIN INTERACTIONS

Department Biochemistry and Molecular Biology

Degree Doctor of Philosophy

In presenting this dissertation in partial fulfillment of the requirements for a graduate degree from the University of North Dakota, I agree that the library of this University shall make it freely available for inspection. I further agree that permission for extensive copying for scholarly purposes may be granted by the professor who supervised my dissertation work or, in his absence, by the Chairperson of the department or the dean of the School of Graduate Studies. It is understood that any copying or publication or other use of this dissertation or part thereof for financial gain shall not be allowed without my written permission. It is also understood that due recognition shall be given to me and to the University of North Dakota in any scholarly use which may be made of any material in my dissertation.

Andrea Nore
November 5, 2015

TABLE OF CONTENTS

LIST OF FIGURES vii

LIST OF TABLES ix

ACKNOWLEDGMENTS x

ABSTRACT xii

CHAPTER

I. INTRODUCTION 1

Significance 1

Hypothesis and Rationale 3

Epithelial Cell Adhesion and Polarity 6

Epithelial-Mesenchymal Transition 8

Cadmium is Nephrotoxic 11

Metallothioneins 16

Metallothionein isoform -3 18

Metallothionein-3 Protein-Protein Interactions 19

II. METHODS 22

Immunohistochemistry 22

Laser-Capture Microdissection 23

Cell Culture 25

Transepithelial Resistance 26

RNA isolation and qRT-PCR 26

Protein Isolation 27

Western Blotting 28

ELISA 30

Statistical Analysis 30

Stable Transfections 31

Transient Transfections 32

Co-immunoprecipitation 33

III. RESULTS 34

Expression of E- and N-Cadherin in Human Kidney Proximal Tubules 34

Expression of E- and N-Cadherin in HK-2 Cells as a Function of Growth Medium Composition 38

Comparison of E- and N-Cadherin Expression in HK-2 and HPT Cell Cultures 39

Alterations in Tight Monolayer Development 44

Association of the Unique C-Terminal Domain of MT-3 With MT-3 Induced MET in HK-2 Cells 46

Effect of Forced E-cadherin Expression on HK-2 Vectorial Active Transport, N-Cadherin Expression, and Cell Morphology 52

Zn_7MT-3 mediated pulldowns in HK-2 lysates 55

V5-mediated immunoprecipitations in MT-3 expressing HK-2 lysates 55

IV. DISCUSSION 60

HK-2 Cells have Features Associated with the Initial Stages of EMT 60

HK-2 Cells Undergo MET Mediated by MT-3 65

MT-3 Interacts with Proteins that Promote an Epithelial Phenotype 67

BIBIOGRAPHY 71

APPENDIX 82

LIST OF FIGURES

Figure Page

III-1. Immunohistochemical staining of E-cadherin and N- Cadherin in the human kidney 35

III-2. Expression of E-and N-cadherin in microdissected proximal tubules 36

III-3. Influence of growth medium on E-and N-cadherin expression in HK-2 cells 40

III-4. Comparison of E-cadherin expression in HPT and HK-2 cell cultures 41

III-5. Comparison of N-cadherin expression in HPT and HK-2 cell cultures 42

III-6. The pattern of E- and N-cadherin expression is unaltered when cells are grown on transwell inserts 43

III-7. Transepithelial resistance comparison of HPT and HK-2 cell cultures 44

III-8. Connexin 32 expression in HK-2, HPT, and HK-2 cells expressing MT-3. 45

III-9. Mutated metallothionein constructs 47

III-10. Effect of the altered domains of MT-3 on the formation of domes in stably transfected HK-2 cells 48

III-11. Effect of the altered domains of MT-3 on the expression of E-and N-cadherin in stably transfected HK-3 cells 51

III-12. Effect of the altered domains of MT-3 on the expression of connexin 32 in stably transfected HK-3 cells 52

III-13. Figure III-13. The effect of forced overexpression of E-cadherin on the expression of N-cadherin and on dome formation in HK-2 cells 54

III-14. Schematic representation of the methodology used to pulldown MT-3 interacting proteins 56

III-15. MT-3 interacts with β-actin, Tropomyosin 3, enolase-1, and aldolase A 57

III-16. Zinc supplementation 6 hours post transient transfection of V5-tagged MT-3 into HK-2 cells increases MT-3 protein expression 57

III-17. MT-3 interacts with several proteins in cultured proximal tubule cells 58

III-18. Co-immunoprecipitation of MT-3 protein complexes in HK-2 cells transfected with V5 tagged-MT-3 59

V-1. Immunostaining of MT-3 in Skin Pigment Lesions 90

V-2. Immunostaining of MT-3 in Nevi and Melanoma Cells 92

V-3. Expression of MT-3 in primary normal human keratinocytes (NHEK), Immortalized Human Keratinocytes (HaCaT), and normal human melanocytes (HEMa-LP) 94

LIST OF TABLES

Table		Page
I-1.	MT-3 interacting proteins	21
II-1.	Primary antibodies used for western blotting	29
III-1.	Transepithelial resistance and dome formation in HK-2 cells overexpressing MT-3 with altered protein domains	49
V-1.	Immunostaining of MT-3 in normal skin, SCC, BCC, Nevi, and Melanoma	89

ACKNOWLEDGMENTS

First and foremost I would like to thank Dr. Don Sens, Dr. Van Doze, Dr. Jim Porter and Dr. Joe Provost for recognizing my potential when I was an undergraduate researcher. Their combined support and mentorship has greatly impacted my scientific success and I am forever grateful.

I would like to recognize the many individuals who made this body of work a possibility. Dr. Xudong Zhou, Dr. Yun Zhen, and Dr. Mary Ann Sens procured the tissue and aided in all of immunohistochemistry related data. I would also like to thank Dr. Chandra Bathula for designing the mutant metallothionein constructs, identifying putative protein interactions with the assistance of Dr. John Shabb, and Wallace Muhonen, and finally for performing the microdissection of proximal tubules from paraffin-embedded blocks of tissue. I would like to thank Dr. Dunlevy for her assistance with microscopy, expertise in cell biology, and mentorship. Dr. Brent Voels performed much of the cloning and purification of the 6.2/V5 vectors prior to kindly giving them to me for linearization and transfection. Dr. Seema Somji and Dr. Scott Garrett have been fantastic mentors as well, always available to assist with any struggles I encountered and their independent strengths have made me a well-rounded researcher.

Finally, I would like to thank my family and friends that have supported me as I achieved my goals. My husband (and best friend) John, who has been with me from the beginning of graduate school, is my rock. The many great friends who started and ended this journey with me, in particular Elizabeth Sandquist, Katie Collette, and Dani Rastedt.

These girls hold a special place in my heart, and I will cherish our many "knit nights," happy hours, potlucks, seminars, practice sessions, comprehensive test review, and cakes. I couldn't have done it without any of you.

ABSTRACT

The proximal tubule of the kidney is particularly susceptible to toxicant-induced damage and cell cultures of human proximal tubule cells are widely utilized to study the role of epithelial-mesenchymal transition (EMT) in renal disease. Cadmium is a toxic metal ion that is known to produce renal tubular necrosis and accumulate in the proximal tubule. This metal binds to a family of cysteine rich metal binding proteins known as metallothioneins (MT) that are found in abundance in the kidney. Previous studies from our laboratory have shown that the third isoform of metallothionein (MT-3) is expressed in the epithelial cells of the human kidney, including those of the proximal tubule. An immortalized proximal tubule cell line does not express MT-3 and does not demonstrate vectorial active transport. Transfection of the MT-3 gene into the HK-2 cells restores vectorial active transport as evidenced by dome formation. This suggests that MT-3 is involved in mesenchymal to epithelial transition (MET), the reverse of EMT, and promotes and epithelial phenotype. The goals of the present study were to examine the role of growth media composition on classic EMT responses, quantitatively evaluate the expression levels of E- and N-cadherin, define the functional epitope of MT-3 that mediates MET in HK-2 cells, and identify proteins that interact with MT-3 to promote epithelial features in the proximal tubule. It was shown that both E- and N-cadherin mRNA and protein are expressed in the human renal proximal tubule. Based on the pattern of cadherin expression, vectorial active transport, and transepithelial resistance, it seems that the HK-2 cell line has already undergone many of the early features associated

with EMT. Our data indicates the unique, six amino acid C-terminal sequence of MT-3 is required to induce MET in HK-2 cells. A combination of co-immunoprecipitation and western blotting indicate that MT-3 interacts with myosin-IIa, β-actin, enolase-1, tropomyosin-3, and aldolase-a *in vitro*. Together, the data suggests the HK-2 cell line can be an effective model to study later stages in the conversion of the renal epithelial cell to a mesenchymal cell and when transfected with MT-3 it may be an effective model to study the process of MET. MT-3 protein-protein interactions provide insight into the potential mechanism by which MT-3 promotes cytoskeletal organization in non-diseased epithelial proximal tubule cells and offers the opportunity to investigate these interactions under pathological conditions.

CHAPTER I

INTRODUCTION

Significance

The incidence of chronic kidney disease (CKD) is steadily rising and has reached epidemic proportions in the western and industrialized world. Chronic kidney disease is associated with albuminuria, decreased creatinine clearance, altered glomerular morphology, and tubular degeneration (Eddy & Neilson, 2006). Epidemiological evidence and animal models have demonstrated chronic cadmium exposure as a significant contributory factor for developing CKD (Gobe & Crane, 2010; Klaassen, Liu, & Diwan, 2009; Walter C Prozialeck & Edwards, 2012; Thévenod, 2003) Clinicopathological studies have shown tubulo-interstitial fibrosis to be the hallmark of CKD progression (Bohle, Müller, Wehrmann, Mackensen-Haen, & Xiao, 1996; Eddy & Neilson, 2006; Fine, Ong, & Norman, 1993; Zeisberg & Neilson, 2010). This suggests that halting the progression of CKD could be achieved by stopping the progression of or even by inducing remission of fibrosis. Renal fibrosis is defined as the scarring of the tubulo-interstitial space after kidney damage of any type. It appears to be initiated at random in small areas that are preceded by interstitial inflammation, then expands to become diffuse if drivers of fibrosis persist (Prunotto et al., 2012). Accumulation and proliferation of activated fibroblasts (myofibroblasts) in these small areas are linked to the risk of progression of fibrosis (Hinz et al., 2007). The exact source

of renal myofibroblasts remains to be definitely defined. Several hypotheses exist in the literature including: migration of circulating fibrocytes to the site of the lesion, differentiation of local fibroblasts or pericytes, direct transformation of resident endothelial cells by endothelial-mesenchymal transition (endoMT), or transformation of resident epithelial cells through epithelial mesenchymal transition (EMT). Studies in experimental models have shown that it is the pericytes that respond to chronic injury and profibrotic signals through proliferation and differentiation into myofibroblasts (S.-L. Lin, Kisseleva, Brenner, & Duffield, 2008; Picard, Baum, Vogetseder, Kaissling, & Le Hir, 2008). Fate tracing of pericytes has shown a direct contribution of these cells to renal fibrosis (Humphreys & Lin, 2010). These studies, taken together, suggest a limited contribution for a direct conversion of renal epithelial cells, through the process of EMT, to produce the proliferative pool of fibroblast and myofibroblast cells seen during chronic kidney injury.

An indirect role for EMT in the progression of CKD can be proposed through alteration of the tubulo-interstitial microenvironment which can promote fibroblast proliferation and myofibroblast activation (Prunotto et al., 2012). This microenvironment would be produced by an alteration in epithelial to mesenchymal cellular cross talk produced by renal epithelial cells undergoing EMT upon renal injury. A role for an alteration in the microenvironment by renal cells undergoing EMT is consistent with early observations which showed that regions of active renal interstitial fibrosis exhibited a predominant peritubular as opposed to a perivascular distribution (Alpers & Hudkins, 1994; Fine, Norman, & Ong, 1995). In addition, some clinical features of CKD can be explained by a hypothesis that tubular epithelial cells can relay fibrogenic signals to

contiguous fibroblasts in diseased kidneys (Coca, Yusuf, & Shlipak, 2009; Venkatachalam & Griffin, 2010). However, a role for EMT of renal epithelial cells producing a pro-fibrotic microenvironment remains a hypothesis supported by general observations, but not one supported by mechanism.

Hypothesis and Rationale

This study tests the hypothesis that epithelial-mesenchymal transition occurs in epithelial cells of proximal tubule origin and that cells cultured in the presence of serum acquire a mesenchymal phenotype. Further, we hypothesize that the hexapeptide insert in the C-terminal domain of MT-3 is required for vectorial active ion transport by interacting with proteins involved in cytoskeletal organization.

One means to study the possible role of EMT in renal epithelial cells and its relationship to a microenvironment promoting fibrosis is the use of human renal epithelial cell cultures to model the mechanistic processes underlying the EMT. An examination of the literature suggests that the HK-2 cell line is the most common human renal epithelial cell line used to model human renal EMT and related renal disorders. The HK-2 cell line was isolated by immortalizing and cloning a cell line from a primary culture of proximal tubule epithelial cells transduced with a construct containing the HPV16 E6/E7 genes (Ryan, Johnson, & Kirk, 1994). The HK-2 cell line proliferates in a serum-free growth medium comprised of keratinocyte serum free medium (KSFM) supplemented with epidermal growth factor and bovine pituitary extract. The HK-2 cell line is available from the American Type Culture Collection (ATCC) with instructions for growth in a KSFM medium supplemented with epidermal growth factor and bovine pituitary extract. The HK-2 cells were shown to have an epithelial morphology and to retain many markers

of proximal tubule cells such as alkaline phosphatase, gamma glutamyltranspeptidase, leucine aminopeptidase, acid phosphatase, cytokeratin, $\alpha_3\beta_1$ integrin and fibronectin. Functional markers of proximal tubule differentiation also retained were: cAMP responsiveness to parathyroid hormone, but not antidiuretic hormone; Na^+ dependent, phlorizin sensitive glucose transport; and, the ability to accumulate glycogen.

The present study is designed to address several concerning studies that use the HK-2 cell line as a model for renal EMT. First, do conditions used for the growth of the HK-2 cell line influence the results of studies examining the mechanism/s underlying renal EMT? This question arises since the growth media conditions recommended in the original publication, and those suggested by the ATCC, have not been employed in many investigations. A cursory review of the literature discloses that many studies that employ this cell line to address human renal EMT grow the HK-2 cells in various growth formulations containing fetal calf serum (Bai, Zeng, Zhou, & Liao, 2012; Berzal, Alique, & Ruiz-Ortega, 2012; W. Ding, Yang, Zhang, & Gu, 2012; Eneling, Brion, Pinto, & Pinho, 2012; Guillén-Gómez, 2012; Q. Li, Liu, Lv, & Ma, 2011; Y. Li et al., 2010; H. Lin, Wang, Wu, & Dong, 2011; Masola, Gambaro, & Tibaldi, 2012; Veerasamy & Nguyen, 2009) as opposed to those using the recommended growth medium (Dudas, Argentieri, & Farrell, 2009; Dudas & Sague, 2011; Grabias & Konstantopoulos, 2012; Sarközi, Flucher, & Haller, 2012; Yuan, Chen, Zhang, & Huang, 2012). One could speculate that growth media containing serum would in itself promote EMT and provide a more profibrotic growth environment than growth medium formulations without serum. To examine this question, the present study determines the expression of two common markers of EMT, E-cadherin and N-cadherin, as a function of the growth media

composition used for the growth of the HK-2 cells. In addition, previous studies from this laboratory demonstrated that the HK-2 cell line grown on serum-free growth medium had lost the ability for vectorial active transport as noted by a lack of dome formation and transepithelial resistance (Bathula, Garrett, & Zhou, 2008; Kim, Garrett, Sens, Somji, & Sens, 2002). The present study is also designed to determine if the loss of vectorial active transport was influenced by the presence or absence of serum in the growth medium of the HK-2 cells.

A second question explored in the present study, to what degree did the immortalization process used to isolate the HK-2 cell line advance the process of EMT compared to the parental cell line? This question is important since it is possible that the HK-2 cells may have already undergone a significant degree of the EMT. Evidence for this concept comes mainly from studies by this laboratory which developed the serum-free culture conditions for the growth of mortal cultures of human proximal tubule (HPT) cells that retain many of the differentiated features of the renal proximal tubule (Detrisac, Sens, Garvin, Spicer, & Sens, 1984; D. A. Sens et al., 1999; Todd, McMartin, & Sens, 1996). Similar cultures are now currently available from a number of commercial suppliers along with kits to support serum-free cell growth (some proprietary). In two related studies, this laboratory compared several properties of the HPT and HK-2 cells when grown on identical serum-free growth media (Bathula et al., 2008; Kim et al., 2002). It was shown that when compared to the HPT cell line, the HK-2 cells had lost the capacity for vectorial active transport as noted by the inability to form doming structures (Kim et al., 2002). In agreement with the absence of domes, the HK-2 cells, when compared to the HPT cells, were also shown to not generate transepithelial resistance and

to lack the presence of tight junctions (Kim et al., 2002). A corresponding analysis of E- and N-cadherin expression between the cell lines demonstrated a decrease in E-cadherin and an increase in N-cadherin when the HK-2 cells were compared to the HPT cells (Bathula et al., 2008). The determination of the E- and N-cadherin protein levels were qualitative in this past study and a goal of the present study is to quantify the differences in E- and N-cadherin expression between the cell lines and to determine if additional differences exist in cell-to-cell junctional communication. The goal is to confirm that early features of EMT, such as the loss of cell-to-cell junctional integrity and a shift between E- and N-cadherin have already taken place in the HK-2 model system. The above studies (Bathula et al., 2008; Kim et al., 2002) also demonstrated that the HK-2 cell line could undergo a reversal of the EMT process (MET) and regain vectorial epithelial transport, undergo a switch in E-, N, and K-cadherin expression, and regain junctional integrity upon stable transfection with the gene encoding the 3rd isoform of the metallothionein protein (MT-3). MT-3 is a multifunctional protein, playing roles in zinc and copper homeostasis, prevention of oxidative damage, protection against heavy metal toxicity, ion transport and it may also potentially maintain epithelial cell polarity, a property postulated to be attributed to the interaction of MT-3 with proteins involved in cytoskeletal organization. An additional goal of the present study, therefore, is to define the functional domain of MT-3 eliciting increased MET in HK-2 cells, and confirm putative MT-3 interacting proteins.

Epithelial Cell Adhesion and Polarity

Polarized epithelial cells are composed of distinct apical, lateral, and basal plasma membrane domains. Cells of transporting epithelia, including proximal tubule epithelial

cells, form specialized junctional complexes that connect lateral domains of adjacent cells and attach the basolateral domain to the ECM, forming epithelial sheets that line organs. These complexes are necessary for both the restriction of permeability and the normal transport of molecules across the cell monolayer, while additionally contributing to the maintenance of proper cell polarity. The lateral complexes include the zona occludens, normally referred to as tight or occluding junctions, the adherens junctions, desmosomes, and gap junctions. Hemidesmosomes are the junctional complex that link the basolateral membrane to the ECM. Specific cell adhesion and junction associated proteins comprise these complexes and include the cadherins, catenins, integrins, connexins, among others. These proteins are associated with actin filaments and cytoskeletal structural elements of individual cells within the epithelial sheet.

The tight junctions function to seal the cytoplasm of adjacent cells from one another, and are primarily comprised of the occluden and claudin family of proteins. These lateral junctions are nearest to the apical surface of epithelial cells, and integrity of these complexes promotes tight association of adjacent cells while also functioning as a barrier against solutes entering the extracellular space between cells and interacting with the lateral domains of adjacent cells.

The adherens junctions are responsible for lateral intercellular anchorage and are mediated by the calcium dependent cell adhesion protein E-cadherin. E-cadherin is a single pass transmembrane protein that is the main structural component of this junctional complex. The intracellular domain is composed of a complex of proteins required for linking E-cadherin to the actin cytoskeleton, and is made up of alpha-catenin, beta-catenin, and alpha actinin. The extracellular domain of E-cadherin is responsible for the

adhesive properties of E-cadherin, containing calcium binding sites in addition to the adhesion domain. Calcium binding to this domain increases the rigidity of the molecule that correctly orients the adhesive region to participate in homotypic interaction with neighboring E-cadherin molecules, ultimately serving to connect the actin cytoskeletons of adjacent cells.

Gap junctions allow for intercellular communication between epithelial cells and are also located at the lateral domain of the plasma membrane of epithelial cells. They are formed by the connexins, a family of channel forming proteins that directly connect the cytoplasms of neighboring cells. These channels allow inorganic ions, glucose, amino acids, nucleotides, and intracellular mediators to pass through mediating communication between not only adjacent cells, but throughout the epithelial sheet.

The basolateral domain is oriented away from the lumen of the tubule and functions to take up metabolic waste into the epithelial cell for transport to the luminal filtrate, where it can ultimately be excreted in the urine. These specialized basolateral membranes are also responsible for transporting ions and substrates, including glucose, from the lumen back to the interstitial fluid. The apical membrane localizes the polarity complexes, Par and Crumbs. The apical membrane is composed of a dense covering of microvilli (also called the brush border) which serve to increase the surface area of this membrane which in turn aids in absorption capabilities from the luminal filtrate into the proximal tubule.

Epithelial-Mesenchymal Transition

EMT is a process where epithelial cells lose cell-cell adhesion, apical basolateral

cell polarity, and gain migratory capabilities ultimately becoming mesenchymal cells. This process is essential for development and wound healing, and dysregulation of EMT can be pathogenic resulting in organ fibrosis or the initiation of metastasis in cancer progression. Mesenchymal-epithelial transition (MET), the reverse process of EMT, also occurs during development.

There are three types of EMT that occur during development, wound healing (or fibrosis), and cancer metastasis. Developmental EMT (Type I) occurs during gastrulation, neural crest cell migration, and organ development. EMT occurs in order to generate mesenchymal cells to form secondary epithelia through MET. Wound healing (Type II) EMT serves to generate fibroblasts following tissue injury. Unfortunately, failure to regain homeostasis by MET of fibroblasts or to attenuate inflammatory mediators leads to organ fibrosis. This is particularly problematic for the kidney, liver, lungs, and intestines as they are more susceptible to fibrotic injury than other tissues. Cancer metastasis (Type III) is the EMT process in which neoplastic cells gain migratory capabilities and are able to leave the primary epithelial tumor site by degrading the extracellular matrix, invading through the basement membrane, intravasating the endothelium to circulate. These cells will extravasate the blood vessel at a favorable site and undergo MET to form a secondary tumor in a different organ.

The steps in the progression of EMT are well characterized. Disassembly of lateral intercellular junctions is one of the earliest steps in EMT, followed by the dissociation of proteins critical for lateral actin anchorage and epithelial cell polarity. Changes in gene expression result in the transcriptional induction of pro-mesenchymal genes and the down-regulation of pro-epithelial gene expression. Finally, actin

reorganization results in the formation of stress fibers attaching the ECM, MMP mediated ECM degradation, and the acquisition of migratory capabilities.

Dissociation of tight junctions, the lateral junctions in closest proximity to the apical surface that seal cells from one another, is one of the earliest steps in EMT. This results in the redistribution of molecules critical for cytoskeletal organization and disrupts the cell polarity complex.

Next the adherens junctions (and desmosomes), intercellular anchoring junctions, are disassembled. E-cadherin is the main structural/scaffolding component of the adherens junction. Disruption of these specialized cell-cell complexes leads to redistribution of these mediators in the cell and no longer anchors adjacent cells to one another. Following the loss of junctional complexes and the down-regulation of E-cadherin, sequestered β-catenin, a key EMT mediator is freed. Under normal physiological circumstances β-catenin is phosphorylated by GSK3β, targeting it for ubiquitination and proteasomal degradation. During EMT, β-catenin escapes phosphorylation, accumulates in the cytosol, ultimately enabling the molecule to translocate the nucleus. Importantly, this translocation event is the convergence of several known EMT inducers and may be the most critical step for the induction of full EMT.

This nuclear translocation event results in β-catenin binding to the TCF/LEF complex, and the promotion of a mesenchymal phenotype. There is a shift in transcription of epithelial markers to mesenchymal markers, controlled by Snail 1/2, Zeb 1/2, Twist-1 and multiple bHLH family of transcription factors. These function to repress E-cadherin and promote N-cadherin expression. Additionally, vimentin, α-

smooth muscle actin, and matrix metalloproteinases (MMPs) are increased. The actin cytoskeleton is disrupted contributing to the loss apical-basolateral polarity and gain of front-back polarity. This reorganization promotes migratory capabilities of cells, further increased MMP production and activation-mediated degradation of the matrix facilitates migration. Transforming growth factor-beta is a potent EMT inducer that acts by binding to heteromeric TGFβ receptor type I/II complexes at the plasma membrane, initiating a signaling cascade involving SMAD 2/3 phosphorylation, colocalization of the phospho-SMAD 2/3 complex with SMAD 4, and nuclear translocation of the complex (Y. Liu, 2009). Nuclear translocation of the complex activates the expression of several target genes that promote a mesenchymal phenotype.

General markers of EMT are well defined; however none appear to be unique to the specific type of EMT. Clinical studies have demonstrated the upregulation of mesenchymal markers in tubular epithelial cells in several progressive kidney disorders, including vimentin, α-smooth muscle actin and FSP1.

Cadmium is Nephrotoxic

Cadmium is a toxic metal ion and is considered an environmental pollutant and has no known physiological function in humans. Cadmium is ranked eighth in the Top 20 Hazardous Substances Priority List (ATSDR, 2012) and is classified as a human carcinogen (IARC, 1993). Cadmium is a naturally occurring element, and is found in the Earth's crust in mineral rich deposits. Naturally occurring events including: soil erosion, rock abrasion, and volcanic eruptions release cadmium into the environment (ATSDR 2012). Additionally, cadmium dust is released during forest fires.

Human exposure to cadmium occurs mainly through the gastrointestinal and respiratory systems. Crops grown in contaminated soil are the largest contributors to gastrointestinal exposure, and smoking leads to the highest respiratory exposure to cadmium. Plants that contain the largest concentrations of cadmium include lettuce, spinach, potatoes, peanuts soybeans, and sunflower seeds (ATSDR 2012). Additional dietary sources of cadmium exposure include shellfish and the livers or kidneys of animals that have ingested cadmium (ATSDR 2012, Satarug 2004). Individuals are also occupationally exposed in industrial settings such as zinc and iron refineries, welding of cadmium coated steel, formulation of cadmium pigments, and production nickel-cadmium batteries or cadmium (NTP, 2011).

Cadmium was first identified in 1817 by Stomeyer as a byproduct of zinc refining. It was not appreciated to have detrimental health consequences until the late 1950's when an outbreak of Itai-Itai disease occurred in the region of the Jinzu River basin, a cadmium-polluted region, in Japan. Zinc mining in this region released significant quantities of cadmium into the Jinzu River, killing nearly all the fish. This river was the irrigation source for nearby rice paddies, and the main source of drinking water. In 1968 Itai-Itai was officially recognized to be caused by cadmium exposure when epidemiological evidence demonstrated that cadmium was the only source that could explain the restricted development of the disease in this area of Japan. The toxicity is exerted on the kidneys where tubular and glomerular injury results in renal dysfunction; gout also occurs as a side effect of kidney dysfunction. Additionally, the bones are damaged due to osteomalacia and osteoporosis.

Cadmium is toxic to several tissues, and the pathological consequences of cadmium are dependent upon the dose and duration of exposure (ATSDR 2012, Liu 2007a,b). Acute cadmium poising primarily targets the liver, with cadmium hepatotoxicity as the major cause of lethality from an acute exposure (Goering 1983, Klassen 1999).The main target organ of chronic exposure to cadmium is the kidney. Cadmium impairs tubular and glomerular function, and accumulates in the proximal tubule. Cadmium is a cumulative toxin with a recommended daily limit of intake in humans of 0.3 ug/kg (Choudry 2001). When levels of cadmium accumulation have reached 150-200 µg cadmium/g tissue in the proximal tubule, dysfunction begins to occur. Deficiencies in glomerular filtration rate (GFR), and impaired reabsorption of various solutes including low molecular weight proteins, glucose, amino acids, phosphate and sodium characterized by proteinuria, glucosuria aminoaciduria, phosphaturia and hyperosmolar polyuria are reliable indications of proximal tubule damage The long biological half-life of cadmium, ranging from 15-30 years (ATSDR 2012), is most likely due to the fact that cadmium is non-biodegradable and relatively redox inert. Information on the biotransformation of cadmium is limited, with literature support for cadmium conjugation to sulfhydryl groups of proteins including MT and glutathione. Most of the cadmium that is absorbed will ultimately be stored in the kidney, and to a lesser extent in the liver for several years with only a small percentage eliminated through excretion in the urine and bile respectively.

While the toxic effects of cadmium are well characterized, the molecular mechanisms of toxicity remain to be fully characterized. Several investigations designed to elucidate its cytoxic effects have revealed cadmium to alter a variety of cellular

functions including alteration in the activity of several enzymes, interference with essential metal ion activities, induction of oxidative stress and apoptosis, inhibition of mitochondrial ATP production, and alterations in gene expression.

As cadmium is a nonessential ion, there are no known ion transporters specific for cadmium. Multivalent cations have relatively small atomic radii, so toxic metal ions such as cadmium appear to gain entry through molecular mimicry of calcium, zinc, iron and magnesium. Cadmium uses molecular mimicry not only to gain entry to the cell, but also to exit the lysosome to return to the cytosol and to enter the mitochondria (Bridges & Zalups, 2005). Cadmium is absorbed from the gastrointestinal tract after ingestion by binding to the divalent metal ion transporter-1 (DMT1 or SLC11A2) in the duodenum. As the name suggests, this transporter carries several other metal ions including iron and zinc (Mn > Cd > Fe > Pb > Zn). Individuals deficient in essential metals such as iron are susceptible to increased cadmium transport into cells due to increased expression of divalent metal ion transporter 1 (Vesey, 2010). Once in the plasma, cadmium binds to albumin and is transported into the liver. Within the liver, cadmium induces metallothioneins, to which it binds with high affinity (Sabolić, Breljak, Skarica, & Herak-Kramberger, 2010). Cadmium binding to glutathione allows for excretion through the bile, while cadmium-metallothionein complexes are transported back into the plasma following necrosis or natural turnover of hepatic cells. Free filtration of these complexes in the glomerulus allows for the subsequent reabsorption of the cadmium-metallothionein complex from the lumen of the proximal tubule at the apical face of the epithelium (Tang, Sadovic, & Shaikh, 1998). This occurs by endocytosis mediated by the megalin receptor. Once in the proximal tubule, stable cadmium –metallothionein complexes are

degraded by the lysosome (Vesey, 2010). Due to the acidic environment of the lysosome, cadmium is displaced from metallothionein, and gains entry back into the cytosol to exert detrimental effects or be sequestered by metallothioneins. Additionally, divalent metal ion transporter 1 is also present on proximal tubule cells, and may be the transporter responsible for free cadmium export from endosomes and lysosomes that have internalized cadmium-metallothionein complexes. Cadmium is also capable of entering the mitochondria where it targets complex III of the electron transport chain impairing ATP generation, lowering the energy status and capabilities of the cell (Gobe & Crane, 2010). The proximal tubule is mitochondria rich in order to maintain the high ATP required for transport. This results in lower capabilities to "rescue" useful substances from the lumen of the proximal tubule. If cadmium concentrations remain high, the mitochondrial disruption generates increasing levels of reactive oxygen species (ROS) with release of cytochrome c, inducing the caspase cascade and subsequent apoptosis. In addition to divalent metal ion transporter 1 and megalin, ZIP8 (SLC39A8), and ZIP14 (SLC39A14) have been identified as transporters capable of allowing cadmium entry into the cell.

Cadmium has also been demonstrated to disrupt adherens junctions in the proximal tubule (W C Prozialeck, 2000; W. Prozialeck, Lamar, & Appelt, 2004; Walter C Prozialeck, Lamar, & Lynch, 2003) by selectively disrupting E-cadherin-dependent intercellular junctions by interfering with calcium binding. Cadmium also disrupts tight junctions by altering the distribution of claudins 2 and 5 (Walter C Prozialeck et al., 2003).

Metallothioneins

The metallothioneins (MT) are a family of cysteine-rich metal binding antioxidant proteins consisting of four functional protein isoforms, MT-1, MT-2, MT-3, and MT-4. These proteins range from 61 to 68 amino acids with highly conserved primary and secondary structure. The investigation and discovery of metallothioneins was initially closely associated with the search for tissues containing cadmium by Valee and Margoshes (Vallee, 1979). The first study to report the presence of cadmium in the human kidney was initially published by Maliuga in 1941, however this report was not available to western scientists until the mid-1950s. This finding led to the identification of cadmium in the kidneys of other mammalian species, and the initial identification of a protein containing cadmium, as well as substantial levels of zinc and iron, fractionated and purified from the kidney cortex of a horse. Chromatographic separation revealed the presence of the two isoforms, MT-1 and MT-2 (19), with a low molecular weight of 6-7 kDa, high sulfur and metal content. Further protein sequencing revealed that of the 61 amino acids composing the single polypeptide chain, 20 residues were cysteines with distinct clustering into Cys-X-Cys, Cys-Cys, and Cys-X-X-Cys (Piscator, 1964). Subsequent toxicological studies involving cadmium administration to small animal models identified increased amounts of MT in the liver. This led to the initial hypothesis that biosynthesis of MT is induced by cadmium for metal detoxification (Piscator, 1964). Later studies found dietary administration of copper and zinc also capable of MT induction in the liver and kidneys of small animal models (Nordberg & Kojima, 1979). Several studies by Valee and others determined the kidney to be the primary site of

cadmium accumulation and toxicity in chronic exposure models, typically in a complex with metallothionein.

Due to the observation that cadmium-metallothionein complexes accumulate in the proximal tubule and exert toxicity in chronic exposure models, it was a long held paradigm that metallothionein was detrimental in the context of cadmium exposed animal models. This paradigm shifted when mice administered cadmium-metallothionein complexes displayed less toxicity than those administered cadmium alone. Further, metallothionein null mice (incapable of producing metallothionein) chronically exposed to cadmium display enhanced sensitivity to cadmium induced nephropathy (J. Liu, Liu, Habeebu, & Klaassen, 1998). It is now generally accepted that metallothioneins are protective against cadmium toxicity.

Metallothioneins readily bind metal cations, and under normal physiological conditions bind preferentially to copper and zinc. There are two distinct metal binding domains in each isoform, the β-domain near the N-terminal region, and the α-domain near the C-terminal region (Vašák & Meloni, 2011). Typically the β-domain binds three-divalent cations, while the α-domain binds four-divalent cations, forming two distinct metal thiolate clusters. Metal bound MTs are more stable than apo-MT (metal free) and are less susceptible to lysosomal degradation. In fact, molecular mechanic-molecular dynamic calculations of apo-MT indicate no structural stability and is predicted to form a random coil conformation (Rigby Duncan & Stillman, 2006). Using a combination of circular dichroism and NMR to evaluate the metal composition of metallothionein, determined that the preferential state contains seven divalent metal ions per one metallothionein molecule (Meloni, Polanski, Braun, & Vasák, 2009), with metal status

ranges from 5-10 divalent metal ions per molecule of metallothionein (Sutherland & Stillman, 2011).

MT-1and MT-2 are ubiquitously expressed at high levels. These isoforms are readily inducible in response to perturbations in cellular homeostasis and are particularly responsive to metal induction in animal models following dietary administration of cadmium copper or zinc. The promoter regions of these genes contain metal response elements (MRE) that induce gene expression when cellular levels of essential or toxic metals are increased. These isoforms are also responsive to hypoxia, oxidative stress, steroids, and hormones. MT-3 and MT-4 exhibit more restricted tissue specific expression, with the highest distributions classically recognized to localized to the CNS and stratified epithelium respectively.

Metallothionein isoform 3

For more than a decade this laboratory has rigorously investigated tissue distribution of MT-3 and the role this isoform may play in cellular homeostasis and disease(S H Garrett, Somji, Todd, & Sens, 1998; Scott H Garrett et al., 2002; S Somji, Garrett, Sens, & Sens, 2006; Seema Somji et al., 2011; Todd et al., 1996). MT-3 was first identified by Uchida and colleagues in 1991 in cortical neurons and to a lesser extent in a distinct population of astrocytes in the gray matter. MT-3 inhibited survival and neurite formation of cortical neurons *in vitro*, and was found to be down regulated in astrocytes from brains affected by Alzheimer's Disease (Uchida, Takio, Titani, Ihara, & Tomonaga, 1991). MT-3 exhibits tissue-specific expression differentiating this isoform from the ubiquitously expressed MT-1 and -2. The distribution of MT-3 is not restricted to central nervous system as the classical view suggests; components of normal skin and

kidney express MT-3 (Scott H. Garrett, Sens, Todd, Somji, & Sens, 1999; Slusser et al., 2014). Additionally, MT-3 is expressed in several types of cancer including breast, bladder, prostate, and skin (Satarug, Garrett, Sens, & Sens, 2010; M. A. Sens et al., 2000; Zhou et al., 2006).

The first unique function, growth inhibitory activity, can be attributed to the β-domain of MT-3, with one study attributing this activity to the proline insert (Sewell, Jensen, & Erickson, 1995) and another to E23 (Z. Ding, Teng, Cai, & Wang, 2006). MT-3 also influences the mechanism of cell death a stressed cell undergoes (apoptosis or necrosis) and that the β-domain influences this activity (Seema Somji, Garrett, Sens, Gurel, & Sens, 2004; Seema Somji, Garrett, Sens, & Sens, 2006). MT-3 can also participate in thiol-disulfide exchange reactions with other cysteine-containing proteins when the β-domain is bound to four-copper ions leaving two cysteine residues free to participate in thiol/disulfide exchange (Ghazi, Martin, & Armitage, 2010; Meloni, Faller, & Vasák, 2007).

The deviations in the primary sequence of MT-3 from the other isoforms are thought to be responsible for unique functions of MT-3. There is an additional threonine in the N-terminal domain, an alanine to proline substitution in the β-domain, and a six amino acid insert in the C-terminal domain. This proline induces a kink in the structure of MT-3 and the six amino acid insert consists of acidic amino acids. These differences manifest structurally and influence the interactions of MT-3 with other proteins.

Metallothionein-3 Protein-Protein Interactions

The existing literature describing protein interactions with MT-3 have been limited to investigations within the CNS (Durand, Meloni, Talmard, Vašák, & Faller,

2010; Meloni & Vašák, 2009). This is not entirely surprising due to the classical view that tissue distribution of MT-3 is restricted to neurons and astrocytes. However, in 1999 Garret and Sens demonstrated that MT-3 is expressed in several epithelial components of the nephron using immunohistochemistry. The highest levels of MT-3 were observed in several components of the renal cortex; moderate staining was observed in components of the glomerulus, including parietal epithelial cells of Bowman's capsule and visceral epithelial cells of the glomerular tuft, moderate staining was observed in epithelial cells of the proximal tubule, and strong cytoplasmic staining in the distal tubule. MT-3 staining was more variable in components of the medulla; staining was weak to moderate in the medullary collecting ducts and absent in the ascending and descending loops of Henle, and transitional epithelium of the renal pelvis (Scott H. Garrett et al., 1999)

The context for studying proteins interacting with MT-3 in the CNS arises from the observation by Uchida in the late 1980s that extracts from Alzheimer's Disease affected brains enhanced the survival of cerebral cortical neurons when compared to normal brain extracts (Uchida 1988). Subsequent comparative analysis of the diseased brain extracts to normal brain extracts attributed this feature to a protein they termed growth inhibitory factor (GIF); it was hypothesized that GIF was involved in the formation of senile plaques and enhanced sprouting (Uchida 1989). However, follow-up studies indicated a correlation to reduced GIF activity and the presence of neurofibrillary tangles, not senile plagues (Uchida 1991). Additionally, GIF was identified to be a metallothionein, the third isoform identified. Since this initial characterization, several laboratories studying AD have sought to characterize the mechanism by which MT-3 contributes to the pathogenesis of AD by investigating protein-protein interactions and

MT-3-mediated metal swap events. Several protein-protein interactions have been identified (Table 1).

The fact that protein interactions with MT-3 are studied in the context of AD where the pathological state is characterized by neurofibrillary tangles (Tau tangles) and senile plagues (Aβ plagues) may provide some insight for studying interacting proteins with MT-3 in the context of CKD. When viewed in simplistic terms, tangles and plagues are an accumulation of dysregulated protein aggregates that contribute to the pathology of AD; the accumulation of dysregulated protein aggregates is a pathological hallmark of fibrosis observed in CKD.

Table I-1. MT-3 interacting proteins

Interacting Protein	Generalized Function	Reference	Tissue
Transthyretin	Thyroxine Transport	Martinho et.al 2010	CNS
Rab3A GTPase	Exocytosis	Kang, Chen, Ren, & Ru, 2001	CNS
Hsp90	Secretion/Stress	Lahti et al. 2005	CNS
Hsp70	Secretion/Stress	Lahti et al. 2005	CNS
Drp2	Neuronal growth	Lahti et al. 2005	CNS
Creatine Kinase	Glycolysis	Lahti et al. 2005	CNS
B-actin	Structure/Scaffolding	Lahti et al. 2005	CNS
Exo84	Exocytosis	Ghazi, Martin, & Armitage, 2011	CNS
14-3-3	Protein signaling	Ghazi, Martin, & Armitage, 2011	CNS
Enolase-1	Glycolysis	Ghazi, Martin, & Armitage, 2011	CNS
Aldolase 1 and 3	Glycolysis	Ghazi, Martin, & Armitage, 2011	CNS
Pyruvate Kinase	Glycolysis	Ghazi, Martin, & Armitage, 2011	CNS
Malate Dehydrogenase	Glycolysis	Ghazi, Martin, & Armitage, 2011	CNS
Tubulin α3	Scaffolding	Ghazi, Martin, & Armitage, 2011	CNS
Gelsolin	Structure/Filament	Bathula, 2010	Kidney
Myosin-9	Cytoskeleton	Bathula, 2010	Kidney
B-actin	Structure/Scaffolding	Bathula, 2010	Kidney
Tropomyosin 3	Cytoskeleton	Bathula, 2010	Kidney

CHAPTER II

METHODS

Immunohistochemistry

Tissue sections for the immunohistochemical analysis of E- and N-cadherin expression in human kidney were obtained from archival paraffin blocks of previously completed patient diagnostic procedures. These archival specimens contained no patient identifiers and use was approved by the University of North Dakota Internal Review Board. Three cases from renal cell carcinomas were utilized in the present analysis and areas of normal kidney were selected for use by a diagnostic pathologist. These archival specimens were routinely fixed in 10% neutral-buffered formalin for 16-18 h and were transferred to 70% ethanol and subsequently dehydrated in 100% ethanol. The dehydrated tissues were cleared in xylene, infiltrated, and embedded in paraffin. Serial sections of formalin fixed and paraffin embedded tissues were cut at 5 μm, deparaffinized in xylene and rehydrated in graded ethanol and water. Prior to immunostaining, antigen retrieval was performed by immersing the sections in Dako Target Retrieval Solution (Code S1699) and heated in a steamer for 20 minutes. The sections were allowed to cool at room temperature for 30 minutes and immersed in TBST (Tris-buffered saline with 0.1% Tween 20) for 10 minutes. The E and N-cadherin were detected by incubating the sections with anti-E cadherin (Santa Cruz; 1:100) and anti-N cadherin (Zymed; 1:100) for 30 minutes at room temperature. The identities of the tubular elements chosen for

subsequent microdissection were identified by the differential immunostaining sections for aquaporin-1 and calbindin (Bedford, Leader, & Walker, 2003; Kirk, Campbell, & Bass, 2010; Kiuchi-Saishin & Gotoh, 2002). Aquaporin-1 and calbindin were detected by incubating sections with anti-aquaporin (Ab9566, Abcam, Cambridge, MA, 1:400) and anti-calbindin (McAb 300, Swant, Switzerland, 1-800) for 30 minutes at room temperature. The sections were then incubated with Dako Envision+ Dual Link System (Code K4061) for 30 minutes at room temperature. Liquid diaminobenzidine (DAB) was used for visualization. After counterstaining with hematoxylin, the slides were rinsed in distilled water, dehydrated in graded ethanol, cleared in xylene, and coverslipped.

Laser-Capture Microdissection

The parafin-embedded specimens were also used to determine the expression of E- and N-cadherin mRNA in proximal tubule cells of human kidney. Five μm thick sections were cut and mounted onto sterile plain glass slides. The slides were heated at 60°C for 25 min followed by incubation in xylene solution for 5 min and transferred into fresh xylene solution for an additional 5 min to deparaffinize the sections. The slides were then washed with 100% ethanol for 30 sec followed by sequential incubation for 30 sec in 100% ethanol, 95% ethanol, and 70% ethanol. The slides were then washed for 30 sec with distilled water and stained with hematoxylin for 30 sec. The slides were washed with distilled water followed by sequential washes with 70% ethanol and 95% ethanol for 60 sec each. The sections were incubated in eosin solution for 30 sec, washed with 95% ethanol for 60 sec, and then with 100% ethanol for 60 sec. The slides were incubated in xylene for 5 min to ensure the dehydration of the sections and excess solution was drained by touching the corner of the slide to a particle-free paper tissue. The slides were

air-dried for 2 min to ensure the evaporation of xylene and were then used for laser capture microdissection. The PixCell II™ LCM system (Arcturus Engineering Inc., Mountain View, CA) was used and proximal tubules were identified by the diagnostic pathologist for microdissection. The microdissected samples were collected on the thermoplastic film of CapSure™ HS LCM caps (Arcturus Bioscience, Mountain View, CA). Total RNA was isolated following the protocol of RNAqueous® –Micro Kit (Life Technologies, Carlsbad CA). The thermoplastic film containing the captured proximal tubule cells was incubated with 100 µl of lysis solution for 30 min at 42°C. Then 3 µl of LCM additive was added to the lysate. The lysate was briefly centrifuged followed by the addition of 1.25 volume of 100% ethanol. The lysate was passed through a pre-wetted microfilter cartridge by centrifugation at 10,000 x g for 1 min. The filter was washed with 180 µl of wash solution and the flow- through was discarded followed by two additional washes with 180 µl of wash solution. The flow-through was discarded and the filter was centrifuged for 1 min to remove the residual fluid. The filter was transferred into a new sterile tube and incubated for 5 min with 10 µl of elution solution preheated to 95°C. The RNA was eluted by centrifugation at 13,000 x g for 1 min and used in real-time reverse transcription polymerase chain reaction (RT-PCR).

The measurement of N-cadherin and E-cadherin was assessed using real time RT-PCR and commercially available primers (Qiagen Company, Valencia, CA. Real time PCR was performed utilizing the SYBR Green kit (Bio-Rad Laboratories) with 2 µl of cDNA, 0.2 µM primers in a total volume of 20 µl in an iCycler iQ Real-Time Detection System (Bio-Rad Laboratories). Amplification was monitored by SYBR Green fluorescence. Cycling parameters consisted of denaturation at 95°C for 15 seconds,

annealing at 55°C for 30 seconds and extension at 72 °C for 30 seconds which gave optimal amplification efficiency of each cadherin isoform. The interpolated numbers of transcripts from three triplicates were divided by the number of 18S rRNA transcripts and averaged for the final reported value (± SE).

Cell Culture

Stock cultures of human proximal tubule cells (HPT) were grown using serum-free condition and collagen coated culture flasks as described previously (Detrisac et al., 1984;Kim et al., 2002). The growth formulation consisted of a 1:1 mixture of Dulbecco's modified Eagles' medium (DME) and Ham's F-12 growth medium supplemented with selenium (5 ng/ml), insulin (5 μg/ml), transferrin (5 μg/ml), hydrocortisone (36 ng/ml), triiodothyronine (4 pg/ml) and epidermal growth factor (10 ng/ml). The cells were fed fresh growth medium every 3 days and were subcultured 1:2 at confluence (normally 3-6 days post subculture) using trypsin-EDTA (0.05% - 0.02%). HK-2 cells were obtained from the American Type Culture Collection, expanded following recommended culture conditions, and aliquots stored under liquid nitrogen. For studies directly comparing properties with HPT cells, the HK-2 cells were cultured under identical growth conditions using the serum-free growth media and subculture conditions described above for the HPT cells. This growth condition was also used for the microarray determinations between HK-2 cells stably transfected with the MT-3 coding sequences and the blank vector control. To determine the effects of serum-free verses serum-contain growth medium on the morphology and expression patterns of the HK-2 cells, the HK-2 cells were grown to confluence on the serum-free medium as suggested by the original publication by Ryan and coworkers (Ryan et al., 1994). At confluence, the serum-free

growth media of the HK-2 cells was replaced by the new media formulations and 24 h later the cells were subcultured using the new media formulations. The cells were allowed to grow under these new conditions for a minimum of 2 passages before use in experimental protocols.

Transepithelial Resistance

Measurement of transepithelial resistance was performed. HK-2 or HPT cells were seeded at a 2:1 ratio in triplicate onto 24-mm-diameter cellulose ester membrane inserts (Corning) placed in six-well trays. Beginning on the third day postseeding, transepithelial resistance (TER) was measured every other day with the EVOM Epithelial Voltohmmeter (World Precision Instruments, Sarasota, FL) with a STX2 electrode set according to the manufactures instructions. The resistance of the bare filter containing medium was subtracted from that obtained from filters containing cell monolayers and multiplied by the surface area (available for growth) of the insert to obtain unit area resistance. Two sets of four readings were taken at two different locations on each filter. The development of the monolayer in parallel 12-well trays was monitored for dome formation. The experiment was repeated twice in triplicate and the final result reported as the mean ± SE.

RNA isolation and RT-qPCR

Total RNA was purified from cultures of HPT cells, human renal cortical tissue or HK-2 cells utilizing TRI Reagent (Molecular Research Center, Cincinnati OH). Gene expression was assessed with real time RT-PCR utilizing gene specific primers. Total RNA (100 ng) was subjected to cDNA synthesis using the iScript cDNA synthesis kit (Bio-Rad) in a total volume of 20 µl. Real-time PCR was performed utilizing SYBR

Green (Bio-Rad) technology with 2 µl of cDNA, 0.2 µM primers in a total volume of 20 µl in an CFX real-time detection system (Bio-Rad). Cycling parameters included a 5 minute hot start followed by 40 cycles of denaturation at 94 ºC (15 s), annealing at 55 ºC-62 °C (30 s), and extension at 72 ºC (30 s). Amplification was monitored by SYBR Green fluorescence and analyzed by interpolation from a standard curve consisting of serial dilutions of known quantities of template. Melt curve analysis confirmed the amplicon was the dominant double stranded species and denatured at the appropriate temperature.

Protein isolation

For EMT studies, HK-2 or HPT cells were lysed in RIPA buffer containing protease inhibitors, PMSF, and sodium orthovandate (Santa Cruz). The monolayer was washed twice with cold phosphate-buffered saline (PBS), scraped in a small volume of cold PBS on ice, rinsed, and pelleted at 4 °C. Pelleted cells were resuspended in an additional volume of PBS and split in to 2-cold microfuge tubes (for parallel RNA analysis), and pelleted. Pellets were either stored at -80 °C or resuspended in cold complete RIPA at a 1:2 w/v ratio (for every 5 mg of cell pellet, 10 uL lysis buffer) and incubated on ice with orbital shaking for 30 minutes. The extracts were then sonicated, placed on ice, and centrifuged at 10,000*g* for 10 minutes at 4°C. Supernatants were transferred to fresh, cold microfuge tubes and either stored at -80 °C or quantified by BCA assay (Thermo-Scientific).

For analysis of protein-protein interactions, HK-2 or HK-2(MT-3-V5) were lysed in a more gentle lysis buffer in the attempt to limit dissociation of protein complexes. Cell monolayers were rinsed on ice with cold PBS twice prior to the addition of 100 uL of cold IP lysis buffer (25 mM Tris-HCl, 150 mM NaCl, 1% NP-40, 5% glycerol, pH

7.4) containing EDTA-free protease inhibitors (Sigma) directly to the monolayer. Plates were incubated on ice for 30 minutes with orbital shaking, and extracts were transferred to cold microfuge tubes and centrifuged at 10,000*g* for 10 minutes to pellet debris. Lysates were transferred to fresh, cold microfuge tubes and quantified by BCA assay. Lysates were used immediately, or stored at -80 °C.

Western Blotting

For western blotting, protein lysates were prepared in equivalent volumes to contain 20 μg of total protein and mixed with Laemmli Buffer (Bio-Rad) containing either TCEP or β-mercaptoethanol, and boiled for 5 minutes at 95 °C to reduce and linearize protein. After cooling, samples were loaded onto 4-20% gradient gels (Bio-Rad), and separated by SDS-PAGE. Proteins were transferred to 0.2 μm PVDF membranes using the Trans-blot Turbo transfer apparatus (Bio-Rad). Following transfer, the membranes were blocked with 5% non-fat milk or bovine serum albumin (BSA) dissolved in 10 mM Tris-buffered saline, 0.1% Tween-20 (TBS-T) for 90 minutes at room temperature. The membranes were incubated with primary antibodies against (human) proteins of interest at dilutions indicated in Table II-1 overnight (16 h) at 4 °C with orbital shaking. Membranes were washed with TBS-T, and incubated with horseradish peroxidase conjugated secondary antibodies against the species the primary antibodies were raised in for 1 h at room temperature with orbital shaking. Anti-rabbit and anti-mouse antibodies were diluted 1:3000 (Cell Signaling), and the anti-goat antibody was diluted 1:1000. Proteins of interest were visualized by chemiluminescent HRP detection (Bio-Rad). Primary and secondary antibodies were diluted in the same buffer used for blocking.

Table II-1. Primary antibodies used for western blotting.						
Antibody	**Dilution**	**Source & Clonality**	**Storage (°C)**	**Company**	**Catalog #**	**Mw (kDa)**
β-actin	(BSA) 1:1000	Mouse monoclonal	-20	Abcam	Ab8226	42
Gelsolin	1:500-1:1000	Mouse monoclonal	-20	Abcam	Ab11081	86
Tropomyosin III	1:1000	Mouse monoclonal	4	Santa-Cruz	Sc12059	29-32
Myosin IIa	1:500	Goat polyclonal	4	Abcam	Ab55456	215
α-enolase	1:3000	Rabbit polyclonal	-20	Abcam	Ab56795	47-51
α-aldolase	1:500	Goat polyclonal	4	Santa-Cruz	Sc12059	40
V5	1:5000	Mouse monoclonal	4	Invitrogen	Ab9116	10-12
E-cadherin	1:500	Rabbit polyclonal	4	Santa-Cruz	Sc	120
N-cadherin	1:1000	Mouse monoclonal	-20	Life Technologies	333900	100
Connexin 32	1:1000	Rabbit polyclonal	-20	Life Technologies		32

ELISA

A sandwich ELISA method was used to quantify the expression of E- and N-cadherin by the cultured cell lines. Both ELISA materials were obtained from Abnova (E-cadherin (#KA0433) and N-cadherin (Abnova, #KA1135). Plates were pre-coated with capture antibodies against either human E-or N-cadherin. Following initial titration to determine the appropriate net amount of protein to load per well, a range of 1-25 ug of total protein (100 μL/well) was used for analysis. The plate was covered and incubated at 37 °C for 90 minutes (E-cadherin) or 2 hours (N-cadherin). The plate contents were discarded and incubated with 100 μL of biotinylated polyclonal antibody against either E- or N-cadherin diluted (1:100) in antibody dilution buffer for 1 hour at 37 °C. The contents of the plate were discarded and each well was washed three times with 10 mM TBS. The plate was incubated with pre-warmed avidin-biotin-peroxidase complex (ABC) prepared 1:100 with ABC-dilution buffer at 37 °C for 30 minutes. The contents were discarded and the plate was washed 5 times. The plate was then incubated with 90 μL of pre-warmed 3, 3′, 5, 5′ tetramethylbenzidine (TMB) substrate solution for 15 minutes at 37°C. Finally, the reaction was quenched by the addition of acidic TMB stop solution halting the colorimetric development. The plate was then analyzed by reading the absorbance of each well on a Biotek plate reader at 450 nm. The data was analyzed via MasterPlex software using 5 parameter logistics to determine the amount of E- or N-cadherin present in each well.

Statistical Analysis

All experiments were performed in triplicate and the results are expressed as the standard error of the mean. Statistical analyses were performed using GraphPad Prism®

software using separate variance t-tests, ANOVA with Tukey post-hoc testing. Unless otherwise stated, the level of significance was 0.05.

Stable Transfections

The HK-2 cells were transfected with wild type MT-3, MT-3 where the unique N-terminal region was altered, and MT-3 where the unique C-terminal sequence was removed from MT-3 (Fig 1). The HK-2 cells were also transfected with MT-1E, MT-1E where the unique C-terminal sequence of MT-3 was added to the corresponding region of MT-1E, and MT-1E in which the sequence of the N-terminal domain was changed to the MT-3 sequence consensus (Fig 1). The Gateway™ cloning system (Invitrogen, Carlsbad, CA) was used for the production MT-3 site-directed mutants. The MT-3 and MT-E coding sequences were cloned into the pENTR vector and site-directed mutagenesis was performed by GeneScript (Piscataway, NJ). The EAEAAE sequence was deleted from the C-terminal domain of MT-3 and this same sequence was inserted in the analogous position of MT-1E, producing the MT-3ΔCT and 1E-CT constructs respectively. The N-terminal sequence of MT-1E (MDPNCSCA) was converted to an MT-3-like sequence (MDPNTCPCP) for the 1E-NT construct. For the mutagenesis of this N-terminal sequence, the last two prolines in the above sequence were converted to threonine for the MT-3-NT mutant. The threonine insert and prolines 7 and 9 of MT-3 were found to be necessary and sufficient to confer growth inhibitory activity and the substitution of the prolines to threonine is sufficient to eliminate this activity (Romero-Isart, Jensen, & Zerbe, 2002). Each metallothionein sequence within the pENTER vector was moved to the pcDNA6.2/V5-DEST destination vector using the Gateway™ LR recombination

reaction. The stop codon was removed from each construct allowing for the translation of the V5 tag on the C-terminus for alternative protein detection.

The HK-2 cells were transfected with the E-cadherin coding sequence using the E-cadherin ORF cloned in pENTR™ 221 vector and was obtained from Invitrogen (Invitrogen, Carlsbad, CA). The E-cadherin gene was transferred into pcDNA™6.2/V5-DEST vector by LR recombination reaction (Invitrogen, Carlsbad,CA). The DNA constructs were linearized with *BspH* I and E-CDH ORF was linearized with *Bcg* I (New England BioLabs, Ipswich, MA) before transfection. The HK-2 cells were transfected using the Effectene™ transfection reagent (Qiagen, Valencia, CA) following the manufacturer's protocol at a ratio of 1:10 plasmid to Effectene ratio, and the lipid complexes were added to the cells at 2 μg of DNA per 9.6 cm^2 well of a 6-well culture plate. For antibiotic selection, transfected cells were seeded 1:10 and clones were selected in 3 μg/ml blasticidin and clones were isolated with cloning rings and propagated in culture medium containing 3 μg/ml blasticidin.

Transient Transfections

HK-2 cells were transiently transfected with 2 μg supercoiled V5-tagged MT-3 DNA construct (described above) using electroporation (Lonza). Subconfluent cell cultures in the log phase of growth were trypsinized from T-75 flasks, pelleted, and resuspended in 100 uL of room temperature Nucleofector Solution V (Lonza). Diluted DNA was added and mixed gently before transferring the reaction to the supplied cuvette. Electroporation program V was ran, and the entire contents of the cuvette were transferred to 1-well of a 6-well plate containing 2 mL of 20/12. Cells were allowed 6 hours to take up the construct and to attach to the tissue culture treated matrix before the

addition of 20/12 supplemented with 30 μM zinc. Cells were harvested 24 hours following transfection.

Co-mmunoprecipitation

For co-immunoprecipitation of immune complexes, 1000 μg of HK-2 or HK-2 (MT-3-V5) lysate was first pre-cleared by incubation with 50 μL of Protein A/G magnetic beads (Thermo-Scientific) and rabbit IgG (to eliminate most of the non-specific protein interactions) for 30 minutes at 4°C with gentle end-over-end mixing (10 RPM). The beads were pelleted with a magnet, and the lysates were transferred to a fresh, cold microfuge tube. Next, 20 μg of the anti-V5 antibody (rabbit monoclonal, Abcam #Ab9116) was added to the tube and the total volume was adjusted to 500 μL. The samples were incubated overnight at 4°C with gentle end-over-end mixing (10 RPM) to allow immune complex formation. The following day, 50 μL of Protein A/G magnetic beads were prepared by first adding 175 uL of IP lysis buffer (described above), mixing, and removal. An additional 1 mL of IP lysis buffer was added, mixed and removed. Immediately following the final bead wash, the immune complexes were transferred to the tubes containing the prepared beads, and incubated at room temperature with gentle end-over-end mixing for 75 minutes to allow the beads to capture the immune complexes. The beads were collected, and the supernatant was removed. The beads were washed 3 times with 500 μL of 25 mM Tris-HCl, 150 mM NaCl, 0.05% Tween-20 (pH 7.4), followed by a final wash with 18Ω H_2O. Bound proteins were eluted from the antibody bound beads through incubation with Laemmli Buffer containing no reducing agent, with mixing at room temperature for 10 minutes. Heat causes Protein A/G to come off the magnetic beads, and reducing agent dissociate the heavy and light chains of the antibody. Controls included were: beads + V5 antibody+ IP lysis buffer (no lysate control); HK-2 (MT-3-V5 lysate) + beads (no antibody control); HK-2 lysate + V5 antibody + beads (no bait control) and were processed in an analogous manner simultaneously.

CHAPTER III

RESULTS

Expression of E- and N-Cadherin in Human Kidney Proximal Tubules

To confirm the expression of E-cadherin in the proximal tubule, serial sections were prepared from three independent specimens of human kidney in order to compare routine H&E histology with expression of E- and N-cadherin. In proximal tubules, staining for E-cadherin was moderate in intensity for all three specimens with staining concentrated on the luminal or apical borders of the cells (Figure III-1 A, B; D, E; G, H). In distal tubules, staining for E-cadherin was usually stronger than that observed for proximal tubules and staining was present around the entire epithelial cell (Fig III-1 A, C; D, F; G, I). In proximal tubules, staining for N-cadherin was also moderate in intensity and often localized to the basolateral side of the tubules (Figure III-1 A, C; D, F; G, I). Distal tubules were negative for the expression of N-cadherin (Figure III-1 A, C; D, F; G, I). The glomeruli were negative for the expression of N-cadherin and negative to very weakly positive for the expression of E-cadherin.

Microdissection was utilized to determine the expression of E- and N-cadherin mRNA in proximal tubules isolated from tissue sections obtained from the three archival specimens of human kidney. Serial sections were stained for calbindin and aquaporin to identify that proximal tubules were selectively chosen for microdissection (Figure III-2A,B

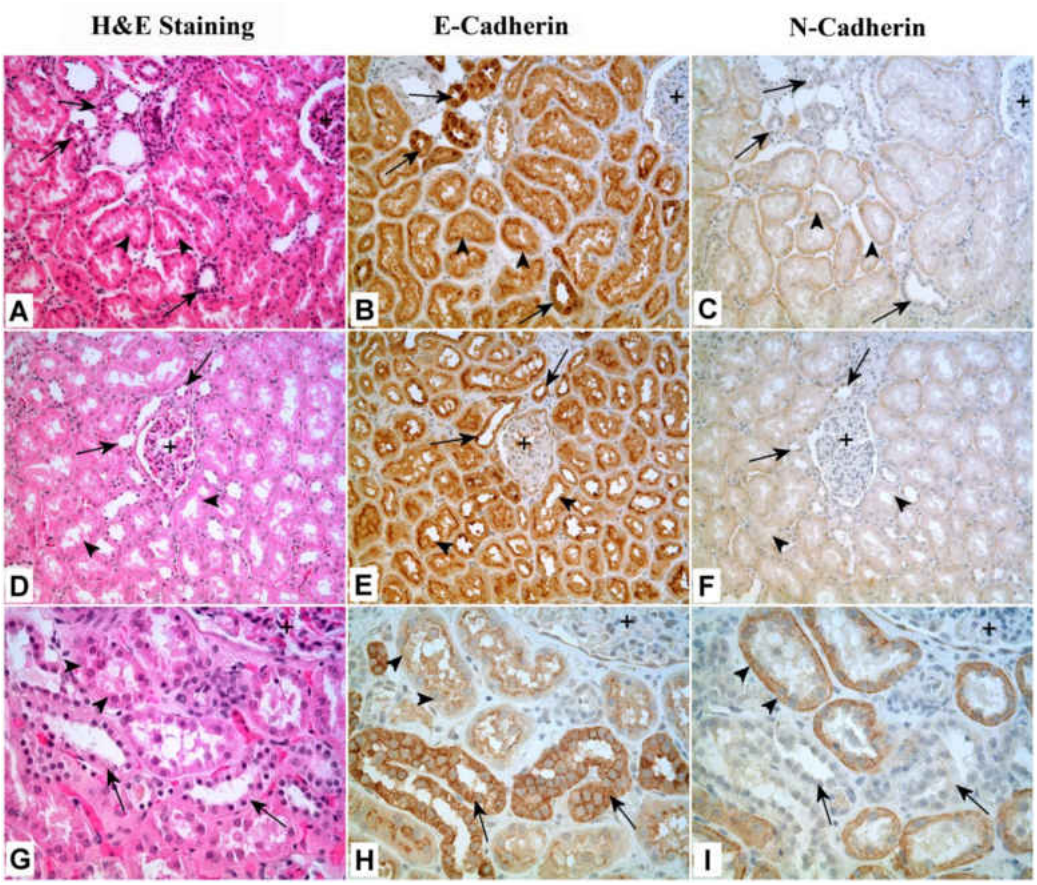

Figure III-1. Immunohistochemical staining of E- and N-Cadherin in human kidney.A-C: The majority of the tubules in the image are proximal tubules (A, arrow heads). These tubules are moderately positive for E-cadherin with stronger staining on the luminal border (B, arrow heads). Proximal tubules are also moderately positive for N-cadherin (C, arrowheads). A few of distal tubules are strongly positive for E-cadherin (B, arrows), but negative for N-cadherin (C, arrows). On the upper right corner is a part of glomerulus (A, +), which shows very weak staining of E-cadherin and no staining of N-cadherin (B, C, +). 200X **D-F:** In the center of the image is a glomerulus (D, +), which is very weakly positive for E-cadherin (E, +) but negative for N-cadherin (F, +). Almost all of the tubules around the glomerulus are proximal tubules, which are moderately to strongly positive for E-cadherin, especially on the luminal or apical border (E, arrowhead), but only weakly positive for N-cadherin (F, arrowhead). The arrows indicate the 2 or 3 distal tubules, which are strongly positive for E-cadherin (E, arrows), but negative for N-cadherin (F, arrows). 200X **G-I:** At higher magnification, it can be clearly seen that the E-cadherin is present around the whole epithelial cells of distal tubules (H, arrows) with stronger staining in the cell borders (H, arrows); while in proximal tubules, E-cadherin is mainly located in the luminal borders (H, arrowheads). For N-cadherin, it is only present in proximal tubules, and its signal is mainly located in the basolateral sides of the tubules (I, arrowheads). Distal tubules are totally negative for N-cadherin (I, arrows). A small part of glomerulus can be seen in upper right corner (G-I +). X400

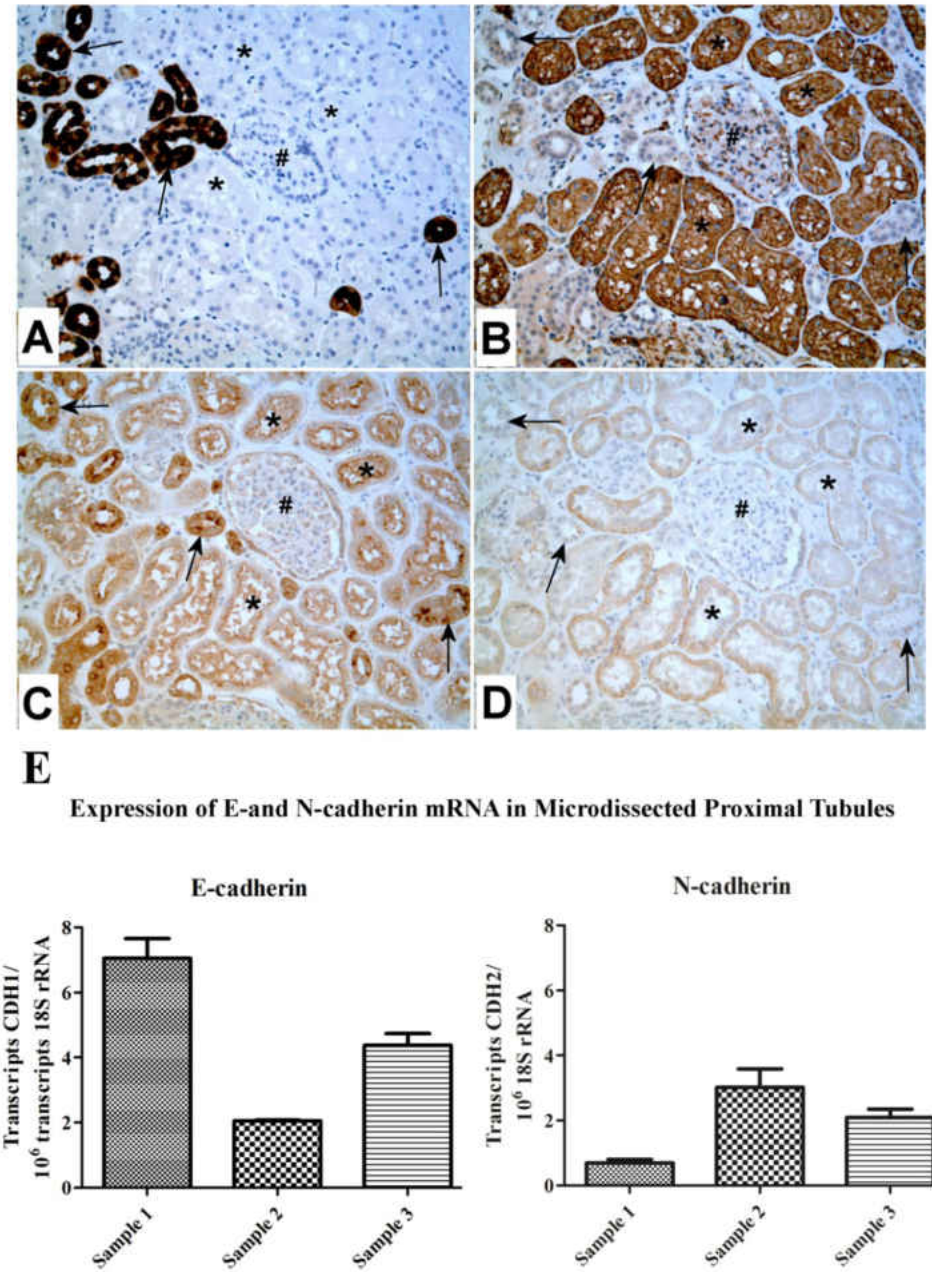

Figure III-2. Expression of E- and N-cadherin in microdissected proximal tubules.

A and B: Identification of proximal tubules by immunohistochemical staining in matched area of normal kidney for calbindin (A)(distal) and aquaporin-1 (B) (proximal). C and D: Verification of E-cadherin (C), N-cadherin (D) expression. The proximal tubules (marked by *) are moderately to strongly positive for E-cadherin (mainly in the luminal side), moderately positive for N-cadherin (mainly in basolateral side), negative for calbindin, and diffusely strongly positive for aquaporin-1. In contrast, the distal tubules (pointed by arrows) show diffuse, strong staining of E-cadherin and calbindin, but no staining or faint staining of N-cadherin and aquaporin-1. The glomeruli (indicated by #) are weakly stained by E-cadherin and aquaporin-1, but negative for N-cadherin and calbindin. Original magnification: X200. Only one example of the serial sections is presented, and all three specimens gave identical results. E: Expression of E- and N-cadherin mRNA in microdissected proximal tubules. RNA was purified from laser-capture microdissected proximal tubules identified in sections of formalin-fix, paraffin-embedded tissue obtained from human renal cortex. Levels of RNA for E- and N-cadherin were determined quantitatively using real-time PCR and normalized to the levels of 18S rRNA also assessed with real-time PCR. The levels of each cadherin isoform were determined in triplicate and expressed as the number of detected cadherin transcripts per million transcripts of rRNA. The results are expressed as the mean of triplicate determinations (±SE). Identification of proximal tubules by immunohistochemical staining in matched area of normal kidney for calbindin (A) (distal) and aquaporin-1 (B) (proximal). C and D: Verification of E-cadherin (C), N-cadherin (D) expression. The proximal tubules (marked by *) are moderately to strongly positive for E-cadherin (mainly in the luminal side), moderately positive for N-cadherin (mainly in basolateral side), negative for calbindin, and diffusely strongly positive for aquaporin-1. In contrast, the distal tubules (pointed by arrows) show diffuse, strong staining of E-cadherin and calbindin, but no staining or faint staining of N-cadherin and aquaporin-1. The glomeruli (indicated by #) are weakly stained by E-cadherin and aquaporin-1, but negative for N-cadherin and calbindin. Original magnification: X200. Only one example of the serial sections is presented, and all three specimens gave identical results. E: Expression of E- and N-cadherin mRNA in microdissected proximal tubules. RNA was purified from laser-capture microdissected proximal tubules identified in sections of formalin-fix, paraffin-embedded tissue obtained from human renal cortex. Levels of RNA for E- and N-cadherin were determined quantitatively using real-time PCR and normalized to the levels of 18S rRNA also assessed with real-time PCR. The levels of each cadherin isoform were determined in triplicate and expressed as the number of detected cadherin transcripts per million transcripts of rRNA. The results are expressed as the mean of triplicate determinations (± SE).xpression of E- and N-cadherin mRNA in microdissected proximal tubules.

Immunohistochemisstry for E-and N-cadherin verified the proximal and distal tubule distribution seen in Figure III-1 (Figure III-2C, D). The results of this determination showed that mRNA for both E- and N-cadherin was expressed in proximal tubule isolated from all three independent specimens (Figure III-2E). The levels of expression of E-cadherin varied between 2 and 7 transcripts and that of N-cadherin between 0.5 and 3 transcripts.

Expression of E- and N-Cadherin in HK-2 Cells as a Function of Growth Medium Composition

In this analysis, the expression of E- and N-cadherin was determined on the HK-2 cell line when grown of three different growth media formulations. The first formulation was that developed by Ryan and coworkers (Ryan et al., 1994), and suggested for use by the ATCC, that is composed of keratinocyte serum free media supplemented with 0.05 mg/ml BPE and 5.0 ng/ml EGF (designated KSFM). The second formulation tested was that used by Detrisac and coworkers (Detrisac et al., 1984) for the growth of human proximal tubule (HPT) cells and is composed of a a 1:1 mixture of DME and F-12 containing selenium (5 ng/ml), insulin (5 μg/ml), transferrin (5 μg/ml), hydrocortisone (36 ng/ml), triiodothyronine (4 pg/ml) and epidermal growth factor (10 ng/ml) (designated 20/12EGF). The third formulation was chosen to be representative of one of the various growth mediums used that contained fetal calf serum (Q. Li et al., 2011) and was a 1:1 mixture of DME and Ham's F-12 growth medium containing 10% fetal calf serum (designated 20/12FCS). In addition, it was also determined if adding 0.05 mg/ml of BPE to the 20/12EGF formulation and if raising the calcium concentration of the KSFM to that of 20/12 had any effect on the expression of E- and N-cadherin.

The results of this determination showed that the expression of E-cadherin mRNA was very low in the HK-2 cells regardless of the growth media formulation, being on the order of 1 mRNA transcript per cell (Figure III-3A). The corresponding matching western blots showed only very faint bands corresponding to the expression of the E-cadherin protein (Figure III-3A). In contrast, the expression of N-cadherin mRNA was much higher in the HK-2 cells when compared to that of E-cadherin, with most conditions exhibiting hundreds of fold greater level of expression regardless of growth formulation (Figure III-3B). The N-cadherin protein was also prominent on western blots (Figure III-3B). Similar to that found for E-cadherin, the growth media composition had little effect on N-cadherin expression. Overall, the analysis demonstrated that the HK-2 cells have a low expression of E- compared to N-cadherin and that growth media composition has only a marginal influence on the levels of mRNA or protein expression.

Comparison of E- and N-Cadherin Expression in HK-2 and HPT Cell Cultures

The expression of E- and N-cadherin was compared between the HK-2 and HPT cells at the level of mRNA and protein expression. Since the results of western analysis can be influenced by the development time used to produce the blot, an ELISA-based method was employed to quantify the amount of E- and N-cadherin that was present in both the HK-2 and HPT cells. Three independent isolates of HPT cells were used in the experiments and these were grown on 20/12EGF. The HK-2 cells were grown on KSFM, 20/12FCS, and 20/12EGF. The results of this analysis confirmed that the HPT cells produced E-cadherin mRNA in substantially higher amounts than the HK-2 cells regardless of growth media composition (Figure III-4A). The levels of E-cadherin mRNA in HPT cells was over 50 fold higher than levels in HK-2 cells.

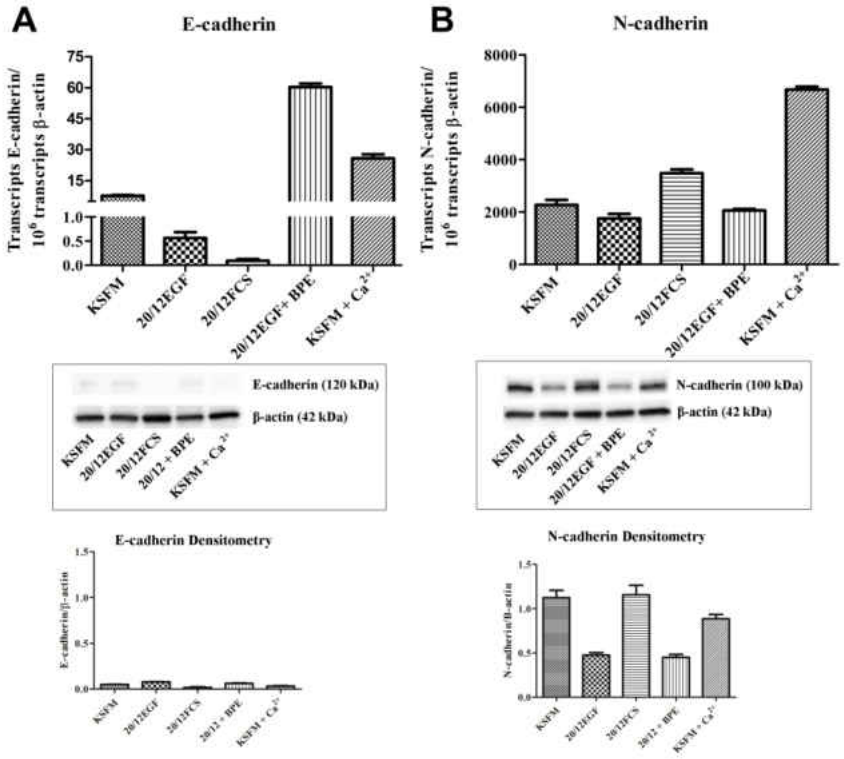

Figure III-3. Influence of growth medium on E- and N-cadherin expression HK-2 cells. A) E-cadherin mRNA expression in HK-2 cells grown in various growth media. Expression was assessed with real-time RT-PCR and expressed as the number of transcripts per million transcripts of β-actin. Western analysis of E-cadherin is shown below the graph. See Materials and Methods for media formulations. B) N-cadherin mRNA expression in HK-2 cells grown in various growth media. Messenger RNA expression was assessed by real-time PCR. Western analysis of N-cadherin is shown below the graph.

This difference in mRNA expression did translate to the amount of E-cadherin protein, with ELISA analysis showing a similar large (>50 fold) increase in E-cadherin protein in the HPT cells compared to the HK-2 cell line (Figure III-4B). An identical analysis of N-cadherin expression confirmed that N-cadherin mRNA expression was higher in the HK-2 cell line compared to the HPT cells (Figure III-5A). An analysis of N-cadherin protein expression also demonstrated that this difference did translate to the differences in the N-cadherin protein (Figure III-5B).

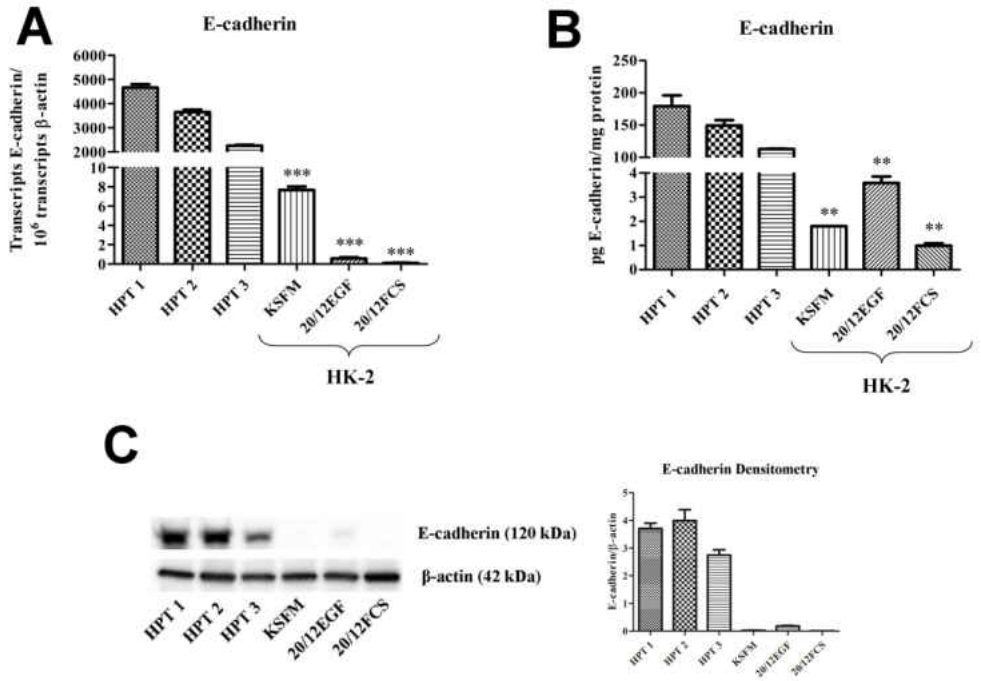

Figure III-4. Comparison of E-cadherin expression in HPT and HK-2 cell cultures. A) Expression of E-cadherin mRNA in three independent HPT isolates (human proximal tubule cells) compared to that in HK-2 cells growth in three different media formulation. HPT cells were grown in the 20/12EGF formulation. B) Levels of E-cadherin protein measured quantitatively using an ELISA. C) Western analysis of E-cadherin in the identical cultures as in A and B. Significant differences between HK-2 and each HPT isolate are designated ***$p < 0.0001$, of ** $p < 0.001$ as determined by one-way ANOVA with Tukey's post-hoc test.

However, the magnitude of the difference between N-cadherin protein expression between the HPT and HK-2 cell lines was much less (4 to 10 fold) than that found for the E-cadherin protein (Figure III-4B versus III-5B). Overall, the results demonstrate that the level of E-cadherin mRNA and protein is significantly higher in HPT cells compared to HK-2 cells and that the expression pattern is reversed for the expression of N-cadherin between the cell lines. To validate that HK-2 cells grown on filters did not alter their E-

cadherin levels, protein extracts were taken from the cells on the filter inserts and subjected to western analysis for both E- and N-cadherin protein expression. The results of this experiment show that the expression level of these cadherins was not altered from culturing in the filter-insert environment (III-6).

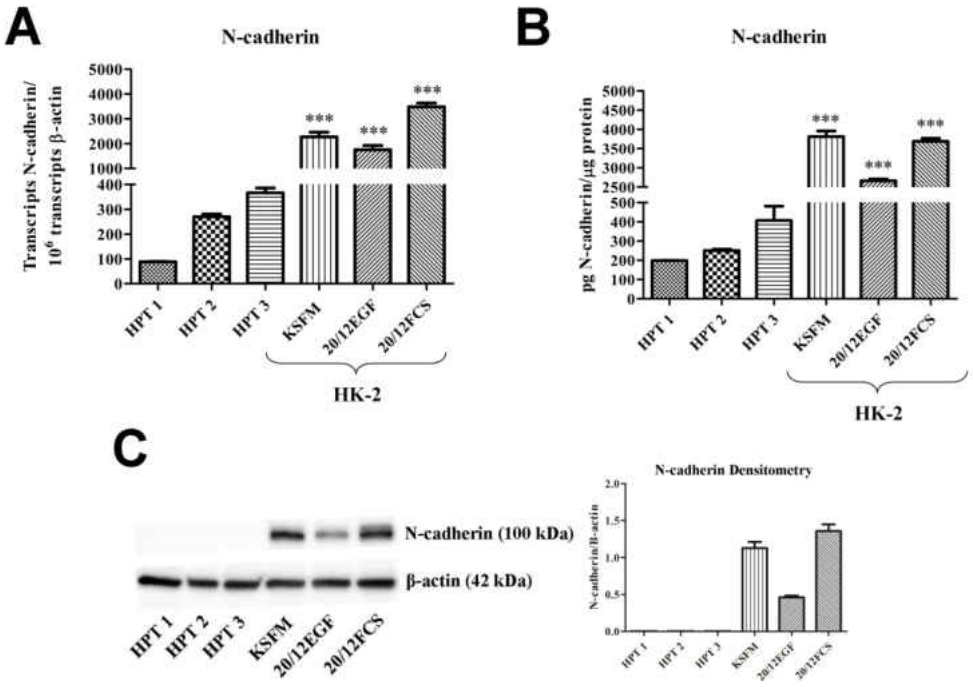

Figure III-5. Comparison of N-cadherin expression in HPT and HK-2 cell cultures. A) Expression of N-cadherin mRNA in three independent HPT isolates (human proximal tubule cells) compared to that in HK-2 cells growth in three different media formulation. HPT cells were grown in the 20/12EGF formulation. B) Levels of N-cadherin protein measured quantitatively using an ELISA. C) Western analysis of N-cadherin in the identical cultures as in A and B.

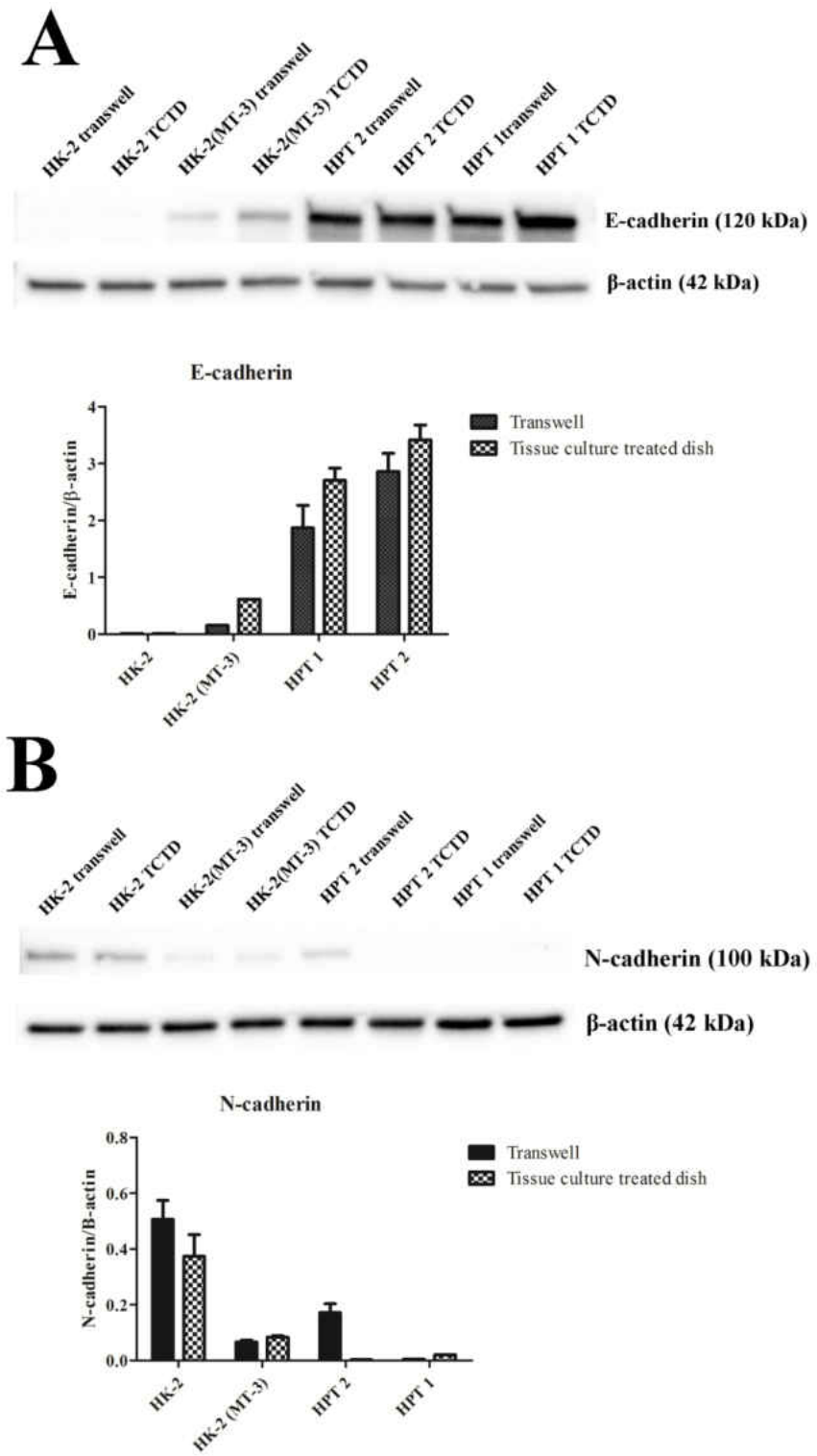

Figure III-6. The pattern of E-and N-cadherin expression is unaltered when cells are grown on transwell inserts. Growing cells on trawnswell inserts allows both the apical and basolateral membranes of proximal tubule cells to have access to the growth medium, a situation that is a better model of proximal tubule transport in vivo that tissue culture treated plastic substrates. E- and N-cadherin expression remains very similar in both growth conditions.

Alterations in Tight Monolayer Development

The transepithelial resistance of the HK-2 and HPT cell monolayers was also determined to confirm that the growth media composition had no effect on the tight junctions between the cells. It was shown that the HK-2 developed no transepithelial resistance (TER), whereas, the HPT cell line developed a TER consistent with a "leaky" epithelium (Figure III-7).

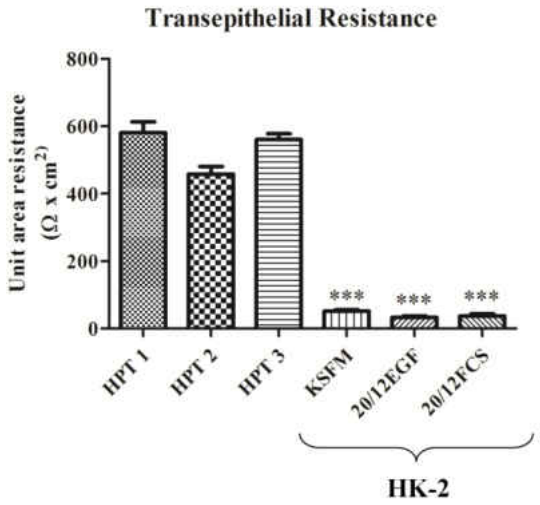

Figure III-7. Transepithelial resistance comparison of HPT and HK-2 cell cultures. Cells were grown on filter supports and the electrical resistance across the monolayer was measured. Resistance is expressed as Ohms-cm2. Three independent HPT isolates (human proximal tubule cells) are compared to that in HK-2 cells growth in three different media formulation. HPT cells were grown in the 20/12EGF formulation. Significant differences between HK-2 and each HPT isolate are designated *$p < 0.0001$ as determined by one-way ANOVA with Tukey's post-hoc test.

As a further validation for an alteration in cell-to-cell junctions, the HK-2(MT-3), HK-2(blank vector) and HPT cells were assessed for the expression of connexin 32. The results of this determination showed that HK-2(BV) had marginal expression of connexin 32 mRNA and protein, while the HK-2(MT-3) and HPT cells each showed significant expression of both connexin 32 mRNA and protein (Figure III-8). These finds further

validate the findings of altered cell-to-cell junctional responsibilities between the HK-2 and the HPT cell line and extend those observations to communication between adjacent cells.

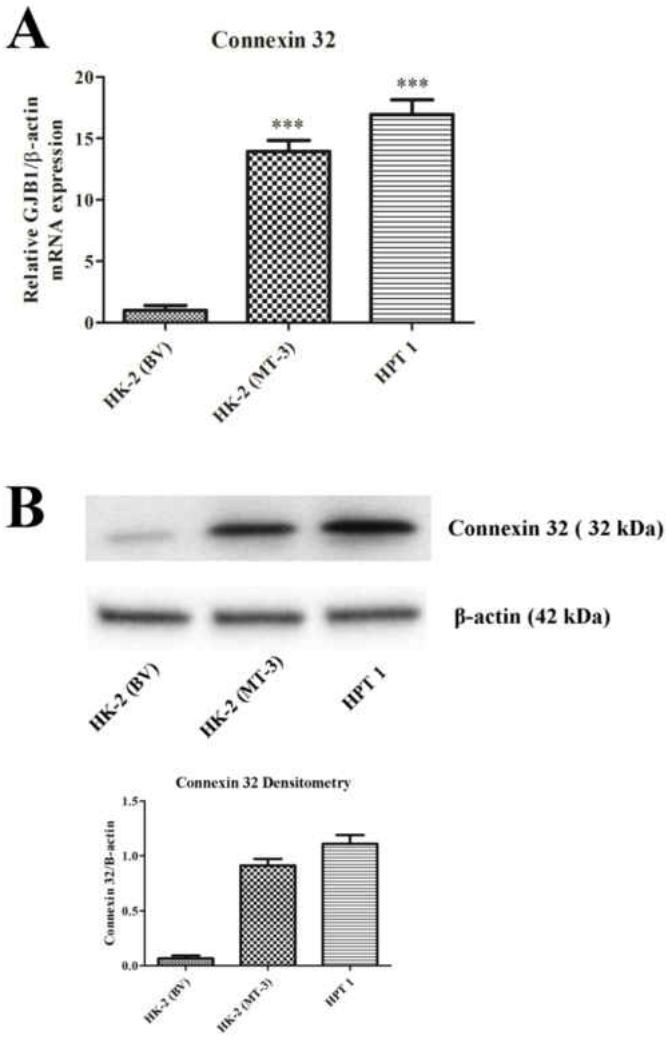

Figure III-8. Connexin 32 expression in HK-2, HPT, and HK-2 cells expressing MT-3. Messenger RNA of connexin 32 was assessed with real-time PCR and expressed as a fold increase of the HK-2 cells stably transfected with the blank vector. The change in connexin 32 expression was normalized to the change in β-actin expression. Western analysis of connexin 32 is shown below the graph.

Association of the Unique C-Terminal Domain of MT-3 With MT-3 Induced MET in HK-2 Cells

The goal of this experiment was to determine the functional domain of the MT-3 protein required for the MT-3 protein to re-establish vectorial active transport, produce an enhanced epithelial morphology, elicit a shift in the expression of E- and N-cadherin, and to increase the expression of connexin 32. Four constructs were used to transfect the HK-2 cells to determine their effect (III-9) on vectorial active transport as judged by the appearance of domes and the generation of a transepithelial resistance. The first construct was MT-3 where the N-terminal sequence was been mutated, the second was MT-3 where the C-terminal sequence was mutated, the third was the MT-1E isoform where the unique C-terminal sequence of MT-3 was inserted into the sequence, and the fourth was the MT-1E isoform where the unique N-terminal sequence of MT-3 was inserted into the sequence. The HK-2 cell line carrying the blank vector or transfected with the MT-1E isoform served as controls. The results of this determination demonstrated that the C-terminal sequence of MT-3 is required for the establishment of vectorial active transport when MT-3 is transfected and expressed in the HK-2 cell line. First, the mutation of the N-terminal sequence of MT-3 had no effect on the ability of HK-2 cells to form domes or generate a transepithelial resistance (Figure III-10 A,B; Table III-1).

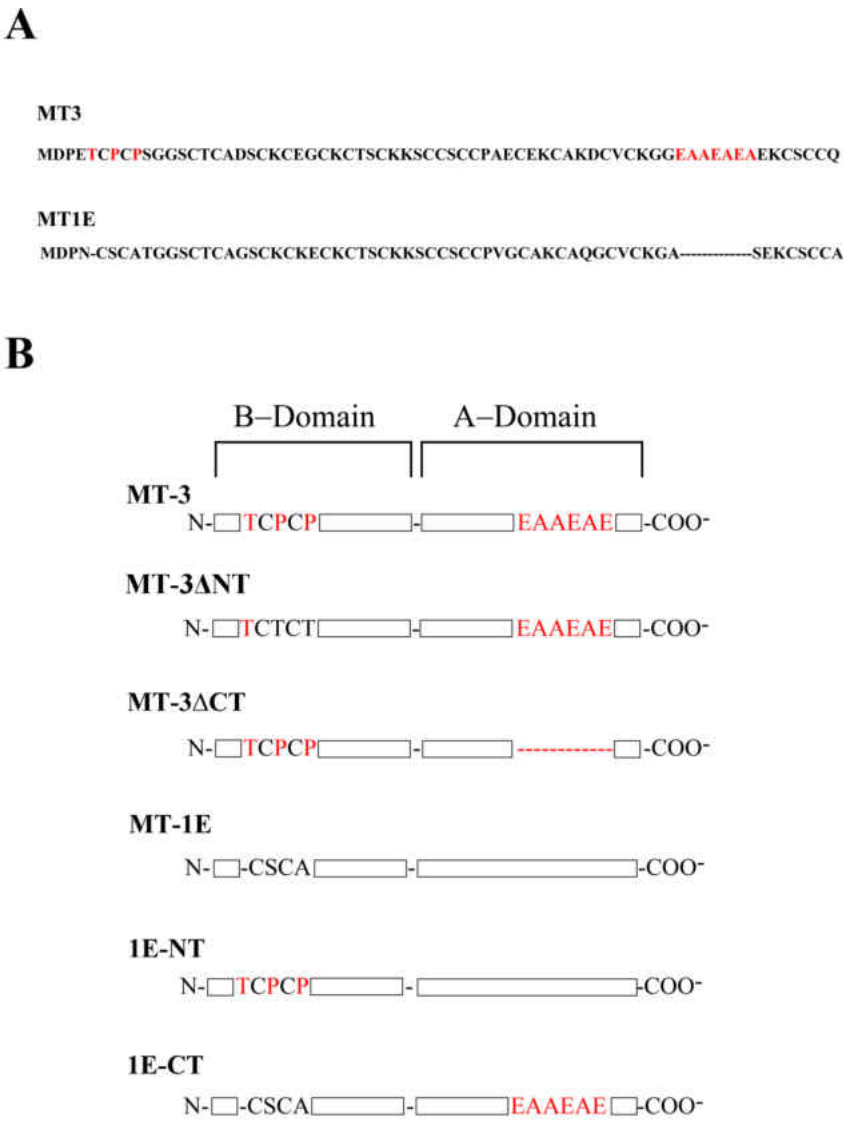

Figure III-9. Mutated metallothionein constructs. A) Amino acid sequence of human MT-3 compared with human MT-1E. Shown in red are the MT-3 specific sequences that are not exhibited in any mammalian MT 1/2 isoform. The N-terminal TCPCP sequence of MT-3 has been shown to confer the unique biological activity of neuronal growth inhibitory activity [38]. These two sequences were independently deleted from MT-3 and inserted into the MT-1E isoform to test for the conference of vectorial active transport. B) Schematic diagram of the various metallothionein constructs with: MT-3 denoting the wild-type sequence; MT-3-ΔNT, the two essential prolines were converted to threonines; MT-3ΔCT, the EAAEAE C-terminal sequence was deleted from MT-3; MT-1E, wild-type 1E isoform of metallothionein; 1E-NT, the N-terminal sequence of MT-3 was inserted into the corresponding position of MT-1E; 1E-CT, the MT-3 C-terminal sequence EAAEAE was inserted into the corresponding position of MT-1E.

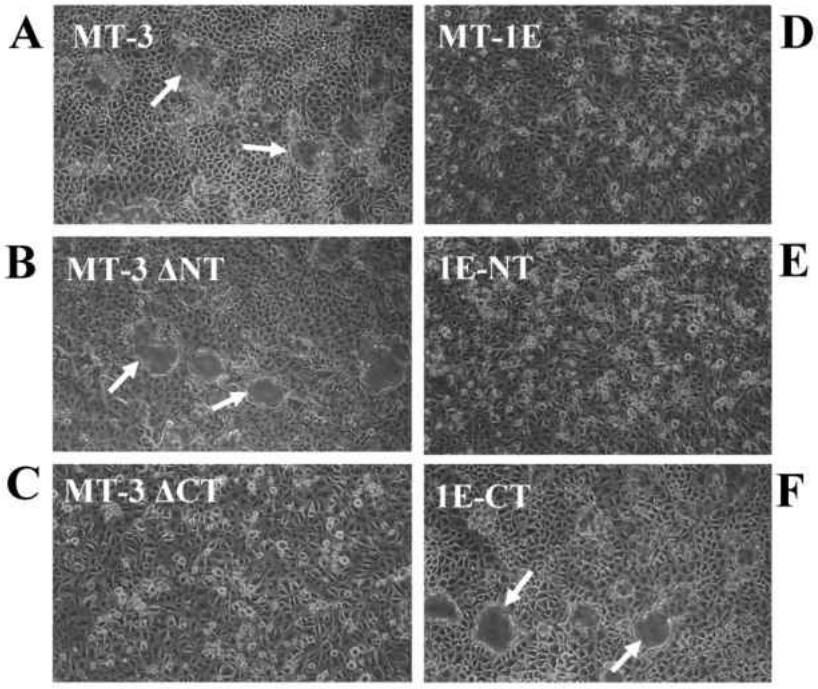

Figure III-10: Effect of the altered domains of MT-3 on the formation of domes in stably transfected HK-2 cells. To assess the domain of MT-3 that is responsible for the ability to confer dome formation, site-directed mutants of MT-3 were produced and the two unique domains of MT-3 were inserted into the non-doming MT isoform, MT-1E, as shown in Figure 1. Each expression construct was stably transfected into HK-2 cells, and expressing clones were assessed for the ability to form domes. A) wild-type MT-3 showing dome formation when stably transfected, B) MT-3-ΔNT where the prolines in the N-terminal domain that confers growth inhibitory activity were converted to threonines, show that the ability to form domes was not compromised, C) MT-3ΔCT where the C-terminal EAAEAE sequence unique to the third isoform of metallothionein was deleted, shows the lack of dome formation, D) MT-1E, wild-type human metallothionein 1E, commonly expressed at high levels in many cell types exhibits no domes when stably transfected, E) 1E-NT, the N-terminal unique sequence of MT-3 was inserted into the corresponding position of MT-3 shows no conference of dome formation, and F) 1E-CT, the EAAEAE sequence of MT-3 was inserted in the corresponding position of MT-1E and when stably transfected into HK-2 cells confers dome formation.

Construct	MT Protein per µg protein	Domes per Field	Trans Epithelial Resistance (Ohm-cm^2)
MT-3-NT Mutant			
#1	3.2 ± 0.25	6.2 ± 0.8	426 ± 36
#2	4.6 ± 0.31	3.5 ± 1.2	493 ± 42
#3	2.8 ± 0.29	3.3 ± 1.0	506 ± 42
MT-3ΔCT			
#1	3.7 ± 0.40	0	17 ± 12
#2	3.8 ± 0.11	0	15 ± 11
#3	2.2 ± 0.16	0	18 ± 18
MT-1E-NT			
#1	5.1 ± 0.72	0	22 ± 17
#2	3.6 ± 0.45	0	23 ±18
#3	4.2 ± 0.33	0	18 ± 9
MT-1E-CT			
#1	3.3 ± 0.26	9.8 ± 0.7	623 ± 31
#2	1.9 ± 0.08	6.7 ± 0.6	446 ± 33
#3	3.3 ± 0.33	4.4 ± 0.2	594 ± 23

In contrast, mutation of the C-terminal sequence of MT-3 abolished both dome formation and the transepithelial resistance of the monolayer (Figure III-10 A,C; Table III-1). The MT-1E isoform of MT does not contain either of the unique C-terminal or N-terminal sequences of MT-3 and transfection of HK-2 cells with MT-1E do not form domes in culture or develop a transepithelial resistance (Figure III-10D). The insertion of the N-terminal sequence of MT-3 into the MT-1E gene and subsequent transfection into the HK-2 cells does not result in dome formation or the development of transepithelial-electrical resistance (Figure III-10E, Table III-1).

In contrast, the insertion of the C- terminal sequence of MT-3 into the MT-1E gene and subsequent transfection into the HK-2 cells results in both dome formation and the generation of a transepithelial resistance (Figure III-10F; Table III-1).

The expression of E- and N-cadherin in HK-2 cells transfected with each MT-3 mutant construct was assessed (Figure III-11). Those constructs that produced domes in culture expressed high levels of E-cadherin. Constructs containing only the N-terminal domain of MT-3 were also able to highly express E-cadherin, despite the lack of the ability to form domes. The repression of N-cadherin, however, required the presence of the C-terminal domain (Figure III-11). The expression of connexin 32 required the presence of both domains with each domain being able to support intermediate levels of connexin 32 (Figure III-12).

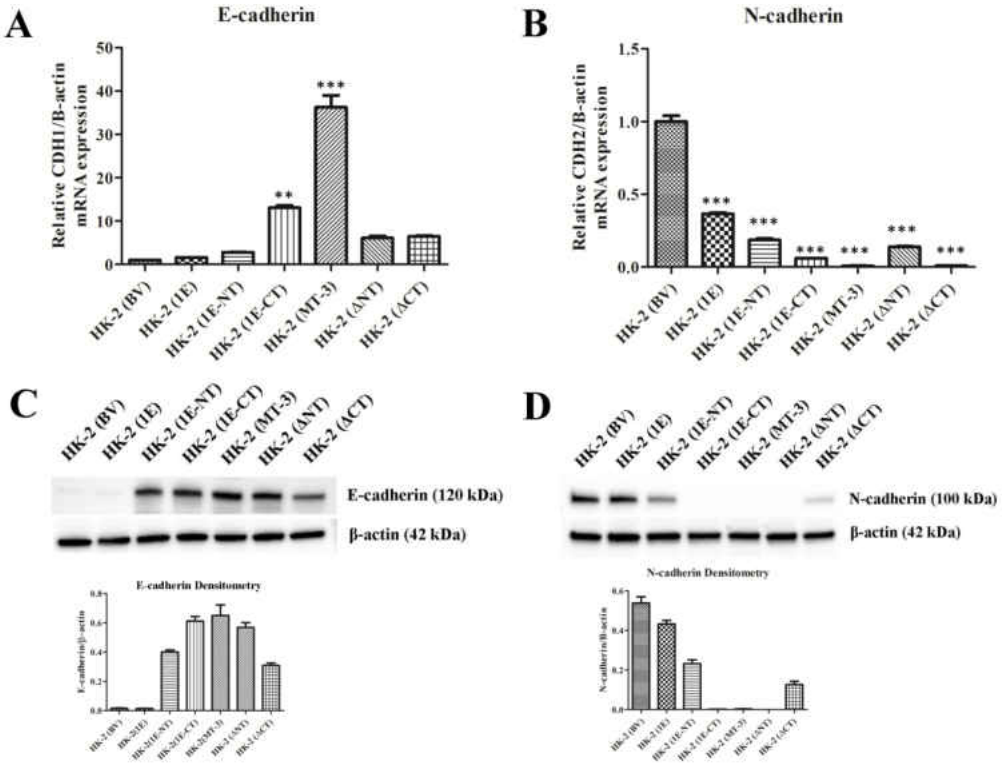

Figure III-11. Effect of the altered domains of MT-3 on the expression of E-and N-cadherin in stably transfected HK-2 cells. Messenger RNA of E-cadherin (A) and N-cadherin (B) were assessed with real-time PCR and expressed as fold change in expression versus HK-2 cells transfected with the blank vector. The change in E- or N-cadherin expression was normalized to the change in β-actin expression. Significant differences from HK-2 (BV) are designated as ** $p < 0.001$,*** $p < 0.0001$. Western analysis of E-cadherin (C) and N-cadherin (D) was conducted in identical cultures as in A and B. β-actin was used as a loading control and for densitometric normalization. Densitometry is shown below the corresponding blot.

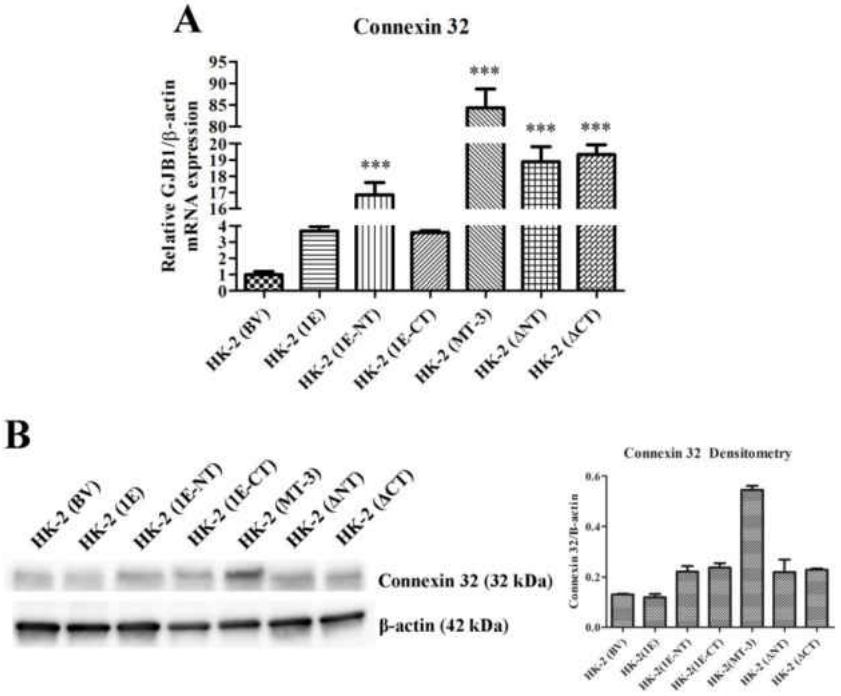

Figure III-12. Effect of the altered domains of MT-3 on the expression of connexin 32 in stably transfected HK-3 cells. A) Messenger RNA of connexin 32 assessed with real-time PCR and expressed as fold change in expression versus HK-2 cells transfected with the blank vector. The change in connexin 32 expression was normalized to the change in β-actin expression. Significant differences from HK-2 (BV) are designated as *** $p < 0.0001$. B) Western analysis of connexin 32 was conducted in identical cultures as in (A). β-actin was used as a loading control and for densitometric normalization. Densitometry is shown beside the corresponding blot.

Effect of Forced E-cadherin Expression on HK-2 Vectorial Active Transport, N-Cadherin Expression, and Cell Morphology

It was previously shown that the stable transfection of HK-2 cells with MT-3 resulted in the re-establishment of vectorial active transport with a corresponding induction of E-cadherin and repression of N-cadherin gene expression [30]. In this study E-cadherin was transfected into the HK-2 cells to determine if the expression of E-cadherin, in the absence of MT-3 expression, could restore vectorial active transport. It was also determined if E-cadherin expression would alter cell morphology or the expression of N-cadherin in the HK-2 cells. Five independent clones were selected and

characterized for their expression of E-cadherin mRNA and protein. Two clones (5 and 15) displayed an elevated expression of E-cadherin, two displayed a very modest elevation (3 and 14) and one (9) displayed no detectable alteration in expression of E-cadherin mRNA and protein (Figure III-13A,C). An analysis of N-cadherin mRNA expression showed that N-cadherin expression was highly repressed in the two isolates of HK-2 cells that expressed an elevated level of E-cadherin expression (Figure III-13A,B). N-cadherin mRNA was modestly repressed in the two isolates of HK-2 cells that expressed very modest elevation of E-cadherin expression (Figure III-13A,B). There was no alteration in the level of N-cadherin mRNA from that found in HK-2 cells for the transfected HK-2 cell clone (#9) that failed to increase their level of E-cadherin (Figure III-13A,B). The correlation between the expression of E-cadherin mRNA and the repression of N-cadherin mRNA was not as pronounced for the corresponding proteins (Figure III-13C). In agreement with the mRNA expression data, it was shown that whenever E-cadherin protein was expressed, there was no expression of the N-cadherin protein. The results also demonstrated that transfection of the HK-2 cells with E-cadherin did not result in the re-establishment of vectorial active transport as evaluated by both dome formation and the development of a transepithelial resistance across the monolayer. None of the 5 independent clones showed any evidence of dome formation by the cell monolayers or developed a transepithelial resistance above a blank filter control (data not shown). The morphology of the cells was also not altered by transfection of E-cadherin into the HK-2 cell lines as noted by a similar morphology between wild type HK-2 cells and clone 5 which had the highest level of E-cadherin protein expression (Figure III-13D,E). This result also correlates with constructs containing the N-terminal but

lacking the C-terminal domain being able to support E-cadherin expression but not sufficient enough to establish vectorial active transport (Figure III-11, Table III-1).

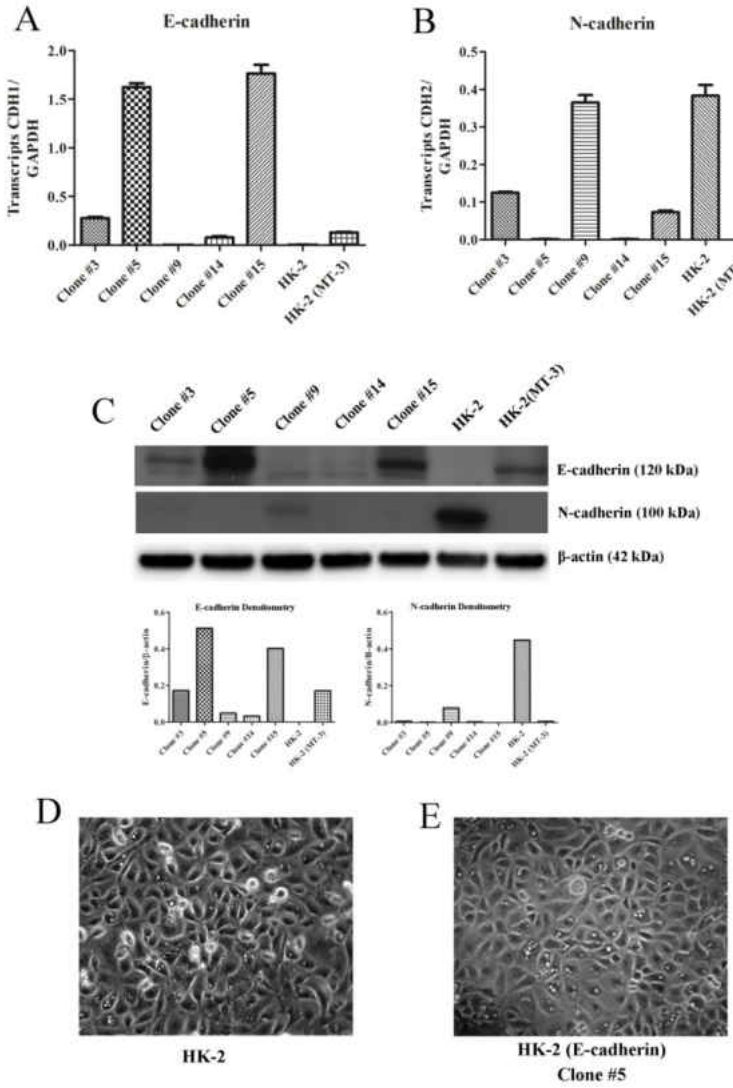

Figure III-13. The effect of forced overexpression of E-cadherin on the expression of N-cadherin and on dome formation in HK-2 cells. E-cadherin was stably transfected into the HK-2 human proximal tubule cell line and individual clones were isolated and assessed for E-cadherin and N-cadherin expression and the formation of domes. A) Expression of E-cadherin mRNA in five individual clones, HK-2 cells and the MT-3 stably transfected HK-2 line, HK-2 (MT-3) assessed quantitatively with real-time PCR and normalized to the levels of transcripts of glyceraldehyde phosphate dehydrogenase; B) Expression of N-cadherin mRNA; C) Expression of E- and N-cadherin protein in each isolated clone, D) and E) Morphology of the highest expressing E-cadherin clone (E) in comparison to the parental HK-2 cells (D) showing the absence of dome formation.

Zn_7MT-3 mediated pulldowns in HK-2 lysates

In order to identify potential protein interactions of MT-3 within the human proximal tubule, Zn_7MT-3 was covalently crosslinked to amine-reactive agarose beads and incubated with lysates isolated from HK-2 cells (Figure III-14). Previous studies indicated β-actin, myosin IIa, gelsolin, and tropomyosin 3 as putative binding partners (Bathula, 2010). Literature review indicated enolase-1 and aldolase-A as MT-3 interacting proteins in cultured astrocytes (Armitage, 2010), and these potential interactions were also evaluated. Eluates were subjected to SDS-PAGE followed by western blotting, probing for potential MT-3 interacting proteins. The results of this determination showed Zn_7MT-3 able to pulldown β-actin, tropomyosin-3, α-enolase, and aldolase-a from HK-2 lysates (Figure III-15).

V5-mediated immunoprecipitations in MT-3 expressing HK-2 lysates

To further support the protein-protein interactions observed through pulldowns, we generated mutant cell lines either stably or transiently expressing MT-3 with a protein tag (V5). The MT-3 antibody is generated against the C-terminal insert not present in the other isoforms. We have hypothesized the C-terminal domain of MT-3 to be the region of protein-protein interactions, as this feature distinguishes MT-3 from MT-1,-2, and -4. This becomes problematic for co-immuoprecipitation if this domain is blocked by the interactions in which we are attempting to determine. For these reasons, the stop codon of MT-3 was removed in order to allow translation of a V5 tag to aid in immunoprecipitation , western blotting, and immunofluorescence. V5 is a relatively small tag in comparison to most other commercially available protein tags, adding an additional 4 kDa. Prior to performing immunoprecipitation, lysates were tested for the

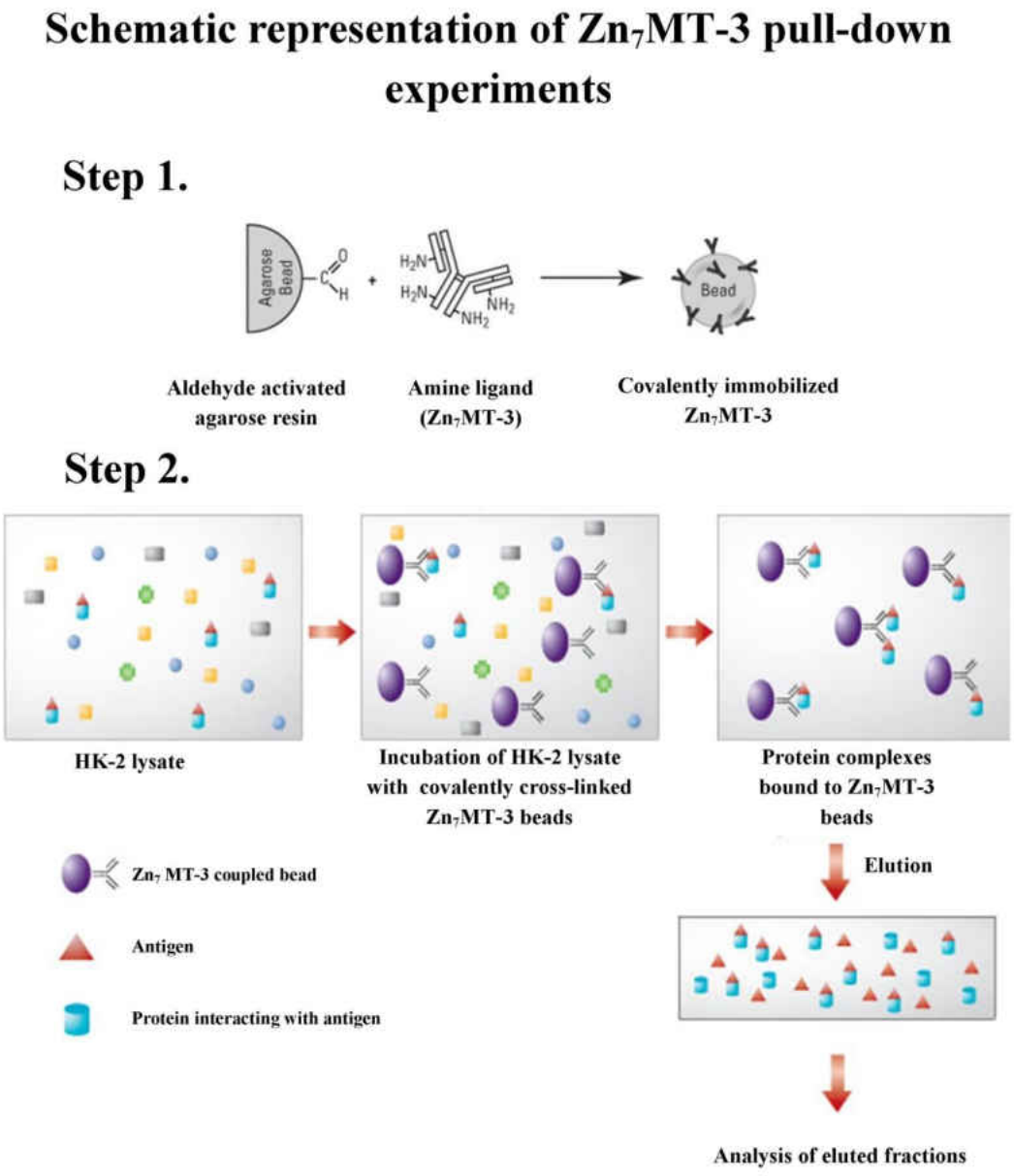

Figure III-14. Schematic representation of the methodology used to pulldown MT-3 interacting proteins. Eluted fractions were subjected to silverstaining to confirm the presence of proteins of the correct molecular weight and western blotting to confirm the identity of these previously identified proteins.

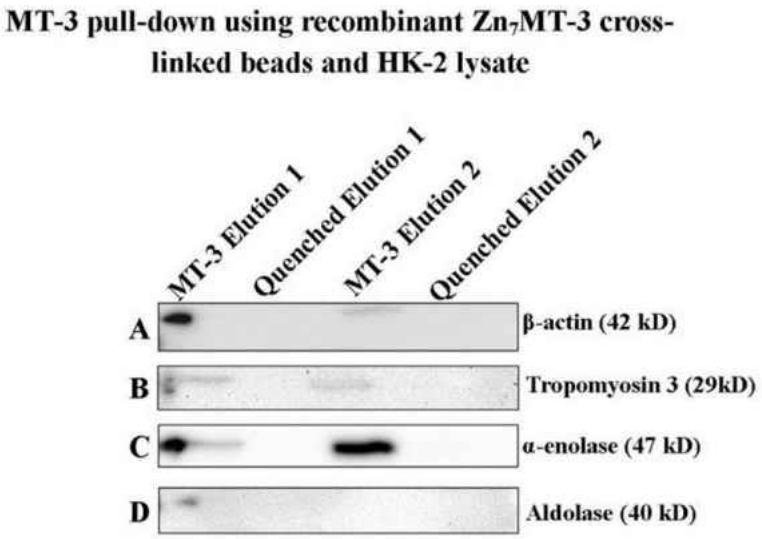

Figure III-15. MT-3 interacts with β-actin, Tropomyosin 3, enolase-1, and aldolase A. MT-3 can pulldown proteins isolated from cultured human proximal tubule cells, suggesting potential protein interactions between MT-3 and B-actin (A), Tropomyosin-3 (B), alpha-enolase (C), and aldolase-a (D) in the human proximal tubule.

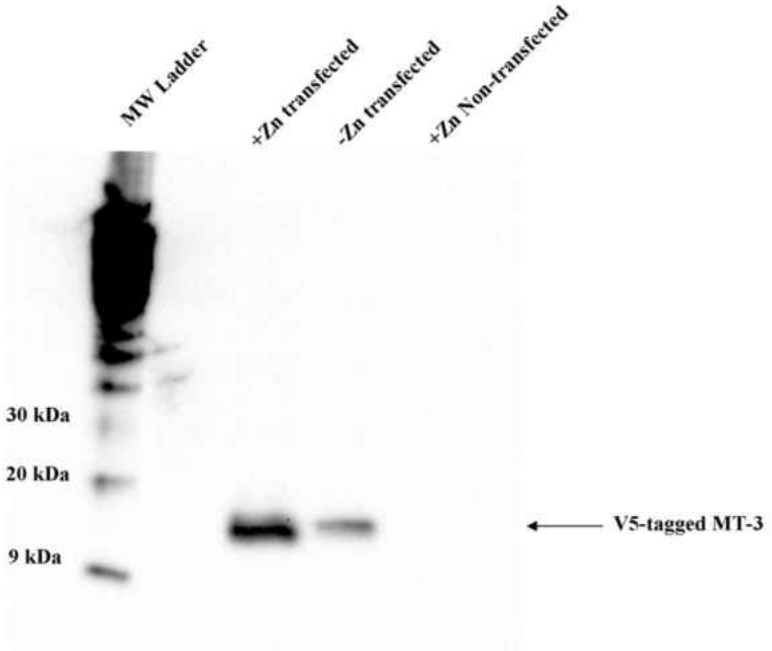

Figure III-16. Zinc supplementation 6 hours post transient transfection of V5-tagged MT-3 into HK-2 cells increases MT-3 protein expression. V5 tagged-MT-3 migrates at the appropriate molecular weight, and zinc supplementations following transfection yields more available V5 tagged-MT-3 available for co-immunoprecipitation.

presence of MT-3 –V5 by western blotting (Figure III-16) . We also confirmed the lack of V5 signal in MT-3 null lysates. Interestingly, cells supplemented with 30 uM zinc in the growth medium six hours-post transient transfection contained more MT-3 protein than those supplemented with the normal growth medium (Figure III-17). MT-3 is not inducible by zinc, so this observation probably correlates to the increased stability of fully zinc-bound MT-3 than apo-MT-3 or less metallated forms of MT-3, resulting in less turnover of this protein. The eluates were subjected to SDS-PAGE followed by silverstaining to test for the presence of proteins in the eluted fractions, and that proteins were present in the eluate that migrated at the approximate molecular weight of those proteins previously identified in 2010 (Figure III-17).

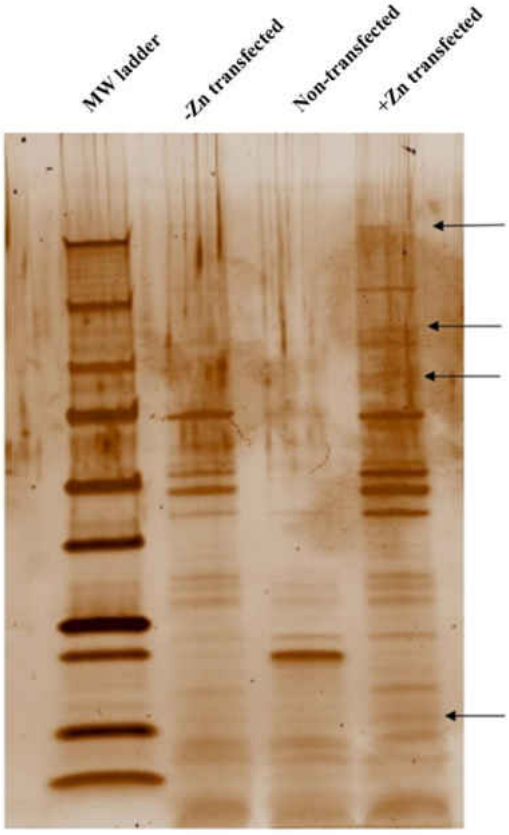

Figure III-17. MT-3 interacts with several proteins in cultured proximal tubule cells. Representative image of a silverstained gel following SDS-PAGE of eluates from a pulldown experiment. Arrows indicate proteins present at the molecular weight of putative interacting proteins identified by Bathula in 2010.

Co-immunoprecipitation of V5-MT-3 complexes and subsequent western blotting confirmed β-actin, myosin IIa, enolase-1, and possibly aldolase-a (Figure III-18) as potential MT-3 interacting proteins in the proximal tubule.

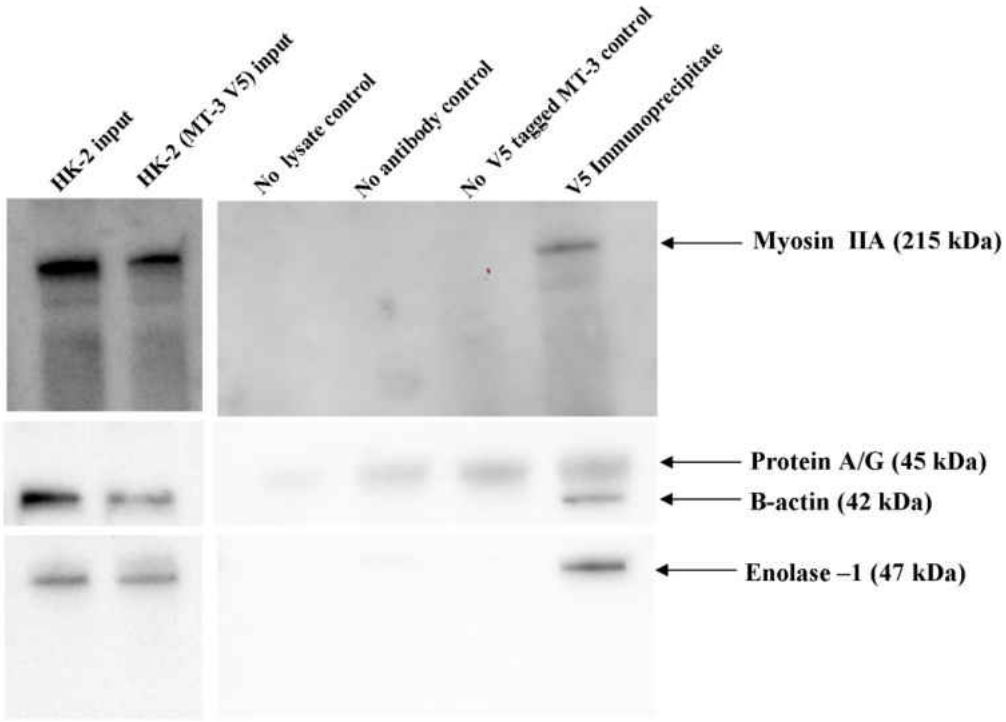

Figure III-18. Co-immunoprecipitation of MT-3 protein complexes in HK-2 cells transfected with V5 tagged-MT-3. V5-tagged MT-3 immunoprecipitates with myosin IIa, β-actin, and enolase-1. Lane 1 and 2 are the lysate inputs used for co-immunoprecipitations, Lane 3 is the eluate from the control reaction that contained all the reaction components (e.g. Protein A/G magnetic beads, V5 antibody, IP lysis buffer) excluding cellular lysate; Lane 4 is the control reaction that contained all reaction components excluding the V5 antibody; Lane 5 is the no prey control, containing all reaction components as lane 6 but incubated with non-transfected HK-2 lysate. Equal volumes were loaded into each lane.

CHAPTER IV

DISCUSSION

HK-2 Cells have Features Associated with the Initial Stages of EMT

EMT is a developmental process where reorganization of the actin cytoskeleton, a loss of apical-basolateral polarity, and loss of cell-to-cell contact, results in conversion of an epithelial cell to a mesenchymal cell. The repression of the epithelial marker, E-cadherin, and upregulation of the mesenchymal marker, N-cadherin, are gene expression changes typically observed during EMT (Wu, Tsai, Wu, Teng, & Wu, 2012). As detailed in the introduction, the HK-2 cell line has seen frequent use as a model to study the process of EMT in the human kidney. This laboratory previously reported that the HK-2 cell line had a very low expression of E-cadherin compared to N-cadherin, an absence of tight junction mediated paracellular barrier function, and a failure to maintain vectorial active transport (Bathula et al., 2008; Kim et al., 2002). These would be features that suggest that the HK-2 cell line may have undergone an appreciable level of EMT during the isolation of the cell line. However, these studies used one of a variety of growth media employed for growth of the HK-2 cell line and therefore may not have been representative of other reports in the literature that use this cell line. Thus, the first goal of the present study was to confirm the levels of expression of the E- and N-cadherin, tight junctional integrity, and vectorial active transport in the HK-2 cell line as a function of growth media composition.. The results of this study confirmed that the HK-2 cells expressed a very low amount of E-cadherin mRNA and

protein and that this expression was largely independent of the composition of the growth media. Similarly, the expression of N-cadherin was very high compared to that of E-cadherin. The HK-2 cell monolayer exhibited no transepithelial resistance on any of the growth media tested, confirming a lack of tight junctional integrity. It was also demonstrated that the HK-2 cell line did not form "domes", a feature of vectorial active transport, on any of the tested growth mediums. The formation of domes is a hallmark of cultured renal epithelial cells that retain the *in situ* property of vectorial active transport (D. A. Sens et al., 1999). These out-of-focus areas of the cell monolayer, seen upon light microscopic examination, represent raised areas where fluid has become trapped underneath the monolayer owing to active transport of ions and water across the cell monolayer in an apical to basolateral direction. These results show that the HK-2 cell line, regardless of the conditions used for growth, have a low expression of E- compared to N-cadherin, an absence of tight junctions, and do not form "domes".

There is agreement in the literature that the renal proximal tubule does express N-cadherin in line with a developmental derivation from mesenchyme (Jung, Dean, Jiang, & Gaylor, 2004; Nürnberger & Feldkamp, 2010; W. Prozialeck et al., 2004; Shimazui & Kojima, 2006). However, the literature is somewhat less clear regarding the expression of E-cadherin. In the developing kidney, it has been shown that the early progenitors of the proximal tubules express cadherin 6 and not E-cadherin (Cho, Patterson, & Brookhiser, 1998). Then, as the proximal tubules mature, cadherin-6 (also called K-cadherin) is down-regulated and E-cadherin is then detected in the mature proximal tubules of the adult kidney (Cho et al., 1998). In this regard, cadherin-6 can be looked upon as a marker for the fetal proximal tubule. Despite this convincing study, there is

some discrepancy in the literature regarding the expression of E-cadherin in the proximal tubule, with some reports indicating no expression (Docherty & Calvo, 2009; Esteban, Tran, & Harten, 2006; Nouwen & Dauwe, 1993; Nürnberger & Feldkamp, 2010; Shimazui & Kojima, 2006), others low expression well below that of N-cadherin (Huby, Rastaldi, & Caron, 2009; Langner, Ratschek, & Rehak, 2004; Mori, Lee, & Rapoport, 2005; W. Prozialeck et al., 2004; Walter C Prozialeck et al., 2003), and some with expression without indication of level (Alami, Williams, & Yeger, 2003; Piepenhagen & Nelson, 1998). Due to this discrepancy in E-cadherin expression, the present study examined the expression of E- and N-cadherin in the human kidney proximal tubule. It was shown using immunohistochemistry on three independent specimens of human kidney that the proximal tubules had expression of both E- and N-cadherin protein. The study was also extended to the level of mRNA expression by microdissection of proximal tubules from 3 independent specimens and determining the expression of E- and N-cadherin by real time PCR. It was found that there was expression of both E- and N-cadherin mRNA in the proximal tubules. The proximal tubules chosen for microdissection were those in close proximity to glomeruli, greatly minimizing any chance for contamination with other types of tubular elements. A plausible reason for the discrepancy in the literature regarding the expression of E-cadherin in the proximal tubule is that most studies relied on immunohistochemistry, both peroxidase and fluorescent based, in attempts to detect and compare the intensity of staining between antibodies for E- and N-cadherin. While it is possible to compare the intensity of staining within each antibody across the differing elements of the kidney, it is not possible to compare the intensity of staining generated between the E- and N-cadherin antibodies and

draw conclusions regarding levels of expression. Each antibody will have its own characteristics of antigen binding and staining can also vary further between antibodies as a function of tissue fixation, antigen retrieval techniques, and incubation conditions to name but a few variables. It is extremely difficult, if not impossible, to compare the level of expression of E-cadherin to N-cadherin using immunohistochemical analysis. Thus, the present study shows that both E- and N-cadherin mRNA and protein are expressed in the human renal proximal tubule.

The present results suggest that the HK-2 cell line has already undergone an appreciable degree of EMT. This is based on several observations. First, the HK-2 cell line does not form "domes" in cell culture. This is in contrast to primary cultures of human renal epithelial cells, isolated and cultured by several different laboratories that have been shown to form "domes"(KEMPSON, 1986; Wilson & Dillingham, 1985), [56], (Detrisac et al., 1984). In fact, the primary culture used in the isolation of the HK-2 cell line was stated to form "domes" prior to being used in the transfection and immortalization procedure (Ryan et al., 1994). Dome formation in epithelial cell cultures is acceptable presumptive evidence of the following processes that are required for its expression: functional plasma membrane polarization, formation of occluding junctions (tight junctions), and vectorial transepithelial active ion transport [57]. Studies from this laboratory demonstrated that the HK-2 cell line does not generate a transepithelial electrical resistance or possess tight junctional sealing strands, both indicative of a loss of tight junctions between adjacent cells (Kim et al., 2002). Second, the present study confirms that the HK-2 cell line has undergone an E-cadherin to N-cadherin shift when compared to the HPT cells. The present study quantified the difference in E-cadherin and

N-cadherin between the HPT and HK-2 cells. This showed high levels of E-cadherin in the HPT cells and very low levels in the HK-2 cell line. The reverse was shown for N-cadherin expression, but the magnitude of the difference was not as large. In addition, when compared to the HPT cells, the HK-2 cell line has increased expression of cadherin-6 (K-cadherin), a marker associated with the proximal tubule of the developing kidney (Bathula et al., 2008; Cho et al., 1998). This finding suggests a more mesenchymal differentiation of the HK-2 cells based on the known development of the proximal tubule (Cho et al., 1998). Third, the human proximal tubule is known to possess gap junctions between adjacent cells. The present study demonstrated that the HPT cells expressed connexin 32; whereas, the HK-2 cell line had a very reduced expression of this connexin. Thus, the present results suggest that the HK-2 cells already displays those features of a cell having undergone appreciable EMT.

The results should not be interpreted to indicate that the HK-2 cell line is an unacceptable model for the study of the overall process of EMT. Too often EMT is looked upon as an all-or-none process rather than a graded series of events. The HPT cell line and all other primary mortal cultures of cells retaining proximal tubule character have lost their brush border. This could be looked upon as a very early feature of EMT that occurs upon placing the cells into culture. Similarly, the HK-2 cell line could be looked upon as a model for a proximal tubule cell that has lost early features associated with EMT such as cell-to-cell contact, a loss of apical to basolateral separation and cadherin switching. However, the HK-2 cells retain many other differentiated features of the proximal tubule. As detailed in the introduction, these include: proteins such as alkaline phosphatase, gamma glutamyltranspeptidase, leucine aminopeptidase, acid

phosphatase, cytokeratin, $\alpha_3\beta_1$ integrin and fibronectin; and functional markers such as, the cAMP responsiveness to parathyroid hormone but not antidiuretic hormone, Na^+-dependent, phlorizin-sensitive glucose transport, and the ability to accumulate glycogen. As such, the HK-2 cell line could be looked upon as a model system where EMT has progressed with regard to a loss of cell junctions and the E- to N-cadherin switch, but with the retainment of many features of proximal tubule differentiation. The HK-2 cell line may be very valuable in elucidating pro-fibrotic factors and in defining the changes necessary for the HK-2 cells to gain further mesenchymal differentiation.

There is also convincing evidence that the differences between the HPT and HK-2 cell line is not an anomaly of the isolation protocol used to develop the HK-2 cell line. The HK-2 cell line is derived from a single clone of cells following transfection with the HPV E6/E7 genes as designated in the ATCC product sheet and the original publication (Ryan et al., 1994) . Thus, a simple explanation for the finding that HK-2 cells have no tight junctions and have undergone an E- to N-cadherin switch is that the HK-2 cell line was derived from an aberrant single cell that possessed these properties in the original primary culture used for isolation of the cell line. Under this scenario, the originating cell would not have been representative of the cells within the primary culture that were able to form domes. However, if the above were the case, the HK-2 cell would not be expected to be able to undergo MET and regain the original characteristics of the cells of the primary culture that are able to form domes.

HK-2 Cells Undergo MET Mediated by MT-3

Studies from this laboratory have shown that the HK-2 cells can undergo MET and regain the features expected of primary cultures of human proximal tubule cells

(Bathula et al., 2008; Kim et al., 2002). This was accomplished by the stable transfection of the MT-3 gene into the HK-2 cell line. The HK-2 cells transfected with the MT-3 gene regained the ability to form domes in culture, displayed increased transepithelial resistance, and a switch from N-cadherin to E-cadherin expression. The present studies also demonstrated that the MT-3 transfected cells regained the expression of the gap junction protein connexin 32, similar to that found in primary cultures. These studies show that the HK-2 cell line can undergo MET and convert back to those phenotypic and genotypic properties of the original primary culture. In addition, the ability of the MT-3 gene to induce MET in HK-2 cells provides a model for the study of MET in the proximal tubule and also might uncover mechanistic approaches to halt the pro-fibrotic microenvironment of the kidney if it indeed wholly or partially develops from EMT of tubular epithelium. There appears to be many more models for the study of renal EMT than that of MET in the adult kidney.

The finding that MT-3 elicited MET-like changes in HK-2 cells was not based on a mechanistic hypothesis regarding EMT or MET. Rather, the laboratory was studying the possible role of the MT-3 gene in cadmium-induced renal toxicity. There is no other existing literature to suggest a role of MT-3 in renal EMT or MET. There is also no literature on how MT-3 might interact with the HPV E6 and E7 genes to promote MET in HK-2 cells. However, MT-3 has two unique sequences that help define the epitope of its participation in EMT and MET. The MT-3 isoform is unique among the MT gene family and these differences from other family members have been highlighted in past reports from this laboratory (Bathula et al., 2008; Kim et al., 2002; Seema Somji et al., 2004). Of importance in the present study is that MT-3 possesses 7 additional amino acids that

are not present in any other member of the MT gene family, a 6 amino acid C-terminal sequence and a Thr in the N-terminal region (Palmiter, 1992; Tsuji, Kobayashi, & Uchida, 1992; Uchida et al., 1991). The current study shows that a unique C-terminal amino acid insert of MT-3 was required to re-establish vectorial active transport and the shift in E- and N-cadherin expression for the HK-2 cells. This would be the first study to define a functional significance to this unique sequence of the MT-3 protein. The only other study was one designed to define how the C-terminal insert in MT-3 would alter metal binding characteristics compared to other members of the MT gene family (Zheng, Yang, Yu, & Cai, 2003). This study demonstrated that the C-terminal hexapeptide insert would lower the stability of the MT-3 α-domain metal-thiolate cluster; an alteration that would render the metal binding site more accessible for metal exchange with potential protein partners. Overall, the present study demonstrates the essential nature of the C-terminal sequence by both deletion of the sequence from the MT-3 gene and by insertion of the sequence into the MT-1E isoform, which resulted in the loss of dome formation and the establishment of dome formation in transfected HK-2 cells, respectively.

MT-3 Interacts with Proteins that Promote an Epithelial Phenotype

The regulation of cytoskeletal organization is an important feature for polarized epithelial cells; apical-basolateral polarity is vital for vectorial active ion transport, intercellular communication, tissue organization, and general cellular homeostasis. Cells that lose lateral cell-cell contacts display impaired cell polarity. Further, formation of lamellipodia protrusions is crucial step in the acquisition of migration. Under normal physiological conditions, homeostasis is promoted by the maintenance of cytoskeletal organization and essential structural components that promote cell shape while also

facilitating cell-cell and cell-extracellular matrix anchorages.

Myosin-IIA is a member of the type II non-muscle myosin family of proteins and is coded for by the *MYH9* gene. This isoform is a conventional heavy chain containing an IQ domain and a myosin-head like domain that is intricately involved in regulation of the actin cytoskeleton, affecting cytokinesis, cell motility, and maintenance of cell shape. Defects in the MYH9 gene have been associated with several types of CKD including sickle cell disease nephropathy, chronic glomerulonephritis, focal segmental glomerulonephritis, diabetic and non-diabetic nephropathies (Ashley-Koch et al., 2011; Cooke et al., 2012; Kao et al., 2008; Kopp et al., 2008; Singh, Nainani, Arora, & Venuto, 2009). During the initiation of cell migration, cells extend their plasma membranes in the form of lamellipodia that requires cytoskeletal reorganization. During this process monomeric G-actin polymerizes into F-actin filaments and is reorganized and depolymerized. Non-muscle myosin II associates with F-actin, and is known to generate contractile forces and tension. There are three-Type II non-muscle myosin members, myosin IIA, IIB, and IIC, coded for by *MYH9, MYH10,* and *MYH14* respectively. Myosin IIA appears to have an opposite function to myosin IIB, acting to confer contractile and retrograde force at the cell margin while IIB confers protrusive force at the cell margin (Betapudi, 2010). Myosin IIa may play a role in the prevention of cell migration, promoting the maintenance of epithelial cell shape though cytoskeletal organization,

Tropomyosin alpha-3 chain, coded for by TPM3, binds to actin filaments in both muscle and non-muscle cells. In non-muscle cells tropomyosin-3 stabilizes cytoskeletal actin filaments and regulate the access of the other actin binding proteins. Tropomyosin-

3 is protective against actin filament depolymerization. Additionally, this protein has been found at the brush border of epithelial cells of the intestine and kidney, and is not found in association with the leading edge migratory lamellipodia, but rather at the base or rear portion. Tropomyosin prevents myosin IIB access to the actin filament, which antagonizes the pro-migratory action of myosin IIB. Working together, tropomyosin-3 and myosin IIA aid in the maintenance of the actin cytoskeleton promoting epithelial cell polarity, a feature we propose MT-3 to contribute to in human proximal tubule cells.

Enolase-1, coded for by the *ENO1* gene, is a metal activated enzyme that catalyzes the dehydration of 2-phosphoglycerate to phosphoenolpyruvate in glycolysis. There are three isoforms of enolase including non-neuronal enolase (enolase-1 or α-enolase); neuron-specific enolase (enolase-2 or γ-enolase); and muscle-specific enolase (enolase-3 or β-enolase). These proteins occur as dimers, with the two monomer subunits orient in an antiparallel manner. The dimerization process is dependent on two magnesium ions, and these divalent cations play a critical role in catalysis (Díaz-Ramos, 2012). These enzymes also bind strongly to zinc ions, however enzyme activity is decreased when bound to these divalent cations (Ghazi et al., 2010). Enolase-1 occurs only as a homodimer (αα), is localized predominantly to the cytoplasm, but can also translocate to the apical plasma membrane and act as a plasminogen receptor. Overexpression of enolase has been associated with a plethora of diseases ranging from AD, cancer, as well as autoimmune diseases rheumatoid arthritis and primary nephropathies from lupus nephritis.(Bruschi et al., 2014). Enolase-1 has also been demonstrated to bind to F-actin microtubules (Walsh, Keith, & Knull, 1989). Further, α-enolase knockdown in tumor derived cell lines increased their sensitivity to

microtubule targeted drugs (Georges, Bonneau, & Prinos, 2011). With respect to MT-3 interactions with enolase-1, it is possible that MT-3 is acting as a zinc donor to facilitate homodimer formation , metal exchange to reduce the enzyme activity, or participating thiol-disulfide exchange (Meloni et al., 2007).

Aldolase A, coded for by ALDOA gene, is an enzyme that catalyzes the conversion of fructose-1,6-bisphosphate to glyceraldehyde 3-phosphate and dihydroxyacetone phosphate in glycolysis (and the reverse reaction during gluconeogenesis). Aldolase-A has been demonstrated to directly interact with both F-actin and enolase-1 (Walsh et al., 1989). Aldolase-A plays a role in actin cytoskeleton organization, regulating actin remodeling though interactions with ADP-ribosylation factor, Arf6 and guanine nucleotide exchange factor, ARNO (D'Souza-Schorey & Chavrier, 2006). Probably acting as a scaffolding protein, aldolase-a plays a role in the coordination of membrane trafficking, and cytoskeleton dynamics at the cell periphery (Merkulova et al., 2011). Alternatively, these protein interactions have a demonstrated role in the regulation of the endosomal/lysosomal protein degradation pathway (Casanova, 2007) so it is possible that the purpose of this interaction is to shuttle MT-3 to the lysosome for degradation.

BIBLIOGRAPHY

Alami, J., Williams, B., & Yeger, H. (2003). Differential expression of E-cadherin and β catenin in primary and metastatic Wilms's tumours. *Molecular Pathology*. Retrieved from http://www.ncbi.nlm.nih.gov/pmc/articles/PMC1187324/

Alpers, C., & Hudkins, K. (1994). Human renal cortical interstitial cells with some features of smooth muscle cells participate in tubulointerstitial and crescentic glomerular injury. *Journal of the American* ….. Retrieved from http://jasn.asnjournals.org/content/5/2/201.short

Ashley-Koch, A. E., Okocha, E. C., Garrett, M. E., Soldano, K., De Castro, L. M., Jonassaint, J. C., … Telen, M. J. (2011). MYH9 and APOL1 are both associated with sickle cell disease nephropathy. *British Journal of Haematology*, *155*(3), 386–94. http://doi.org/10.1111/j.1365-2141.2011.08832.x

Bai, S., Zeng, R., Zhou, Q., & Liao, W. (2012). Cdc42-interacting protein-4 promotes TGF-B1-induced epithelial-mesenchymal transition and extracellular matrix deposition in renal proximal tubular. ... *Journal of Biological* ….. Retrieved from http://www.ncbi.nlm.nih.gov/pmc/articles/PMC3385008/

Bathula, C., Garrett, S., & Zhou, X. (2008). Cadmium, vectorial active transport, and MT-3–dependent regulation of cadherin expression in human proximal tubular cells. *Toxicological* ….. Retrieved from http://toxsci.oxfordjournals.org/content/102/2/310.short

Bedford, J., Leader, J., & Walker, R. (2003). Aquaporin expression in normal human kidney and in renal disease. *Journal of the American* ….. Retrieved from http://jasn.asnjournals.org/content/14/10/2581.short

Berzal, S., Alique, M., & Ruiz-Ortega, M. (2012). GSK3, snail, and adhesion molecule regulation by cyclosporine A in renal tubular cells. *Toxicological* ….. Retrieved from http://toxsci.oxfordjournals.org/content/127/2/425.short

Betapudi, V. (2010). Myosin II motor proteins with different functions determine the fate of lamellipodia extension during cell spreading. *PloS One*, *5*(1), e8560. http://doi.org/10.1371/journal.pone.0008560

Bohle, A., Müller, G. A., Wehrmann, M., Mackensen-Haen, S., & Xiao, J. C. (1996). Pathogenesis of chronic renal failure in the primary glomerulopathies, renal vasculopathies, and chronic interstitial nephritides. *Kidney International. Supplement*, *54*, S2–9. Retrieved from http://www.ncbi.nlm.nih.gov/pubmed/8731185

Bridges, C. C., & Zalups, R. K. (2005). Molecular and ionic mimicry and the transport of toxic metals. *Toxicology and Applied Pharmacology*, *204*(3), 274–308. http://doi.org/10.1016/j.taap.2004.09.007

Bruschi, M., Sinico, R. A., Moroni, G., Pratesi, F., Migliorini, P., Galetti, M., … Ghiggeri, G. M. (2014). Glomerular autoimmune multicomponents of human lupus nephritis in vivo: α-enolase and annexin AI. *Journal of the American Society of Nephrology : JASN*, *25*(11), 2483–98. http://doi.org/10.1681/ASN.2013090987

Casanova, J. E. (2007). Regulation of arf activation: the sec7 family of guanine nucleotide exchange factors. *TRAFFIC*, *8*(11), 1476–1485. http://doi.org/10.1111/j.1600-0854.2007.00634.x

Cho, E., Patterson, L., & Brookhiser, W. (1998). Differential expression and function of cadherin-6 during renal epithelium development. …. Retrieved from http://dev.biologists.org/content/125/5/803.short

Coca, S., Yusuf, B., & Shlipak, M. (2009). Long-term risk of mortality and other adverse outcomes after acute kidney injury: a systematic review and meta-analysis. *American Journal of* …. Retrieved from http://www.sciencedirect.com/science/article/pii/S0272638609000791

Cooke, J. N., Bostrom, M. A., Hicks, P. J., Ng, M. C. Y., Hellwege, J. N., Comeau, M. E., … Bowden, D. W. (2012). Polymorphisms in MYH9 are associated with diabetic nephropathy in European Americans. *Nephrology, Dialysis, Transplantation : Official Publication of the European Dialysis and Transplant Association - European Renal Association*, *27*(4), 1505–11. http://doi.org/10.1093/ndt/gfr522

D'Souza-Schorey, C., & Chavrier, P. (2006). ARF proteins: roles in membrane traffic and beyond. *NATURE REVIEWS MOLECULAR CELL BIOLOGY*, *7*(5), 347–358. http://doi.org/10.1038/nrm1910

Detrisac, C., Sens, M., Garvin, A., Spicer, S., & Sens, D. (1984). Tissue culture of human kidney epithelial cells of proximal tubule origin. *Kidney Int*. Retrieved from http://www.nature.com/ki/journal/v25/n2/abs/ki198428a.html

Díaz-Ramos, À. (2012). α-Enolase, a multifunctional protein: its role on pathophysiological situations. *BioMed Research* …. Retrieved from http://downloads.hindawi.com/journals/biomed/2012/156795.pdf

Ding, W., Yang, L., Zhang, M., & Gu, Y. (2012). Reactive oxygen species-mediated endoplasmic reticulum stress contributes to aldosterone-induced apoptosis in tubular epithelial cells. *Biochemical and Biophysical Research* …. Retrieved from http://www.sciencedirect.com/science/article/pii/S0006291X12000605

Ding, Z., Teng, X., Cai, B., & Wang, H. (2006). Mutation at Glu23 eliminates the neuron growth inhibitory activity of human metallothionein-3. *Biochemical and …*. Retrieved from http://www.sciencedirect.com/science/article/pii/S0006291X06018882

Docherty, N., & Calvo, I. (2009). Increased E-cadherin expression in the ligated kidney following unilateral ureteric obstruction. *Kidney …*. Retrieved from http://www.nature.com/ki/journal/v75/n2/abs/ki2008482a.html

Dudas, P., Argentieri, R., & Farrell, F. (2009). BMP-7 fails to attenuate TGF-β1-induced epithelial-to-mesenchymal transition in human proximal tubule epithelial cells. *Nephrology Dialysis …*. Retrieved from http://ndt.oxfordjournals.org/content/24/5/1406.short

Dudas, P., & Sague, S. (2011). Proinflammatory/profibrotic effects of interleukin-17A on human proximal tubule epithelium. *Nephron Experimental …*. Retrieved from http://www.karger.com/Article/FullText/320177

Durand, J., Meloni, G., Talmard, C., Vašák, M., & Faller, P. (2010). Zinc release of Zn_7 -metallothionein-3 induces fibrillar type amyloid-β aggregates. *Metallomics : Integrated Biometal Science*, *2*(11), 741–4. http://doi.org/10.1039/c0mt00027b

Eddy, A. A., & Neilson, E. G. (2006). Chronic kidney disease progression. *Journal of the American Society of Nephrology : JASN*, *17*(11), 2964–6. http://doi.org/10.1681/ASN.2006070704

Eneling, K., Brion, L., Pinto, V., & Pinho, M. (2012). Salt-inducible kinase 1 regulates E-cadherin expression and intercellular junction stability. *The FASEB Journal*. Retrieved from http://www.fasebj.org/content/26/8/3230.short

Esteban, M., Tran, M., & Harten, S. (2006). Regulation of E-cadherin expression by VHL and hypoxia-inducible factor. *Cancer Research*. Retrieved from http://cancerres.aacrjournals.org/content/66/7/3567.short

FINE, L. G., ONG, A. C. M., & NORMAN, J. T. (1993). Mechanisms of tubulo-interstitiaI injury in progressive renal diseases. *European Journal of Clinical Investigation*, *23*(5), 259–265. http://doi.org/10.1111/j.1365-2362.1993.tb00771.x

Fine, L., Norman, J., & Ong, A. (1995). Cell-cell cross-talk in the pathogenesis of renal interstitial fibrosis. *Kidney International. Supplement*. Retrieved from http://europepmc.org/abstract/med/7674594

Garrett, S. H., Phillips, V., Somji, S., Sens, M. A., Dutta, R., Park, S., … Sens, D. A. (2002). Transient induction of metallothionein isoform 3 (MT-3), c-fos, c-jun and c-myc in human proximal tubule cells exposed to cadmium. *Toxicology Letters*,

126(1), 69–80. http://doi.org/10.1016/S0378-4274(01)00448-9

Garrett, S. H., Sens, M. A., Todd, J. H., Somji, S., & Sens, D. A. (1999). Expression of MT-3 protein in the human kidney. *Toxicology Letters*, *105*(3), 207–214. http://doi.org/10.1016/S0378-4274(99)00003-X

Garrett, S. H., Somji, S., Todd, J. H., & Sens, D. A. (1998). Exposure of human proximal tubule cells to cd2+, zn2+, and Cu2+ induces metallothionein protein accumulation but not metallothionein isoform 2 mRNA. *Environmental Health Perspectives*, *106*(9), 587–95. Retrieved from http://www.pubmedcentral.nih.gov/articlerender.fcgi?artid=1533161&tool=pmcentrez&rendertype=abstract

Georges, E., Bonneau, A., & Prinos, P. (2011). RNAi-mediated knockdown of α-enolase increases the sensitivity of tumor cells to antitubulin chemotherapeutics. *International Journal of* …. Retrieved from http://www.ncbi.nlm.nih.gov/pmc/articles/PMC3242425/

Ghazi, I. El, Martin, B., & Armitage, I. (2010). New proteins found interacting with brain metallothionein-3 are linked to secretion. *International Journal of Alzheimer's* …. Retrieved from http://www.hindawi.com/journals/ijad/2011/208634/abs/

Gobe, G., & Crane, D. (2010). Mitochondria, reactive oxygen species and cadmium toxicity in the kidney. *Toxicology Letters*, *198*(1), 49–55. http://doi.org/10.1016/j.toxlet.2010.04.013

Grabias, B., & Konstantopoulos, K. (2012). Epithelial-mesenchymal transition and fibrosis are mutually exclusive reponses in shear-activated proximal tubular epithelial cells. *The FASEB Journal*. Retrieved from http://www.fasebj.org/content/26/10/4131.short

Guillén- Gómez, E. (2012). New role of the human equilibrative nucleoside transporter 1 (hENT1) in Epithelial- to- mesenchymal transition in renal tubular cells. *Journal of Cellular* …. Retrieved from http://onlinelibrary.wiley.com/doi/10.1002/jcp.22869/full

Hinz, B., Phan, S. H., Thannickal, V. J., Galli, A., Bochaton-Piallat, M.-L., & Gabbiani, G. (2007). The myofibroblast: one function, multiple origins. *The American Journal of Pathology*, *170*(6), 1807–16. http://doi.org/10.2353/ajpath.2007.070112

Huby, A., Rastaldi, M., & Caron, K. (2009). Restoration of podocyte structure and improvement of chronic renal disease in transgenic mice overexpressing renin. *PLoS One*. Retrieved from http://dx.plos.org/10.1371/journal.pone.0006721

Humphreys, B., & Lin, S. (2010). Fate tracing reveals the pericyte and not epithelial

origin of myofibroblasts in kidney fibrosis. *The American Journal of* …. Retrieved from http://www.sciencedirect.com/science/article/pii/S0002944010603276

Jung, K., Dean, D., Jiang, J., & Gaylor, S. (2004). Loss of N-cadherin and α-catenin in the proximal tubules of aging male Fischer 344 rats. *Mechanisms of Ageing* …. Retrieved from http://www.sciencedirect.com/science/article/pii/S0047637404000739

Kao, W. H. L., Klag, M. J., Meoni, L. A., Reich, D., Berthier-Schaad, Y., Li, M., … Parekh, R. S. (2008). MYH9 is associated with nondiabetic end-stage renal disease in African Americans. *Nature Genetics*, *40*(10), 1185–92. http://doi.org/10.1038/ng.232

KEMPSON, S. (1986). PROXIMAL TUBULE CHARACTERISTICS OF CULTURED HUMAN RENAL-CORTEX EPITHELIUM. *IN VITRO* …. Retrieved from https://scholar.google.com/scholar_lookup?title=Proximal+tubule+characteristics+of+cultured+human+renal+cortex+epithelium&author=Kempson&publication_year=1989#0

Kim, D., Garrett, S. H., Sens, M. A., Somji, S., & Sens, D. A. (2002). Metallothionein isoform 3 and proximal tubule vectorial active transport. *Kidney International*, *61*(2), 464–72. http://doi.org/10.1046/j.1523-1755.2002.00153.x

Kirk, A., Campbell, S., & Bass, P. (2010). Differential expression of claudin tight junction proteins in the human cortical nephron. *Nephrology Dialysis* …. Retrieved from http://ndt.oxfordjournals.org/content/early/2010/02/01/ndt.gfq006.short

Kiuchi-Saishin, Y., & Gotoh, S. (2002). Differential expression patterns of claudins, tight junction membrane proteins, in mouse nephron segments. *Journal of the* …. Retrieved from http://jasn.asnjournals.org/content/13/4/875.short

Klaassen, C. D., Liu, J., & Diwan, B. A. (2009). Metallothionein protection of cadmium toxicity. *Toxicology and Applied Pharmacology*, *238*(3), 215–20. http://doi.org/10.1016/j.taap.2009.03.026

Kopp, J. B., Smith, M. W., Nelson, G. W., Johnson, R. C., Freedman, B. I., Bowden, D. W., … Winkler, C. A. (2008). MYH9 is a major-effect risk gene for focal segmental glomerulosclerosis. *Nature Genetics*, *40*(10), 1175–84. http://doi.org/10.1038/ng.226

Langner, C., Ratschek, M., & Rehak, P. (2004). Expression of MUC1 (EMA) and E-cadherin in renal cell carcinoma: a systematic immunohistochemical analysis of 188 cases. *Modern* …. Retrieved from http://www.nature.com/modpathol/journal/v17/n2/abs/3800032a.html

Li, Q., Liu, B., Lv, L., & Ma, K. (2011). Monocytes induce proximal tubular epithelial–mesenchymal transition through NF- kappa B dependent upregulation of ICAM- 1. *Journal of Cellular* …. Retrieved from http://onlinelibrary.wiley.com/doi/10.1002/jcb.23074/full

Li, Y., Zhang, J., Fang, L., Luo, P., Peng, J., & Du, X. (2010). Lefty A attenuates the TGF-β1-induced epithelial to mesenchymal transition of human renal proximal epithelial tubular cells. *Molecular and Cellular* …. Retrieved from http://link.springer.com/article/10.1007/s11010-010-0389-6

Lin, H., Wang, D., Wu, T., & Dong, C. (2011). Blocking core fucosylation of TGF-β1 receptors downregulates their functions and attenuates the epithelial-mesenchymal transition of renal tubular cells. *American Journal of* …. Retrieved from http://ajprenal.physiology.org/content/300/4/F1017.short

Lin, S.-L., Kisseleva, T., Brenner, D. A., & Duffield, J. S. (2008). Pericytes and perivascular fibroblasts are the primary source of collagen-producing cells in obstructive fibrosis of the kidney. *The American Journal of Pathology*, *173*(6), 1617–27. http://doi.org/10.2353/ajpath.2008.080433

Liu, J., Liu, Y., Habeebu, S. S., & Klaassen, C. D. (1998). Susceptibility of MT-null mice to chronic CdCl2-induced nephrotoxicity indicates that renal injury is not mediated by the CdMT complex. *Toxicological Sciences : An Official Journal of the Society of Toxicology*, *46*(1), 197–203. http://doi.org/10.1006/toxs.1998.2541

Liu, Y. (2009). New Insights into Epithelial-Mesenchymal Transition in Kidney Fibrosis. *Journal of the American Society of Nephrology*, *21*(2), 212–222. http://doi.org/10.1681/ASN.2008121226

Masola, V., Gambaro, G., & Tibaldi, E. (2012). Heparanase and syndecan-1 interplay orchestrates fibroblast growth factor-2-induced epithelial-mesenchymal transition in renal tubular cells. *Journal of Biological* …. Retrieved from http://www.jbc.org/content/287/2/1478.short

Meloni, G., Faller, P., & Vasák, M. (2007). Redox silencing of copper in metal-linked neurodegenerative disorders: reaction of Zn7metallothionein-3 with Cu2+ ions. *The Journal of Biological Chemistry*, *282*(22), 16068–78. http://doi.org/10.1074/jbc.M701357200

Meloni, G., Polanski, T., Braun, O., & Vasák, M. (2009). Effects of Zn(2+), Ca(2+), and Mg(2+) on the structure of Zn(7)metallothionein-3: evidence for an additional zinc binding site. *Biochemistry*, *48*(24), 5700–7. http://doi.org/10.1021/bi900366p

Meloni, G., & Vašák, M. (2009). Control of Abnormal Metal-Protein Interactions in

Neurodegenerative Disorders by Metallothionein-3. *CHIMIA International Journal for Chemistry*, *63*(4), 211–213. http://doi.org/10.2533/chimia.2009.211

Merkulova, M., Hurtado-Lorenzo, A., Hosokawa, H., Zhuang, Z., Brown, D., Ausiello, D. A., & Marshansky, V. (2011). Aldolase directly interacts with ARNO and modulates cell morphology and acidic vesicle distribution. *American Journal of Physiology. Cell Physiology*, *300*(6), C1442–55. http://doi.org/10.1152/ajpcell.00076.2010

Mori, K., Lee, H., & Rapoport, D. (2005). Endocytic delivery of lipocalin-siderophore-iron complex rescues the kidney from ischemia-reperfusion injury. *Journal of Clinical* …. Retrieved from http://www.ncbi.nlm.nih.gov/pmc/articles/pmc548316/

Nouwen, E., & Dauwe, S. (1993). Stage-and segment-specific expression of cell-adhesion molecules N-CAM, A-CAM and L-CAM in the kidney. *Kidney International*. Retrieved from http://www.nature.com/ki/journal/v44/n1/abs/ki1993225a.html

Nürnberger, J., & Feldkamp, T. (2010). N-cadherin is depleted from proximal tubules in experimental and human acute kidney injury. *Histochemistry and Cell* …. Retrieved from http://link.springer.com/article/10.1007/s00418-010-0702-1

Palmiter, R. (1992). MT-III, a brain-specific member of the metallothionein gene family. *Proceedings of the* …. Retrieved from http://www.pnas.org/content/89/14/6333.short

Picard, N., Baum, O., Vogetseder, A., Kaissling, B., & Le Hir, M. (2008). Origin of renal myofibroblasts in the model of unilateral ureter obstruction in the rat. *Histochemistry and Cell Biology*, *130*(1), 141–55. http://doi.org/10.1007/s00418-008-0433-8

Piepenhagen, P. A., & Nelson, W. J. (1998). Biogenesis of polarized epithelial cells during kidney development in situ: roles of E-cadherin-mediated cell-cell adhesion and membrane cytoskeleton organization. *Molecular Biology of the Cell*, *9*(11), 3161–77. Retrieved from http://www.pubmedcentral.nih.gov/articlerender.fcgi?artid=25604&tool=pmcentrez&rendertype=abstract

Prozialeck, W. C. (2000). Evidence that E-cadherin may be a target for cadmium toxicity in epithelial cells. *Toxicology and Applied Pharmacology*, *164*(3), 231–49. http://doi.org/10.1006/taap.2000.8905

Prozialeck, W. C., & Edwards, J. R. (2012). Mechanisms of cadmium-induced proximal tubule injury: new insights with implications for biomonitoring and therapeutic

interventions. *The Journal of Pharmacology and Experimental Therapeutics*, *343*(1), 2–12. http://doi.org/10.1124/jpet.110.166769

Prozialeck, W. C., Lamar, P. C., & Lynch, S. M. (2003). Cadmium alters the localization of N-cadherin, E-cadherin, and beta-catenin in the proximal tubule epithelium. *Toxicology and Applied Pharmacology*, *189*(3), 180–95. Retrieved from http://www.ncbi.nlm.nih.gov/pubmed/12791303

Prozialeck, W., Lamar, P., & Appelt, D. (2004). Differential expression of E-cadherin, N-cadherin and beta-catenin in proximal and distal segments of the rat nephron. *BMC Physiology*. Retrieved from http://www.biomedcentral.com/1472-6793/4/10/

Prunotto, M., Budd, D. C., Gabbiani, G., Meier, M., Formentini, I., Hartmann, G., … Moll, S. (2012). Epithelial-mesenchymal crosstalk alteration in kidney fibrosis. *The Journal of Pathology*, *228*(2), 131–47. http://doi.org/10.1002/path.4049

Rigby Duncan, K. E., & Stillman, M. J. (2006). Metal-dependent protein folding: metallation of metallothionein. *Journal of Inorganic Biochemistry*, *100*(12), 2101–7. http://doi.org/10.1016/j.jinorgbio.2006.09.005

Romero-Isart, N., Jensen, L., & Zerbe, O. (2002). Engineering of metallothionein-3 neuroinhibitory activity into the inactive isoform metallothionein-1. *Journal of Biological …*. Retrieved from http://www.jbc.org/content/277/40/37023.short

Ryan, M., Johnson, G., & Kirk, J. (1994). HK-2: an immortalized proximal tubule epithelial cell line from normal adult human kidney. *Kidney …*. Retrieved from http://www.nature.com/ki/journal/v45/n1/abs/ki19946a.html

Sabolić, I., Breljak, D., Skarica, M., & Herak-Kramberger, C. M. (2010). Role of metallothionein in cadmium traffic and toxicity in kidneys and other mammalian organs. *Biometals : An International Journal on the Role of Metal Ions in Biology, Biochemistry, and Medicine*, *23*(5), 897–926. http://doi.org/10.1007/s10534-010-9351-z

Sarközi, R., Flucher, K., & Haller, V. (2012). Oncostatin M inhibits TGF-β1-induced CTGF expression via STAT3 in human proximal tubular cells. *Biochemical and …*. Retrieved from http://www.sciencedirect.com/science/article/pii/S0006291X12013253

Satarug, S., Garrett, S. H., Sens, M. A., & Sens, D. A. (2010). Cadmium, environmental exposure, and health outcomes. *Environmental Health Perspectives*, *118*(2), 182–90. http://doi.org/10.1289/ehp.0901234

Sens, D. A., Detrisac, C. J., Sens, M. A., Rossi, M. R., Wenger, S. L., & Todd, J. H. (1999). Tissue culture of human renal epithelial cells using a defined serum-free

growth formulation. *Experimental Nephrology*, *7*(5-6), 344–52. http://doi.org/20632

Sens, M. A., Somji, S., Lamm, D. L., Garrett, S. H., Slovinsky, F., Todd, J. H., & Sens, D. A. (2000). Metallothionein isoform 3 as a potential biomarker for human bladder cancer. *Environmental Health Perspectives*, *108*(5), 413–8. Retrieved from http://www.pubmedcentral.nih.gov/articlerender.fcgi?artid=1638035&tool=pmcentrez&rendertype=abstract

Sewell, A., Jensen, L., & Erickson, J. (1995). Bioactivity of Metallothionein-3 Correlates with Its Novel. beta. Domain Sequence Rather Than Metal Binding Properties. *Biochemistry*. Retrieved from http://pubs.acs.org/doi/abs/10.1021/bi00014a031

Shimazui, T., & Kojima, T. (2006). Expression profile of N-cadherin differs from other classical cadherins as a prognostic marker in renal cell carcinoma. *Oncology …*. Retrieved from http://www.spandidos-publications.com/or/15/5/1181

Singh, N., Nainani, N., Arora, P., & Venuto, R. C. (2009). CKD in MYH9-related disorders. *American Journal of Kidney Diseases : The Official Journal of the National Kidney Foundation*, *54*(4), 732–40. http://doi.org/10.1053/j.ajkd.2009.06.023

Slusser, A., Zheng, Y., Zhou, X. D., Somji, S., Sens, D. a, Sens, M. A., & Garrett, S. H. (2014). Metallothionein isoform 3 expression in human skin, related cancers and human skin derived cell cultures. *Toxicology Letters*. http://doi.org/10.1016/j.toxlet.2014.09.028

Somji, S., Garrett, S. H., Sens, M. A., Gurel, V., & Sens, D. a. (2004). Expression of metallothionein isoform 3 (MT-3) determines the choice between apoptotic or necrotic cell death in Cd+2-exposed human proximal tubule cells. *Toxicological Sciences*, *80*(2), 358–366. http://doi.org/10.1093/toxsci/kfh158

Somji, S., Garrett, S. H., Sens, M. A., & Sens, D. A. (2006). The unique N-terminal sequence of metallothionein-3 is required to regulate the choice between apoptotic or necrotic cell death of human proximal tubule cells exposed to Cd+2. *Toxicological Sciences : An Official Journal of the Society of Toxicology*, *90*(2), 369–76. http://doi.org/10.1093/toxsci/kfj089

Somji, S., Garrett, S. H., Toni, C., Zhou, X. D., Zheng, Y., Ajjimaporn, A., … Sens, D. a. (2011). Differences in the epigenetic regulation of MT-3 gene expression between parental and Cd+2 or As+3 transformed human urothelial cells. *Cancer Cell International*, *11*(1), 2. http://doi.org/10.1186/1475-2867-11-2

Somji, S., Garrett, S., Sens, M., & Sens, D. (2006). The unique N-terminal sequence of metallothionein-3 is required to regulate the choice between apoptotic or necrotic

cell death of human proximal tubule cells. *Toxicological Sciences*. Retrieved from http://toxsci.oxfordjournals.org/content/90/2/369.short

Sutherland, D. E. K., & Stillman, M. J. (2011). The "magic numbers" of metallothionein. *Metallomics : Integrated Biometal Science*, *3*(5), 444–63. http://doi.org/10.1039/c0mt00102c

Tang, W., Sadovic, S., & Shaikh, Z. A. (1998). Nephrotoxicity of cadmium-metallothionein: protection by zinc and role of glutathione. *Toxicology and Applied Pharmacology*, *151*(2), 276–82. http://doi.org/10.1006/taap.1998.8465

Thévenod, F. (2003). Nephrotoxicity and the proximal tubule. Insights from cadmium. *Nephron. Physiology*, *93*(4), p87–93. http://doi.org/70241

Todd, J. H., McMartin, K. E., & Sens, D. A. (1996). Enzymatic isolation and serum-free culture of human renal cells : retaining properties of proximal tubule cells. *Methods in Molecular Medicine*, *2*, 431–5. http://doi.org/10.1385/0-89603-335-X:431

Tsuji, S., Kobayashi, H., & Uchida, Y. (1992). Molecular cloning of human growth inhibitory factor cDNA and its down-regulation in Alzheimer's disease. *The EMBO …*. Retrieved from http://www.ncbi.nlm.nih.gov/pmc/articles/PMC556960/

Uchida, Y., Takio, K., Titani, K., Ihara, Y., & Tomonaga, M. (1991). The growth inhibitory factor that is deficient in the Alzheimer's disease brain is a 68 amino acid metallothionein-like protein. *Neuron*. Retrieved from http://www.sciencedirect.com/science/article/pii/0896627391902722

Vallee, B. L. (1979). Metallothionein: historical review and perspectives. *Experientia. Supplementum*, *34*, 19–39. Retrieved from http://www.ncbi.nlm.nih.gov/pubmed/400521

Vašák, M., & Meloni, G. (2011). Chemistry and biology of mammalian metallothioneins. *Journal of Biological Inorganic Chemistry : JBIC : A Publication of the Society of Biological Inorganic Chemistry*, *16*(7), 1067–78. http://doi.org/10.1007/s00775-011-0799-2

Veerasamy, M., & Nguyen, T. (2009). Differential regulation of E-cadherin and α-smooth muscle actin by BMP 7 in human renal proximal tubule epithelial cells and its implication in renal fibrosis. *American Journal of …*. Retrieved from http://ajprenal.physiology.org/content/297/5/F1238.short

Venkatachalam, M., & Griffin, K. (2010). Acute kidney injury: a springboard for progression in chronic kidney disease. *American Journal of …*. Retrieved from http://ajprenal.physiology.org/content/298/5/F1078.short

Vesey, D. A. (2010). Transport pathways for cadmium in the intestine and kidney proximal tubule: focus on the interaction with essential metals. *Toxicology Letters*, *198*(1), 13–9. http://doi.org/10.1016/j.toxlet.2010.05.004

Walsh, J. L., Keith, T. J., & Knull, H. R. (1989). Glycolytic enzyme interactions with tubulin and microtubules. *Biochimica et Biophysica Acta (BBA) - Protein Structure and Molecular Enzymology*, *999*(1), 64–70. http://doi.org/10.1016/0167-4838(89)90031-9

Wilson, P., & Dillingham, M. (1985). Defined human renal tubular epithelia in culture: growth, characterization, and hormonal response. *American Journal of …*. Retrieved from http://ajprenal.physiology.org/content/248/3/F436.short

Wu, C., Tsai, Y., Wu, M., Teng, S., & Wu, K. (2012). Epigenetic reprogramming and post-transcriptional regulation during the epithelial–mesenchymal transition. *Trends in Genetics*. Retrieved from http://www.sciencedirect.com/science/article/pii/S0168952512000807

Yuan, Y., Chen, Y., Zhang, P., & Huang, S. (2012). Mitochondrial dysfunction accounts for aldosterone-induced epithelial-to-mesenchymal transition of renal proximal tubular epithelial cells. *Free Radical Biology …*. Retrieved from http://www.sciencedirect.com/science/article/pii/S0891584912001864

Zeisberg, M., & Neilson, E. G. (2010). Mechanisms of tubulointerstitial fibrosis. *Journal of the American Society of Nephrology : JASN*, *21*(11), 1819–34. http://doi.org/10.1681/ASN.2010080793

Zheng, Q., Yang, W., Yu, W., & Cai, B. (2003). The effect of the EAAEAE insert on the property of human metallothionein- 3. *Protein …*. Retrieved from http://peds.oxfordjournals.org/content/16/12/865.short

Zhou, X. D., Sens, M. A., Garrett, S. H., Somji, S., Park, S., Gurel, V., & Sens, D. A. (2006). Enhanced expression of metallothionein isoform 3 protein in tumor heterotransplants derived from As+3- and Cd+2-transformed human urothelial cells. *Toxicological Sciences : An Official Journal of the Society of Toxicology*, *93*(2), 322–30. http://doi.org/10.1093/toxsci/kfl065

APPENDIX

METALLOTHIONEIN ISOFORM 3 EXPRESSION IN HUMAN SKIN, RELATED CANCERS AND HUMAN SKIN DERIVED CELL CULTURES

Abstract

Human skin is a well known target site of inorganic arsenic with effects ranging from hyperkeratosis to dermal malignancies. The current study characterizes the expression of a protein known to bind inorganic, As^{3+}, metallothionein 3 (MT-3). Expression of this protein was assessed immunohistochemically with a specific MT-3 antibody on human formalin-fixed, paraffin-embedded biopsy specimens in normal skin, squamous cell carcinoma (SCC), basal cell carcinoma (BCC) and melanoma. Assessment in normal skin using nine normal specimens showed moderate to intense MT-3 staining in epidermal karatinocytes with staining extending into the basal cells and moderate to intense staining in melanocytes of nevi. MT-3 immunoexpression was shown to be moderate to intense in 12 of 13 of SCC, low to moderate in 8 of 10 BCC, and moderate to intense in 12 melanoma samples. MT-3 expression in cell culture models (normal human epidermal keratinocytes, normal human melanocytes, and HaCaT cells) showed only trace expression of MT-3, while exposures to the histone deacytalase inhibitor, MS-275, partially restored expression levels. These results indicate that the epidermis of human skin and resulting malignancies express high level of MT-3 and potentially impact on the known association of arsenic exposure and the development of skin disorders and related cancers.

Introduction

Inorganic arsenic is a potent human carcinogen, and skin is known to be one of the most susceptible human organs affected by chronic environmental exposure to this

metalloid (Bolt, 2012). Chronic arsenic exposure causes a dry skin phenotype characterized by melanosis, hyperplasia and hyperkeratosis (Komissarova and Rossman, 2010). The most common arsenic-induced skin cancers include Bowen's disease (BD, SCC *in situ*), squamous cell carcinoma (SCC), and basal cell carcinoma (BCC) (Yeh et al., 1968). There is less evidence for a potential contribution of arsenic exposure to the development of melanoma. However, there is emerging evidence for such an association, especially for melanomas that might arise from co-exposure to ultraviolet radiation (Cooper et al., 2014, Pearce et al., 2012 and Dennis et al., 2010). Cell culture models have seen frequent use to investigate the mechanisms involved in arsenic-induced toxicity and cancer development due to the lack of valid animal models. These studies have led to several theories to explain the carcinogenic effects of arsenic exposure and include the generation of reactive oxygen species (ROS), oxidative DNA damage, genomic instability, aneuploidy, gene amplification, inhibition of DNA repair, and epigenetic dysregulation (Ren et al., 2011, Straif et al., 2009 and Lee et al., 2012). This laboratory is interested in how the metallothionein (MT) gene family might participate in the above processes that are associated with arsenic-induced carcinogenesis. A role for this family of proteins might be expected since all MT family members can bind and sequester 6 atoms of As^{+3} and can also serve as an antioxidant (Vasak and Meloni, 2011, Irvine et al., 2013 and Garla et al., 2013). In humans, there are four MT isoforms, designated MT-1 through MT-4. The MT-1 and MT-2 isoforms have been the subject of extensive study over the last 50 years and the subject of numerous reviews (see Vasak and Meloni, 2011). The MT-1 and MT-2 isoforms are inducible in almost all tissues by a variety of stress conditions and compounds including glucocorticoids, cytokines, ROS,

and metal ions. In contrast, the identification of the MT-3 and MT-4 isoforms is relatively recent (1990s) and both isoforms are largely unresponsive to the above inducers and their expression believed to be confined to far fewer tissue types. The four MT isoforms share a high degree of sequence homology and a specific antibody cannot be produced that can separately identify the MT-1, 2 and 4 isoforms. The MT-3 isoform is unique in that it possesses 7 additional amino acids that are not present in any other member of the MT gene family, a 6 amino acid C-terminal sequence and a Thr in the N-terminal region (Palmiter et al., 1992, Tsuji et al., 1992 and Uchida et al., 1991). An MT-3 specific antibody can be generated against the C-terminal sequence (Garrett et al., 1999). Functionally, MT-3 has also been shown to possess several activities not shared by the other MT isoforms. These include a neuronal cell growth inhibitory activity (Uchida et al., 1991), the participation in the regulation of EMT in human proximal tubule cells (Kim et al., 2002 and Kim et al., 2002), and the ability to influence the choice between apoptotic and necrotic cell death in proximal tubule cells exposed to cadmium (Somji et al., 2004). This non-duplication of function occurs despite a 63‑69% homology in amino acid sequence among MT-3 and the other human MT isoforms (Sewell et al., 1995). These unique features of MT-3, along with its ability to bind and sequester As^{+3}, motivated the present study designed to examine the expression of MT-3 in human skin and related skin cancers. A related question was to determine if human cell culture models used to study As^{+3} effects on skin faithfully recapitulate the *in situ* expression of MT-3.

Materials and Methods

Specimens of human skin

Specimens of normal human skin and associated cancers were obtained from archival paraffin blocks 10 years post diagnosis and scheduled for disposal as medical waste. These archival specimens contained no patient identifiers and are in the exempt category for human research. Tissues within these paraffin blocks were routinely fixed in 10% neutral buffered formalin for 16–18 h. The tissues were transferred to 70% ethanol and dehydrated in 100% ethanol. Dehydrated tissues were cleared in xylene, infiltrated, and embedded in paraffin. Tissue sections were cut at 3–5 μm for use in routine histology and immunohistochemical protocols.

Immunostaining for MT-3 in human skin and associated cancers

Serial sections were cut at 3–5 μm for use in immunohistochemical protocols. Staining was performed by a Leica Bond-Max automatic immunostainer. Major reagents for this procedure were contained in the Bond Polymer Refine Detection kit (Leica, DS9800). Paraffin sections were processed in the machine from deparaffinization to counterstaining by hematoxyline according to the manufacturer's recommended program settings with the following modifications. Briefly, the major steps in the protocol include deparaffinization, antigen retrieval for 20 min in Bond Epitope Retrieval Solution 1 (Leica, Catalog No AR9961), peroxide block for 5 min, incubation with rabbit anti-MT-3 antibody (1:200) for 25 min at room temperature, incubation with Post Primary for 10 min (source of the anti-rabbit IgG antibody), incubation with Polymer (source of the anti-rabbit Poly-HRP antibody) for 10 min, visualization with DAB (diaminobenzidine substrate for color development) for 10 min, counterstaining with

hematoxylin for 5 min. Slides were rinsed in distilled water, dehydrated in graded ethanol, cleared in xylene, and coverslipped.The presence and degree of MT-3 immunoreactivity in the specimens was judged by two pathologists. The scale used was 0 to +3 with 0 indicating no staining, +1 staining of mild intensity, +2 staining of moderate intensity, and +3 staining of strong intensity.

Cell culture

The HaCaT cell line was obtained from Cell Line Services (Eppelheim, Germany). HaCaT were initially isolated from normal skin of a 62 year old Caucasian male donor and spontaneously immortalized through p53 mutation; they are nontumorigenic *in vivo* (Boukamp et al., 1988). The cells were maintained in Dulbecco ' s Modified Eagles Medium (DMEM) supplemented with 4.5 g/L glucose, 2 mM L-glutamine, 10% v/v fetal bovine serum (FBS), 0.25 μ g/mL fungizone, 100 U/mL penicillin and 100 μ g/mL streptomycin. HaCaT cells were given fresh medium every 72 h and subcultured at a ratio of 1:5. Normal human epidermal keratinocyte (NHEK) primary cells were obtained from Lonza (Walkersville, MD). NHEK were isolated from a 68 year old Caucasian male donor. The cells were maintained in KBM-Gold (Lonza, Walkersville, MD) supplemented with KGM-Gold™-BulletKit™ (Lonza, # 00192060). NHEK were seeded at a density of 3500 cells/cm^2 and given fresh media the day after seeding and then every 48 h until reaching 70-80% confluency. The human epidermal melanocyte primary cells isolated from a light pigmented donor were obtained from Gibco (HEMa-LP) (Carlsbad, CA), and are referred to as normal human melanocytes (NHM). NHM cells were maintained in Medium 254 supplemented with PMA-free Human Melanocyte Growth Supplement-2 (HMGS-2, Gibco, # S-016-5) 0.25 μg/mL

fungizone, 100 U/mL penicillin and 100 µg/mL streptomycin. The cells were seeded at a density of 5000 cells/cm^2 and given fresh media the day after seeding and then every 48 h until reaching 80% confluency.

Treatment of cultured cells with 5-Aza-2-deoxycytidine and histone deacetylase inhibitor MS-275

HaCaT, NHEK and Primary Melanocytes were seeded at a 1:10 ratio and the next day they were treated with 1 or 3 μM 5-Aza-2′-deoxycytidine (5-AZC) (Sigma-Aldrich, St. Louis, MO) or 1, 3 or 10 μM MS-275 (ALEXIS Biochemicals, Lausen, Switzerland). The cells were allowed to grow to confluency and then harvested for RNA isolation.

RNA Isolation and RT-PCR analysis

Total RNA was isolated from the cells according to the protocol supplied with TRI REAGENT (Molecular Research Center, Inc. Cincinnati, OH) as described previously by this laboratory (Somji et al., 2006). Real time RT-PCR was used to measure the expression level of MT-3 mRNA utilizing a previously described MT-3 isoform-specific primer (Somji et al., 2006). For analysis, 1 μg was subjected to complementary DNA (cDNA) synthesis using the iScript cDNA synthesis kit (Bio-Rad Laboratories, Hercules, CA) in a total volume of 20 μl. Real-time PCR was performed utilizing the SYBR Green kit (Bio-Rad Laboratories) with 2 μl of cDNA, 0.2 μM primers in a total volume of 20 μl in an iCycler iQ real-time detection system (Bio-Rad Laboratories). Amplification was monitored by SYBR Green fluorescence and compared to that of a standard curve of the MT-3 isoform gene cloned into pcDNA3.1/hygro (+) and linearized with *Fsp* I. Cycling parameters consisted of denaturation at 95° C for

30 s and annealing at 65 ° C for 45 s which gave optimal amplification efficiency of each standard. The level of MT-3 expression was normalized to that of β-actin assessed by the same assay with the primer sequences being sense, CGACAACGGCTCCGGCATGT, and antisense, TGCCGTGCTCGATGGGGTACT, with the cycling parameters of annealing/extension at 62 ° C for 45 s and denaturation at 95 ° C for 15 s.

Results

MT-3 expression in human skin and related cancers

The expression of MT-3 was determined in normal human skin, *in situ* squamous cell carcinoma, squamous cell carcinoma, basal cell carcinoma, nevus, dysplastic nevus, *in situ* melanoma, superficial spreading melanoma, and deeply invasive melanoma (Table V-1). Nine independent specimens of human skin were evaluated for the expression of MT-3. All nine specimens displayed immunoreactivity for MT-3 in the epidermis. For each specimen, the immunoreactivity for MT-3 was uniform throughout the epidermis and included staining of the basal keratinocytes (Fig V-1A). Six of the specimens exhibited moderate to strong staining for MT-3 while the other 3 displayed mild to strong intensity of staining (Table V-1). All squamous cell carcinomas (SCC) exhibited staining for MT-3 (Table 1), five strongly (Fig 1C), six moderately (Fig V-1E), and one mild to moderate, whereas many of the basal cell carcinomas (BCC) exhibited low staining (Table 1) with two being totally devoid of MT-3 expression (Fig 2F), three weakly, and the rest (five samples) were either mild or mild to moderate (Fig 1D) in MT-3 staining. The staining of MT-3 was determined on 9 specimens of nevus.

Table V.

Immunostaining of MT-3 in Normal Skin, SCC[a], BCC[b], Nevi, and Melanoma

Sample #	Diagnosis	Intensity[c]	Percentage[d]	Comments[e]
T06-02611	normal skin	2-3+		
T06-04747	normal skin	2+		
T06-08104	normal skin	2-3+		
T06-12296	normal skin	2-3+		
T06-13822	normal skin	2-3+		
T06-15093	normal skin	1-2+		
T06-15738	normal skin	2-3+		
T06-16832	normal skin	1-2+		
T06-17515	normal skin	1-2+		
T06-05920-2	SCC	3+	90	normal skin 2+
T06-08560-1	SCC	2-3+	80	normal skin 2+
T06-10237-1	SCC	1+	60	normal skin 1-2+
T06-17492-3	SCC	2+	80	normal skin 2+
T06-18288	SCC	2-3+	90	no normal skin
T06-19042-2	SCC	2+	80	no normal skin
T07-02859-3	SCC	2-3+	70	normal skin 2+
T07-04441-1	SCC	2+	60	normal skin 2-3+
T07-05223-3	SCC	2+	80	normal skin 1+
T07-07073-2	SCC	1-2+	30	no normal skin
T08-11243	SCC	2+	60	normal skin 2+
T09-09643-1	SCC	2-3+	80	normal skin 2+
T06-13947-1	SCC, in situ	2+	80	no normal skin
T06-00002	BCC	0-1+	30	normal skin 1-2+
T06-03724-2	BCC	1+	60	no skin
T06-06686-8	BCC	0-1+	80	normal skin 1-2+
T06-06889	BCC	1-2+	80	normal skin 2+
T06-07160-2	BCC	0-1+	40	normal skin 2+
T06-08133-2	BCC	NEG	0	normal skin 1-2+
T06-09327-1	BCC	1+	60	normal skin 1-2+
T06-10671-1	BCC	1+	40	normal skin 1-2+
T07-00753-2	BCC	NEG	0	no normal skin
T07-07197-3	BCC	1-2+	60	normal skin 1-2+
T06-05434	nevus	2-3+	80	
T06-13829	nevus	2-3+	80	
T06-15352	nevus	2-3+	80	
T06-16045	nevus	2-3+	80	
T06-16174	nevus	2-3+	80	
T06-16832	nevus	2-3+	80	
T06-16983	nevus	2+	80	
T06-18076	nevus	2+	80	
T06-18753	nevus	2-3+	80	
T06-17364	dysplastic nevus	2-3+	80	
T06-02621	in situ melanoma	2-3+	80	
T06-09160	in situ melanoma	2-3+	80	
T06-11933	in situ melanoma	2-3+	80	
T06-08497	superficial spreading melanoma	2-3+	80	
T06-11336	superficial spreading melanoma	2-3+	80	
T06-11854	superficial spreading melanoma	2-3+	80	
T06-17070	superficial spreading melanoma	2-3+	80	
T06-02282	deeply invasive melanoma	2-3+	80	
T06-03697	deeply invasive melanoma	2-3+	80	
T06-05435	deeply invasive melanoma	2-3+	80	
T06-07039	deeply invasive melanoma	2-3+	80	
T06-16580	deeply invasive melanoma	2+	80	

The sample number indicates the case the tissue source is associated with. MT-3 reactivity was assessed in normal skin, basal cell carcinoma (BCC), squamous cell carcinoma, melanoma, and nevi (moles)

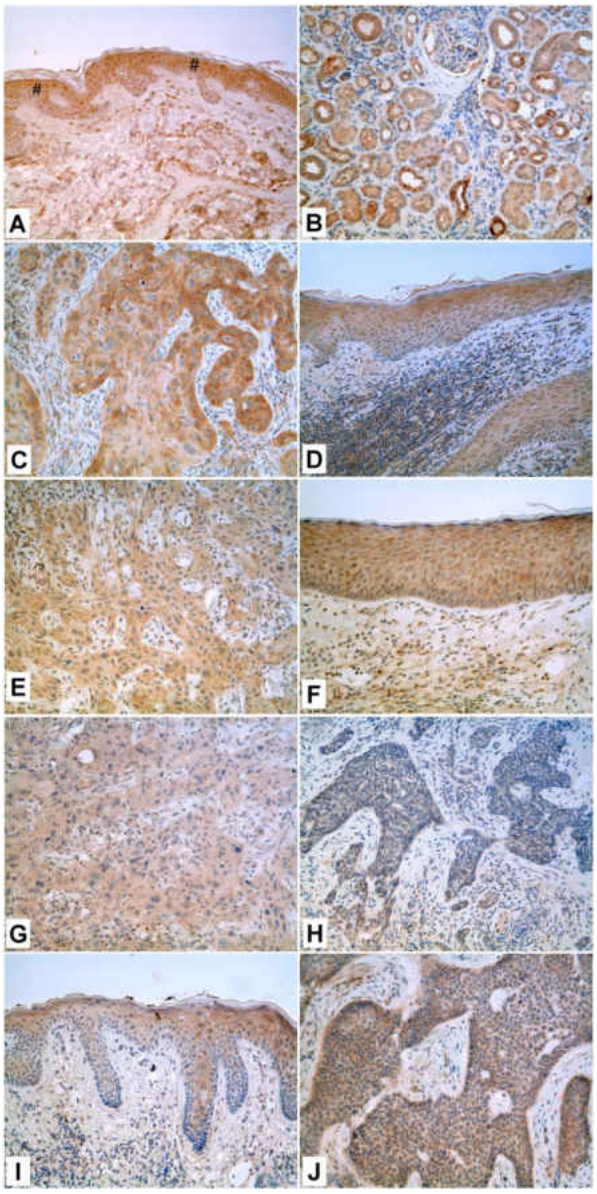

Figure V-1. Immunostaining of MT-3 in Skin Pigment Lesions. A: normal skin shows mild to moderate staining of MT in epidermis (#). In some cases the staining of MT-3 in epidermis can be moderate to strong (not shown); B: normal kidney as positive control; C: squamous cell carcinoma (SCC) (T06–5920) with strong staining of MT-3 (3 +); D: normal skin from the same slide in "C", showing moderate positivity of MT-3 (2 +); E: SCC (T07–4411) with mild staining of MT-3 (2 +); F: normal skin from the same slide as shown in "E", showing moderate staining of MT-3 (2 +); G: SCC (T06–10237) with mild staining of MT-3 (1 +); H: basal cell carcinoma (BCC) (T06–00002) with focal, very weak staining of MT-3 (0–1 +); I: Normal skin from the same slide as shown in "H", showing mild to moderate staining of MT-3 (1–2 +); J: BCC (T06–7889) with mild-moderate staining of MT-3 (1–2 +). All images taken at 200X magnification.

Staining for MT-3 was found for all 9 specimens, exhibited moderate to strong intensity, and was present in over 80% of the cells comprising the nevus (Table 1, Fig 2A). Staining of MT-3 was also performed on 1 case of dysplastic nevus and 3 cases of *in situ* melanoma. The staining was similar to that found in the nevus with all specimens displaying moderate to strong staining in over 80% of the cells (Table 1, Fig 2B). Staining of MT-3 was also performed on 4 cases of superficial spreading melanoma and 5 cases of deeply invasive melanoma. Again, the staining was similar to that found for *in situ* melanoma with moderate to strong staining of MT-3 in over 80% of the melanoma cells (Table V-1, Fig V-2C, D, E).

MT-3 expression in primary normal human keratinocytes (NHEK) and immortalized human HaCaT keratinocytes

Proliferating and confluent cultures of NHEK and HaCaT cells were assessed for their expression of MT-3 mRNA and protein. Real time PCR demonstrated that both resting and dividing NHEK and HaCaT cells had only background levels of MT-3 mRNA expression (Fig V-3A, B). Both sets of cells were also shown to express only background levels of MT-3 protein (data not shown). Both the NHEK and HaCaT cells were treated with MS-275, a histone deacetylase inhibitor, and 5-aza-2-deoxycytidine, a DNA methylation inhibitor, to determine if MT-3 expression might be silenced by a mechanism involving histone modification or DNA methylation. The results demonstrated that treatment with MS-275 was effective in restoring MT-3 mRNA expression in both the NHEK and HaCaT cells (Fig V-3A,B).

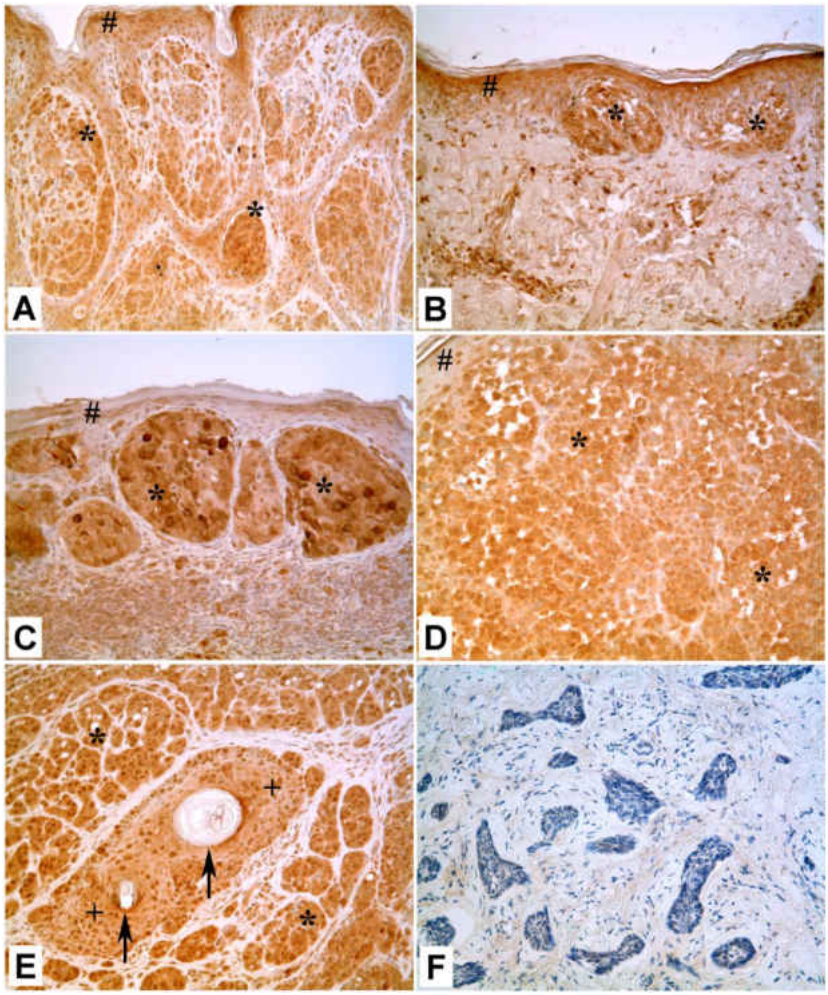

Figure V-2. Immunostaining of MT-3 in Nevi and Melanoma Cells. A: in this intradermal nevus, the neval cells, which located in the dermis, show moderate to strong expression of MT-3 (*). The epidermis at the top of the image is moderately positive for MT-3 (#); B: in this case of in situ melanoma, two nests of melanoma cells in the epidermis are moderately to strongly positive for MT-3 (*). The epidermis is moderately positive for MT-3 (#); C: in this superficial spreading melanoma, some melanoma nests, located in the superficial dermis, show strong staining of MT-3. The overlying epidermis is mildly positive for MT-3 (#); D: in this deeply invasive melanoma, the tumor cells are strongly positive for MT-3 (*). In the top-left corner is a small section of epidermis (#), which is mildly positive for MT-3 (#); E: another case of deeply invasive melanoma. In the center of this image is a hair follicle (+) with two keratin pearls (arrows) in it. The hair follicle shows moderate staining of MT-3. Around the follicle are nests of invasive melanoma cell (*), which show strong staining of MT-3. F: BCC (T06–8133) with negative staining of MT-3.

While MS-275 treatment was effective in both cell lines, MS-275 increased MT-3 mRNA levels in NHEK cells 10 to 20 fold greater than those of the HaCaT cell line. Treatment of the NHEK and HaCaT cells with 5-aza-2′ -deoxycytidine, resulted in a small, but statistically insignificant increase in MT-3 mRNA expression for both cell types (Fig V-3A, B).

MT-3 expression in normal human melanocytes (NHM)

Normal human melanocytes (from a light pigmented donor) were assessed in proliferating and confluent cultures for expression of MT-3 mRNA and protein. Both cell cultures showed only background levels of mRNA as demonstrated with real-time PCR (Fig V-3C) and only background levels of protein (data not shown).

In order to test for epigenetic regulation, cultures were treated with the histone deacetylase inhibitor, MS-275 and the DNA methylation inhibitor, 5-aza-20-doxycytidine. The results demonstrated that treatment with MS-275 was effective in restoring MT-3 mRNA expression in the NHM cells (Fig V-3C). Treatment of the HEMa-LP with 5-Aza-20-deoxycytidine, resulted in only a slight but statistically significant increase in MT-3 mRNA expression (Fig V-3C).

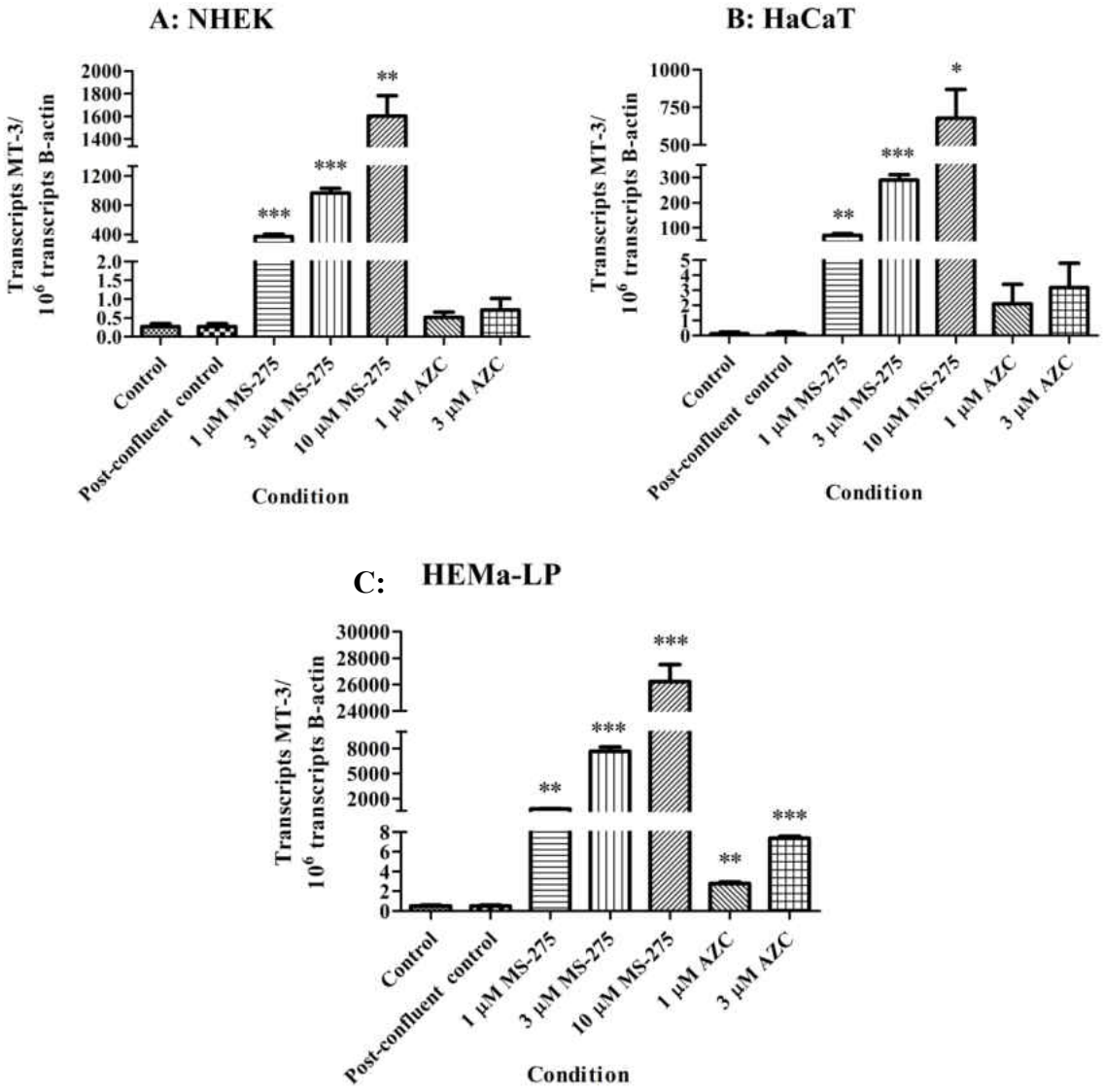

Figure V-3. Expression of MT-3 in primary normal human keratinocytes (NHEK), Immortalized Human Keratinocytes (HaCaT), and normal human melanocytes (HEMa-LP). NHEK (A) HaCaT (B) and HEMa-LP (C) cells were exposed to 1, 3, or 10 μM of the histone deacetylase inhibitor MS-275 for up to 72 h, or to 1 or 3 μM 5-azacytidine for 24 h. The post-confluent control was held at confluency for at least 72 h. Messenger RNA levels for MT-3 were assessed using real-time PCR and gene specific primers on RNA isolated from cells in culture. Expression levels are expressed as transcripts per 1000,000 transcripts of β-actin which was also assessed using real-time PCR. Significant differences from control groups are designated as **$p < 0.005$, ***$p < 0.0005$ as determined by student's unpaired t-test.

Discussion

The present study establishes that MT-3 is expressed in human skin. The immunoreactivity for MT-3 was present in all viable keratinocytes comprising the epidermis. The finding that MT-3 was present in the epidermal keratinocytes has a potential impact on the known association of arsenic exposure and the development of skin disorders and related cancers. All members of the MT gene family (MT-1, -2, -3 and -4) are known to bind heavy metals, including As^{+3} (Vasak and Meloni, 2011, Irvine et al., 2013 and Garla et al., 2013). Previous studies employing a monoclonal antibody against the E-9 epitope of the MT-1, -2, and -4 isoforms demonstrated that these 3 isoforms are poorly expressed in human skin and with expression restricted to the basal keratinocytes (Van den Oord and Delay, 1994, Karasawa et al., 1991 and Zamirska et al., 2012). The high sequence homology of these 3 isoforms prevents the generation of specific antibodies to the individual isoforms. In contrast, the present study shows that a large majority of keratinocytes in the epidermis of normal human skin are moderately to strongly immunoreativity for MT-3. These findings were consistent for 9 independent samples of human skin. The antibody used for the localization of MT-3 is specific since it was generated against the unique C-terminal amino acid sequence that is present only in this MT isoform (Garrett et al., 1999). The fact that human keratinocytes contain substantial levels of MT-3, and that MT-3 can bind As^{+3}, suggests a possible role for MT-3 in the selective accumulation and sequestering of As^{+3} in skin. One hypothesis to explain why skin is highly responsive to arsenic exposure and cancer development is that skin localizes and store As^{+3} due its high keratin content and the corresponding favorable interaction with sulfhydryl groups (Kitchen, 2001 and Lindgren et al., 1982). The current

finding suggests that MT-3 might play an additive, or possibly larger, role in the ability of skin to sequester and store As^{+3} in individuals chronically exposed to this metalloid. Evidence to support the concept that MT expression in a normal target tissue can elicit chronic effects can be found in the nephropathy associated with chronic exposure to cadmium. The MT-1 and MT-2 isoforms are predominantly expressed in the proximal tubules of the human kidney, and this expression is initiated during the early development of the kidney (Mididoddi et al., 1996). The MT-3 isoform is also expressed in the proximal tubules and other tubular elements of the human kidney (Garrett et al., 1999). The cortex of the human kidney has been shown to accumulate cadmium, as a function of age, in humans without occupational exposure (Satarug et al., 2002 and Satarug et al., 2010). Accumulation is assumed to occur through cadmium's interaction with MT and accumulation has been shown to reach a plateau at approximately 50 years of age. Despite the MT's being looked upon as having a protective role against heavy metal toxicity in general, and the proximal tubule in particular (Liu et al., 1995, Liu et al., 1998, Liu et al., 2000 and Masters et al., 1994), the fact remains that the kidney and the proximal tubule is the cell type critically affected by chronic exposure to cadmium (Andrews, 2000, Bernard et al., 1976, Bosco et al., 1986 and Gonich et al., 1980). It has been shown in human population studies that even low exposure to cadmium alters renal tubule function (Akesson et al., 2005). Thus, there is evidence in the kidney that pre-existing expression of MT in the renal tubules both protects the kidney from cadmium exposure, but this expression might also render the organ susceptible to the chronic effects of the metal. There is little evidence, either for or against, that would support a similar role for MT-3 expression in human skin as regards the chronic effects of exposure

to arsenic. The present study demonstrates that MT-3 is prominently expressed in the majority of cells comprising the nevus, dysplastic nevus, *in situ* melanoma, superficial melanoma, and deeply invasive melanoma. Although the sample set was relatively small, there was no indication that expression was variable within or between disease categories. A consequence of this pattern of constant MT-3 expression is that the melanocytes, in all stages of progression, are able to continue to bind and accumulate As^{+3} in an environment where exposure to As^{+3} is at elevated levels. Unfortunately, there is very little information in the literature on conditions or mechanisms *in vivo* that would influence the release of As^{+3} from MT-3 inside a cell or tissue. One could speculate that if ultraviolet radiation influenced the release of As^{+3} from MT-3, it might impact on emerging research which suggests a linkage between the development of melanoma and co-exposure to As^{+3} and ultraviolet radiation (Cooper et al., 2014). The expression of MT-1 and -2 has been examined in patients with melanoma. It was shown that a gain of expression of MT-1 and -2 is an adverse prognostic and survival factor for patients with this cancer (Weinlich et al., 2003 and Weinlich et al., 2006). In contrast to MT-3, MT-1 and -2 is not expressed in the nevus and is gained later during the development of the cancer. The present study also shows that MT-3 is expressed in the normal human epidermal keratinocytes that would give rise to these cancers. The examination of these cancers show that all SCC exhibit robust expression of MT-3, and that the majority of BCC express MT-3 although a significant proportion express mild levels and some BCC failed to immunostain for this protein. The results of the present study also show that cell cultures of NHEK, HaCaT immortalized human keratinocytes, and normal human melanocytes do not express MT-3 as would be unexpected from their *in situ* patterns of

MT-3 expression. This observation shows that these cell lines are lacking a protein that can both bind and sequester As^{+3} as well as serving as an antioxidant. The MT-3 protein has also been shown to have growth inhibitory activity outside the neural system (Gurel et al., 2003), be involved in necrotic and apoptotic cell death (Somji et al., 2004 and Somji et al., 2006) and in the epithelial to mesenchymal transition (Kim et al., 2002 and Bathula et al., 2014). Exactly how this might impact on studies using these cell lines to elucidate the mechanism/s of As^{+3} toxicity and carcinogenicity is unknown, but may need to be considered in the interpretation of past and future studies. The loss of MT-3 expression in cell cultures derived from tissues where MT-3 is expressed may be a result of the cell culture environment. This is suggested by studies on MT-3 expression in bladder cancer and breast cancer cell lines. This laboratory has shown that the epithelial cells of the human bladder and breast do not express MT-3, but that the majority of patient specimens of breast and bladder cancers do express MT-3 (Sens et al., 2000, Sens et al., 2001, Zhou et al., 2006 and Somji et al., 2010). In studies examining MT-3 expression in As^{+3} and Cd^{+2}transformed bladder cancer cell lines and in MCF-7, T-47D, Hs 578 t, MDA-MB-231 breast cancer cell lines it was demonstrated that none of the cell lines expressed MT-3 (Zhou et al., 2006). However, when these cell lines were transplanted into immune compromised mice, all the resulting tumors showed prominent expression of MT-3. It has also been shown that the expression of MT-3 mRNA could be induced under cell culture conditions in the MT-3 non-expressing cell lines following treatment with MS-273, a histone deacetylase inhibitor (Somji et al., 2010 and Somji et al., 2011). These results suggest that MT-3 is silenced under cell culture conditions by a mechanism involving histone acetylation. Previous to the submission of this manuscript,

no studies of MT-3 expression in human skin or derived cancers existed in the literature; however, recently a study was published during the review process that documents the expression of MT-3 in human skin, both in normal as well as BCC and SCC (Pula et al., 2014). The findings of this study are in overall agreement with the above findings with the exception that they have found higher levels of MT-3 in SSC whereas the current study did not. Nevus, melanoma and cultured cell models were not assessed in this study.

References

1. Bolt, H.M., 2012. Arsenic: an ancient toxicant of continuous public health impact, from Iceman ötzi until now. Arch. Toxicol. 86, 825–830.

2. Komissarova, E.V., Rossman, T.G., 2010. Arsenite induced poly(ADP-ribosylation) of tumor suppressor P53 in human skin keratinocytes as a possible mechanism for carcinogenesis associated with arsenic exposure. Toxicol. Appl. Pharmacol. 243, 399–404.

3. Yeh, S., How, S.W., Lin, C.S., 1968. Arsenical cancer of skin. Histologic study with special reference to Bowen0s disease. Cancer 21, 312–339.

4. Cooper, K.L., Yager, J.W., Hudson, L.G., 2014. Melanocytes and keratinocytes have distinct and shared reponses to ultraviolet radiation and arsenic. Toxicol. Lett. 224, 407–415.

5. Pearce, D.C., Dowling, K., Sim, M.R., 2012. Cancer incidence and soil arsenic exposure
in a historical gold mining area in western Victoria, Australia: a geospatial analysis. J. Exposure Sci. Environ. Epidemiol. 22, 248–257.

6. Dennis, L.K., Lynch, C.F., Sandler, D.P., Alavanja, M.C., 2010. Pesticide use and cutaneous melanoma in pesticide applicators in the agricultural health study. Environ. Health Perspect. 118, 812–817.

7. Ren, X., McHale, C.M., Skibola, C.F., Smith, A.H., Smith, M.T., Zhang, L., 2011. An emerging role for epigenetic dysregulation in arsenic toxicity and carcinogenesis. Environ. Health Perspect. 119, 11–19.

8. Straif, K., Benbrahim-Tallas, L., Baan, R., Grosse, Y., Secretan, B., El Ghissassi, F., Bouvard, V., Guha, N., Freeman, C., Galichet, L., Cogliano, V., 2009. WHO International Agency for Research on Cancer Monograph Working Group: A

review of human carcinogens-part C: metals, arsenic, dusts, and
fibres. Lancet Oncol. 10, 453–454.

9. Lee, J.-C., Son, Y.-O., Pratheeshkumar, P., Shi, X., 2012. Oxidative stress and metal carcinogenesis. Free Rad. Biol. Med. 53, 742–757.

10. Vasak, M., Meloni, G., 2011. Chemistry and biology of mammalian metallothioneins. J. Biol. Inorg. Chem. 16, 1067–1078.

11. Irvine, G.W., Summers, K.L., Stillman, M.J., 2013. Cysteine accessibility during As3+ metalation of the a- and b-domains of recombinant human MT1a. Biochem. Biophys. Res. Comm. 433, 477–483.

12. Garla, R., Mohanty, B.P., Ganger, R., Sudarshan, M., Bansai, M.P., Garg, M.L., 2013. Metal stoichiometry of isolated and arsenic substituted metallothionein: PIXE and ESI–MS study. Biometals 26, 887–896.

13. Palmiter, R.D., Findley, S.D., Whitmore, T.E., Durnam, D.M., 1992. MT-III, a brainspecific member of the metallothionein gene family. Proc. Natl. Acad. Sci. U.S.A. 89, 6333–6337.

14. Tsuji, S., Kobayashi, H., Uchida, Y., Ihara, Y., Miyatake, T., 1992. Molecular cloning of human growth inhibitory factor cDNA and its down-regulation in Alzheimer's disease. EMBO J. 11, 4843–4850.

15. Uchida, Y., Takio, K., Titani, K., Ihara, Y., Tomonaga, M., 1991. The growth inhibitory factor that is deficient in Alzheimer's disease is a 68 amino acid metallothionein-like protein. Neuron 7, 337–347.

16. Garrett, S.H., Sens, M.A., Todd, J.H., Somji, S., Sens, D.A., 1999. Expression of MT-3 protein in the human kidney. Toxicol. Lett. 105, 207–214.

17. Kim, D., Garrett, S.H., Sens, M.A., Somji, S., Sens, D.A., 2002. Metallothionein isoform
3 and proximal tubule vectorial active transport. Kidney Int. 61, 464–472.

18. Somji, S., Garrett, S.H., Sens, M.A., Gurel, V., Sens, D.A., 2004. Expression of metallothionein isoform 3 (MT-3) determines the choice between apoptotic or necrotic cell death in Cd+2-exposed human proximal tubule cells. Toxicol. Sci. 80, 358–366.

19. Sewell, A.K., Jensen, L.T., Erickson, J.C., Palmiter, R.D., Winge, D.R., 1995. The bioactivity of metallothionein-3 correlates with its novel (domain sequence rather than metal binding properties. Biochemistry 34, 4740–4747.

20. Boukamp, P., Dzarlieva-Petrusevska, R.T., Breitkreuz, D., Hornung, J., Markham, A.,

Fusenig, N.E., 1988. Normal keratinization in a spontaneously immortalized aneuploid human keratinocyte cell line. J. Cell Biol. 106, 761–771.

21. Somji, S., Garrett, S.H., Sens, M.A., Sens, D.A., 2006. The unique N-terminal sequence
of metallothionein-3 is required to regulate the choice between apoptotic or necrotic cell death of human proximal tubule cells exposed to Cd+2. Toxicol. Sci. 90, 369–376.

22. Van den Oord, J.J., Delay, M., 1994. Distribution of metallothionein in normal and pathological human skin. Arch. Dermatol. Res. 286, 62–68.

23. Karasawa, M., Nishimura, N., Nishimura, H., Tohyama, C., Hashiba, H., Kuroki, T., 1991. Localization of metallothionein in hair follicles of normal skin and the basal cell layer of hyperplastic epidermis: possible association with cell proliferation. J. Invest Dermatol. 97, 97–100.

24. Zamirska, A., Matusiak, L., Dziegiel, P., Szybejko-Machaj, G., Szepietowski, J.C., 2012. Expression of metallothioneins in cutaneous squamous cell carcinoma and actinic keratosis. Pathol. Oncol. Res. 18, 849–855.

25. Kitchen, K.T., 2001. Recent advances in arsenic carcinogenesis: modes of action, animal model systems, and methylated arsenic metabolites. Toxicol. Appl. Pharmacol. 172, 249–261.

26. Lindgren, A., Vahter, M., Dencker, L., 1982. Autoradiographic studies on the distribution of arsenic in mice and hamsters administered 74As-arsenite or -arsenate. Acta Pharmacol. Toxicol. 51, 253–265.

27. Mididoddi, S., McGuirt, J.P., Sens, M.A., Todd, J.H., Sens, D.A., 1996. Isoform-specific
expression of metallothionein mRNA in the developing and adult human kidney. Toxicol. Lett. 85, 17–27.

28. Satarug, S., Baker, J.R., Reilly, P.E., Moore, M.R., Williams, D.J., 2002. Cadmium levels in the lung, liver, kidney cortex, and urine samples from Australians without occupational exposure to metals. Arch. Environ. Health 57, 69–77.

29. Satarug, S., Garrett, S.H., Sens, M.A., Sens, D.A., 2010. Cadmium: environmental exposure and heath outcomes. Environ. Health Perspect. 118, 182–190.

30. Liu, Y., Liu, J., Iszard, M.B., Andrews, G.K., Palmiter, R.D., Klaassen, C.D., 1995. Trangenic mice that overexpress metallothionein-1 are protected from cadmium lethality and hepatotoxicity. Toxicol. Appl. Pharmacol. 135, 222–228.

31. Liu, J., LiuYP, Habeebu, S.M., Klaassen, C.D., 1998. Susceptibility of MT-null mice to chronic CdCl2-induced nephrotoxicity indicates that renal injury is not mediated by the CdMT complex. Toxicol. Sci. 46, 197–203.

32. Liu, Y., Liu, J., Habeebu, S.M., Waalkes, M.P., Klaassen, C.D., 2000. Metallothionein-I/IInull mice are sensitive to chronic oral cadmium-induced nephrotoxicity. Toxicol. Sci. 57, 167–176.

33. Masters, B.A., Kelly, E.J., Quaife, C.J., Brinster, R.L., Palmiter, R.D., 1994. Targeted disruption of metallothionein 1 and II genes increases sensitivity to cadmium. Proc. Natl. Acad. Sci. U.S.A. 91, 584–588.

34. Andrews, G.K., 2000. Regulation of metallothionein gene expression by oxidative stress and metal ions. Biochem. Pharmacol. 59, 95–104.

35. Bernard, A., Roels, H., Hubermont, G., Buchet, J.P., Masson, P.L., Lauwerys, R., 1976. Characterization of the proteinuria in Cd exposed workers. Int. Arch. Occu. Environ. Health 38, 19–30.

36. Bosco, E., Porta, N., Diezi, J., 1986. Renal handling of cadmium: a study by tubular microinjections. Arch. Toxicol. 7, 371–373.

37. Gonich, H.C., Indraprasit, S., Rosen, V.J., Neustein, H., Van de Velde, R., Raghavan, S.R.V., 1980. Effect of cadmium on renal tubular function, the ATP-Na-ATPase transport system and renal tubular ultrastructure. Miner. Electrol. Metab 3, 21–35.

38. Akesson, A., Lundh, T., Vahter, M., Bjellerup, P., Lidfeldt, J., Nerbrand, C., Samsioe, G.,Stromberg, U., Skerfving, S., 2005. Tubular and glomerular kidney effects in Swedish women with low environmental cadmium exposure. Environ. Hlth Perspect. 113, 1627–1631.

39. Weinlick, G., Bitterlich, W., Mayr, V., Fritsch, P.O., Zelger, B., 2003. Metallothioneinoverexpression as a prognostic factor for progression and survival in melanoma:
a prospective study on 520 patients. Br. J. Dermatol. 149, 535–541.

40. Weinlich, G., Eisendle, K., Hassler, E., Baltaci, M., Fritsch, P.O., Zelger, B., 2006. Metallothionein overexpression as a highly significant prognostic factor in melanoma: a prospective study of 1270 patients. Brit. J. Cancer 94, 835–841.

41. Gurel, V., Sens, D.A., Somji, S., Garrett, S.H., Nath, J., Sens, M.A., 2003. Stable transfection and overexpression of metallothionein isoform 3 inhibits the growth of MCF-7 and Hs578T cells but not that of T-47D or MDA-MB-231 cells. Breast Cancer Res. Treat. 80, 181–191.

42. Bathula, C.S., Garrett, S.H., Zhou, X.D., Sens, M.A., Sens, D.A., Somji, S., 2014. Cadmium, vectorial active transport, and MT -3-dependent regulation of cadherin expression in human proximal tubular cells. Toxicological Sciences: an Official Journal of the Society of Toxicology 102, 310–318.

43. Sens, M.A., Somji, S., Lamm, D.L., Garrett, S.G., Slovinsky, F., Todd, J.H., Sens, D.A.,2000. Metallothionein Isoform 3 as a potential biomarker for human bladder cancer. Environ. Health Perspect. 108, 413–418.

44. Sens, M.A., Somji, S., Garrett, S.H., Sens, D.A., 2001. Metallothionein isoform 3 (MT-3) overexpression is associated with breast cancers having a poor prognosis. Am. J. Pathol. 159, 21–26.

45. Zhou, X.D., Sens, M.A., Garrett, S.H., Somji, S., Park, S., Gurel, V., Sens, D.A., 2006. Enhanced expression of metallothionein isoform 3 (MT-3) protein in tumor heterotransplants derived from As+3 and Cd+2 transformed human urothelial cells. Toxicol. Sci. 93, 322

46. Somji, S., Garrett, S.H., Zhou, X.D., Zheng, Y., Sens, D.A., Sens, M.A., 2010. Absence of
metallothionein 3 expression in breast cancer is a rare, but favorable marker of outcome that is under epigenetic control. Toxicol. Environ. Chem. 92, 1673–1695.

47. Somji, S., Garrett, S.H., Toni, C., Zhou, X.D., Zheng, Y., Ajjimaporn, A., Sens, M.A., Sens, D.A., 2011. Differences in the epigenetic regulation of MT-3 gene expression between parental and Cd+2 or As+3 transformed human urothelial cells. Cancer Cell Int. 11, 2.

48. Pula, B., Tazbierski, T., Zamirska, A., Werynska, B., Bieniek, A., Szepietowski, J., Rys, J.,Dziegiel, P., Podhorska-Okolow, M., 2014. Metallothionein 3 expression in normal skin and malignant skin lesions. Pathol. Onocl. Res July 13 [Epub ahead of print].